TECHNISCHE UNIVERSITÄT
KAISERSLAUTERN

Metabolic channeling during phycoerythrobilin biosynthesis

vom Fachbereich Biologie der Universität Kaiserslautern zur Verleihung des akademischen Grades „Doktor der Naturwissenschaften“ genehmigte Dissertation

angefertigt im

Fachbereich Biologie

Abteilung Mikrobiologie

Wissenschaftliche Aussprache: Kaiserslautern, 16.10.2018

vorgelegt von

Marco Aras

Referent:	Prof. Dr. Nicole Frankenberg-Dinkel
Korreferent:	Prof. Dr. Ekkehard Neuhaus
Vorsitz:	Prof. Dr. Johannes Herrmann

Kaiserslautern, 2018 – D 386

Für meine Familie

Table of contents

Danksagung 7

Abbreviations 8

1 Introduction 10

1.1 The importance of oxygenic photosynthesis 10

1.2 Marine Cyanobacteria – The power plants of the earth 12

1.3 Phycobiliproteins of cyanobacteria and their role in light-harvesting 15

1.4 The biosynthesis of light-harvesting pigments in cyanobacteria 16

1.4.1 Heme oxygenases and biliverdin formation 17

1.4.2 Ferredoxin-dependent bilin reductases and phycobilin formation 18

1.4.3 The biosynthesis of phycoerythrobilin in cyanobacteria 20

1.5. The metabolic channeling of DHBV during PEB formation 24

1.6 Objectives of this work 27

2 Materials and Methods 28

2.1 Chemicals and reagents 28

2.1.1 Equipment 28

2.1.2 Enzymes, kits, antibodies and special chemicals 29

2.1.3 Microbial strains 31

2.1.4 Plasmids 31

2.1.5 Oligonucleotides 34

2.2 Microbial methods 36

2.2.1 Sterilization 36

2.2.2 Media and supplements 36

2.2.3 Cultivation of *E. coli* cells 37

2.2.4 Preparation of chemically competent *E. coli* cells 37

2.2.5 Preparation of electro-competent *E. coli* cells 37

2.2.6 Transformation of chemically competent *E. coli* cells 37

2.2.7 Transformation of electro-competent *E. coli* cells 38

2.3 Molecular biological methods 38

2.3.1 Preparation of plasmid DNA 38

2.3.2 Determination of the concentration of nucleic acids 38

2.3.3 Analysis of nucleic acids by agarose gel electrophoresis 38

2.3.4 The polymerase chain reaction (PCR) 39

2.3.5 Restriction Endonuclease digestion of nucleic acids 40

2.3.6 Ligation of DNA molecules 40

2.3.7 Gibson Assembly® of DNA molecules 40

2.3.8 Construction and validation of expression plasmids 41

2.3.9 Site-directed mutagenesis and construction of a fusion protein 41

2.3.10 λ – Red recombineering – a phage mediated gene disruption 42

2.4. Protein biochemical and analytical methods 43

2.4.1 Production of recombinant proteins in *E. coli* BL21 (DE3) 43

2.4.2 Purification of recombinant proteins 44

2.4.3 SDS-polyacrylamide gel electrophoresis (SDS-PAGE) 46

2.4.4. Immuno-detection of immobilized proteins (Western Blot) 47

2.4.5 Determination of protein and phycobilin concentrations 48

2.4.6 Gel permeation chromatography (GPC) 49

2.4.7 Anaerobic bilin reductase assay (FDBR assay) 49

2.4.8 Development of "on-column" FDBR assays with immobilized enzymes 52

2.4.9 HPLC analysis and phycobilin extraction 53

2.4.10 Fluorescence titration and Microscale Thermophoresis (MST) 54

2.4.11 Bacterial Two-Hybrid System (BacTH) 55

2.4.12 *In-vivo* crosslinking with Strep-protein interaction experiments (SPINE) 57

3 Results 58

3.1 Substrate affinities of FDBR:DHBV complexes 58

3.1.1 New evaluation of affinity binding constants of FDBRs to DHBV 58

3.1.2 Analysis of the activity of purified PebA and PebB 60

3.1.3 The FDBRs PebA and PebB form a fluorescent complex with DHBV 62

3.1.4 Binding affinities of FDBRs to DHBV point to metabolic channeling 62

3.2 Development of "on-column" FDBR assays 65

3.2.1 FDBRs show activity after immobilization on chromatography beads 65

3.2.2 The intermediate DHBV is transferred from PebA to PebB on the column 65

3.2.3 Column immobilized PebA and PebB are still functional and show activity 67

3.2.4 UV-Vis spectroscopy confirmed the FDBR:bilin complex 68

3.3 Creating a fusion protein of PebA and PebB 68

3.3.1 A simple base insertion leads to the fusion of PebA and PebB 68

3.3.2 The PebAgB translational fusion protein shows PebS-like activity 69

3.4 Time-coursed experiments of different FDBRs to produce PEB 71

3.5 Bacterial Two-Hybrid system shows slight interactions 73

3.6 PebA and PebB can be crosslinked with formaldehyde 76

3.7 Integration of genes for phycobilin biosynthesis into *E. coli* BL21 (DE3) 78

4 Discussion 80

4.1 High affinity to DHBV is the key step in PEB formation 80

4.2 Immobilized FDBRs are still active and "on-column" assay confirmed the substrate channeling 83

4.3 The fusion protein PebAgB shows PebS-like activity 85

4.4 Alternative interaction studies confirmed a transient interaction 87

4.5 The colored future – pigment biosynthesis in *E. coli* 89

5 Summary 92

6 Zusammenfassung 93

Appendix 94

References 98

Curriculum vitae 109

Eidesstattliche Erklärung 111

Danksagung

Mein besonderer Dank gilt zunächst meiner Doktormutter Prof. Dr. Nicole Frankenberg-Dinkel für die Vergabe dieses interessanten und farbenfrohen Themas sowie der Möglichkeit, meine Doktorarbeit in ihrer Arbeitsgruppe anzufertigen. Ich danke ihr sehr für ihre hervorragende Diskussionsbereitschaft und ihre durchgehende Unterstützung sowohl für die experimentellen Aufgaben als auch für die Ermöglichung an internationalen Konferenzen teilzunehmen.

Bei Prof. Dr. Ekkehard Neuhaus bedanke ich mich für die freundliche Übernahme des Korreferats sowie bei Prof. Dr. Johannes Hermann für die Bereitschaft, den Vorsitz der Prüfungskommission zu übernehmen.

PD Dr. Marc Nowaczyk von der Ruhr-Universität Bochum danke ich für die Bereitschaft zur Kooperation sowie für die Möglichkeit, die Microscale Thermophorese bei ihm durchzuführen.

Ich danke Prof. Dr. Eckhard Hofman und Johannes Sommerkamp von der Ruhr-Universität Bochum für die langjährige Kooperation, die vielfachen wissenschaftlichen Austausche und den freundlichen Umgang innerhalb des gemeinsamen Projektes.

Ich danke Dr. Vinko Misetic von NanoTemper GmbH für den technischen und analytischen Support, meine Messdaten zu evaluieren und meine Experimente zu optimieren.

Danke an Dr. Michelle Gehringer für den tollen Support und die Kooperation während dieser Arbeit

Für die letzten 8 Jahre in Nicoles Gruppe möchte ich mich zunächst herzlichst bei allen Mitgliedern der alten FKB Familie aus Bochum bedanken: Kristina, Sabrina, Julia, Björn, Carina, Basti, Mark, Max und Kathrin. Mit euch fühlte sich arbeiten wie Urlaub an.

Für die Zeit in Kaiserslautern geht mein besonderer Dank an die neuen „Mikros“ für die fantastische Zeit im Labor und die vielen Aktivitäten außerhalb der Forschung. Danke an Benni für die produktiven Kaffeemeetings und die tolle Zeit auf Konferenzen und Tagungen. Danke an Anne für deine ständige Hilfsbereitschaft und dein offenes Ohr in jeder Lebenslage. Danke an meine Studentinnen Jana und Emma für die großartige Zusammenarbeit im Labor. Ein wirklich sehr großer Dank geht an die Laborkollegen & Freunde Loriana, Martina, Katrin, Natascha, Kerstin, Susanne, Christine und Julia für die mehr als tolle Arbeitsatmosphäre, die Diskussionsbereitschaft und die permanente Unterstützung, die wir alle projektübergreifend gepflegt haben.

Meinen allergrößten Dank richte ich an meine Familie, ohne deren permanente Unterstützung mein Studium sowie meine Doktorarbeit nicht möglich gewesen wären. Danke Papa, Mama, Claudio und Sonja sowie Luise und Ella.

Abbreviations

A	absorbance
A%	peak area in percentages
APC	allophycocyanin
APS	ammonium persulfate
AU	absorbance units
BCIP	5-Bromo-4-chloro-3-indolyl phosphate
bp	base pairs
BR	bilirubin
BV	biliverdin IXα
Chl	chlorophyll
CV	column volume
Da	Dalton
DAD	diode array detector
DHBV	15,16-dihydrobiliverdin
DMF	dimethylformamide
DMSO	dimethyl sulfoxide
DNA	desoxyribonucleic acid
DTT	dithiothreitol
Fd	ferredoxin
FDBR	ferredoxin-dependent bilin reductase
Fig	figure
FPLC	fast protein liquid chromatograhphy
LB	Luria Bertani
HO	heme oxygenase
HPLC	high performance liquid chromatography
M	molar
MST	microscale thermophoresis
MW	molecular weight
MWCO	molecular weight cut off
NADPH	nicotinamide adenine dinucleotide phosphate
NBT	nitro blue tetrazolium chloride
nm	nanometer
NRS	NADPH-regenerating system
OD_{578}	optical density at 578 nm
OCA	“on-column” assay

PBP	phycobiliprotein(s)
PBS	phycobilisome(s)
PBS buffer	phosphate buffered saline buffer
PC	phycocyanin
PCB	phycocyanobilin
PCR	polymerase chain reaction
PDB	protein data bank
PE	phycoerythrin
PEB	phycoerythrobilin
PEC	phycoerythrocyanin
PΦB	phycochromobilin
PUB	phycourobilin
PVB	phycoviolobilin
PVDF	polyvinylidene fluoride
rpm	rounds per minute
SDS	sodium dodecyl sulfate
SDS-PAGE	sodium dodecyl sulfate polyacrylamide gel electrophoresis
SPINE	strep-protein interaction experiment(s)
TEMED	N,N,N′,N′-Tetramethylethane-1,2-diamine
TES	N-[Tris(hydroxymethyl)methyl]-2-aminoethanesulfonic acid
TFA	trifluoroacetic acid
UV/Vis	ultraviolet/visible
v/v	volume per volume
w/v	weight per volume
X-Gal	5-bromo-4-chloro-3-indolyl-β-D-galactopyranoside

1 Introduction

1.1 The importance of oxygenic photosynthesis

Oxygenic photosynthesis, the conversion of solar energy into biomass, is one of the most important biochemical processes on earth. Cyanobacteria are the first and only prokaryotes known to have evolved the ability to conduct oxygenic photosynthesis and are thought to have been responsible for oxygenating the early Earth's atmosphere ~ 2.4 billion years ago, allowing the evolution of the variety of oxygen dependent life forms we know today (Nisbet and Nisbet, 2008). Endosymbiosis of these phototrophic organisms about 2.1 billion years ago gave rise to the chloroplast lineage in land plants. In a set of redox reactions these organisms achieve the conversion of light energy into chemical energy in the form of the fixation of CO_2 to carbohydrates. The simplified equation of the oxygenic photosynthesis is written below:

$$6\,CO_2 + 6\,H_2O + hv \rightarrow C_6H_{12}O_6 + 6\,O_2$$

$$(hv = photon\ energy)$$

The biggest biomass of primary producers is located in oceanic environments and is mainly composed of cyanobacteria, algae and cryptophytes while cyanobacteria make up the greatest part in this group (Margulis, 1970; Stoebe and Maier, 2002). Since almost 71% of the earth's surface is covered with water the vast majority of phototrophic organisms in the oceans have a high impact on global CO_2- and O_2 cycles (Siegel and Franz, 2010). Cyanobacteria are therefore key players in the maintenance of the global oxygen level and their involvement in the macrocycle of oxygen is more than important. The sunlight is captured by special molecules which can be excited to use this energy for photosynthetic processes. The majority of light-harvesting molecules belong to the class of tetrapyrroles, including the chlorophyll (Chl) as the most abundant pigment (Bryant *et al.*, 1991; de Marsac and Cohen-bazire, 1977; Glazer, 1985; MacColl, 1998; Redlinger and Gantt, 1981). Chlorophylls are used by all photosynthetic active phototrophs and they are embedded in the photosystem I (PSI) and photosystem II (PSII) for light-harvesting. Furthermore, the most eukaryotic phototrophs (besides red algae and cryptophytes) employ light-harvesting antennae complexes (LHC) in which chlorophylls are used as light-harvesting pigments to distribute the collected light energy to the reactive center of photosynthesis. As chlorophyll absorb mostly blue and red light they leave a vast amount of light energy unused – called the "green gap" between 500 – 600 nm (Fig. 1.1). This gap is filled by the utilization of additional pigments which can absorb mostly green light. In aquatic environments the light conditions are clearly different depending on the depth of water. Red light for example is not able to penetrate deeper levels of water so red-light absorption occurs closer to the water surface or in shaded terrestrial environments (Nürnberg *et al.*, 2018). In contrast, blue light is energy-rich and can penetrate deeper into the water column and therefore the light absorbing pigment composition in this region differ from those of the upper

levels. During their evolution cyanobacteria developed different light-harvesting antenna structures to adapt to these variable light conditions. In order to fill the “green gap” of the chlorophyll absorbance (Fig. 1.1) these organisms developed phycobilisomes (PBS), large light-harvesting complexes, to enhance their access to the available light (Glazer *et al.*, 1985; Kehoe, 2010).

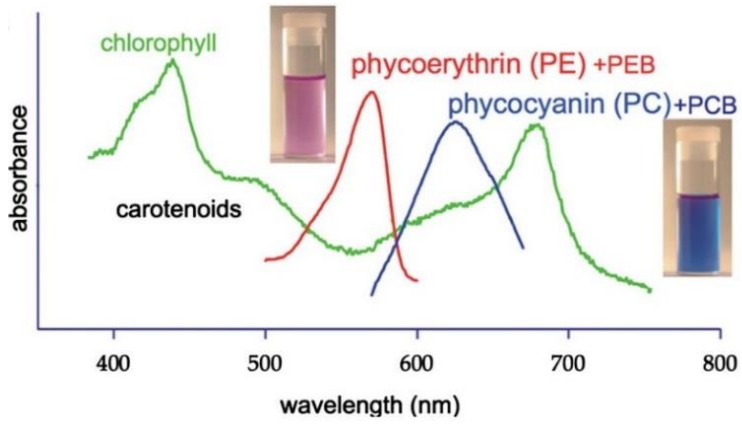

Figure 1.1: Phycobiliproteins fill the green gap of chlorophyll absorbance.

The two most abundant phycobiliproteins are phycocyanin (PC) and phycoerythrin (PE) and they absorb light in the region of the visible spectrum which is not covered by the chlorophyll absorbance. (taken from Kehoe, 2010).

The phycobilisomes (PBS) of cyanobacteria are anchored in an internal membrane system specialized for photosynthesis and respiration, the thylakoid (Liberton *et al.*, 2013; Wildman and Bowen, 1974). This membrane possesses a special feature for electron transduction since the elements of both the photosynthetic apparatus as well as the respiration chain are embedded in the thylakoid (Mullineaux, 2014; Vermaas, 2001). The phycobilisome is directly associated with the photosystem II and the accessory light-harvesting elements are organized in a special antenna structure (Fig. 1.2). A dominant feature of the phycobilisome is a species-specific composition of the light-harvesting elements, depending on the ambient light conditions (see section 1.3) (Glazer, 1977; Grossman *et al.*, 1993). The excitation energy of the sunlight can be transferred to the reaction centers which are embedded into the thylakoid membrane, the photosystem II or photosystem I. Here, the actual photosynthesis process is located and the absorbed light energy drives the fixation of carbohydrates via the Calvin-cycle. The typical phycobilisome of *Synechococcus* is composed of phycocyanin (PC), phycoerythrin (PE) and allophycocyanin (APC) (Glazer, 1977). APC forms the core unit of the PBS and the PCs and PE are connected via core linker proteins to the PBS center (Glazer, 1985; Six *et al.*, 2007; Wilbanks and Glazer, 1993). By stacking several phycobiliproteins a rod-shape antenna structure is formed composed by PCs closer to the center and PEs distal to the core (Fig 1.2) Interestingly, the attachment of the PBS is unstable and some studies observed a mobility of this complex on the membrane’s surface between PSII and PS I.

This phenomenon is believed to regulate the light-harvesting or the repair mechanisms of membrane components (Joshua and Mullineaux, 2004; Mullineaux *et al.*, 1997). The formation and maintenance of a phycobilisome is highly dynamic process in order to maximize the light-harvesting efficiency including protein synthesis, repairing or rod assembly (Liu, 2016).

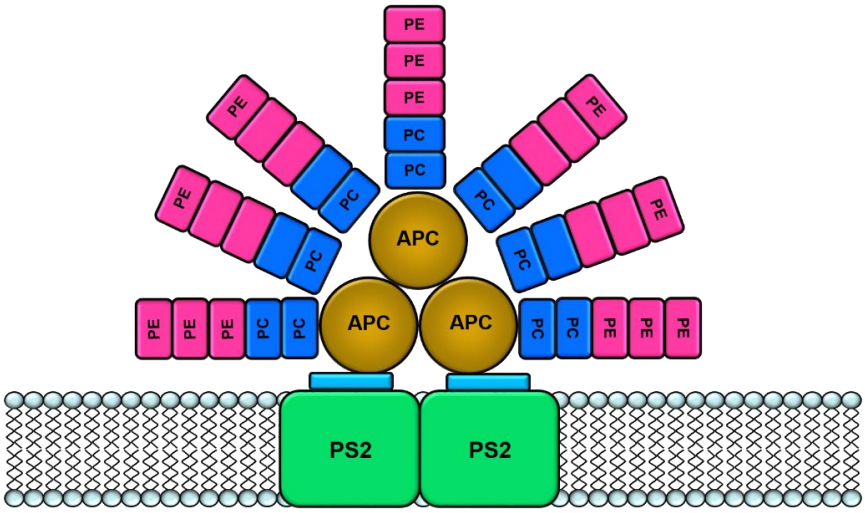

Figure 1.2: Model of the photosynthetic machinery in cyanobacterial thylakoid membranes of *Synechococcus sp.* WH8020

The core unit of the phycobilisome (PBS) is composed of allophycocyanin (APC) which is directly associated with the photosystems in the thylakoid membrane. Extrinsic light-harvesting antenna structure are formed by connecting phycocyanin (PC) and phycoerythrin (PE) to the core unit of the PBS by core-linker proteins. The composition of this structural element is responsible for the vivid colors (blue, blue-green, red or orange) the *Synechococcus* strain appear in nature (modified from (Wiethaus *et al.*, 2010)). PS 2 = photosystem II

1.2 Marine Cyanobacteria – The power plants of the earth

The marine cyanobacterial species *Prochlorococcus* and *Synechococcus* are two of the most abundant species of the marine phytoplankton. They occur in almost every oceanic region and their production of oxygen is substantial for life on earth (Flombaum *et al.*, 2013). *Prochlorococcus* strains occur mostly in warm oceanic regions, mostly in the east Pacific Ocean and the Indian sea in water depths between 100 to 200 m and are the most abundant photosynthetic organisms in the ocean.

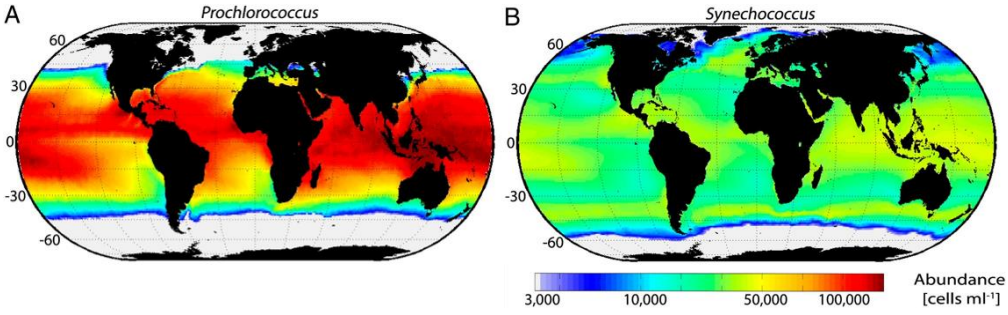

Figure 1.3: Global distribution of the two most abundant oceanic cyanobacteria.

(A) *Prochlorococcus* is mainly found in warm oceanic regions like the east pacific or Indian sea. **(B)** *Synechococcus* is also found in similar regions as *Prochlorococcus* but their occurrence is also expanded to colder areas like the arctic oceans (taken from Flombaum *et al.*, 2013).

The estimated cell density in these regions was estimated as 2.8 x 10^5 cells ml^{-1} and they are only outcompeted in growth by other phytoplanktonic organisms in areas containing high nutrition levels (Fig. 1.3 A). The second most abundant member of the cyanobacterial community are the *Synechococcus* strains which often dominate coastal waters. They appear in similar regions as *Prochlorococcus* strains but also expand their occurrence to colder oceanic regions like the arctic sea (Fig. 1.3 B). It is suggested that both cyanobacterial species compete for the same ecological niche, with the season determining which one of these species dominates (Chisholm, 1992). In general, *Prochlorococcus* strains can be divided into two different groups regarding their light-harvesting ability: The high-light strains (HL) which grow at light intensities up to 200 µmol photons m^{-2} s^{-1} and strains which are adapted to low-light (LL) conditions which can only grow at light intensities ranging from 30 – 50 µmol photons m^{-2} s^{-1}. HL-strains (for example *Prochlorococcus marinus* MED4) typically colonize nutrient poor shallow waters since their photosynthetic apparatus is optimized for this condition. In contrast, the LL-strains (for example *Prochlorococcus marinus* CCMP 1375) tend to live in deeper levels of the water column with nutrient rich conditions (Moore and Chisholm, 1999; Moore *et al.*, 1998). Interestingly, *Prochlorococcus* do not employ phycobilisomes for light-harvesting which is in contrast to other cyanobacterial species.

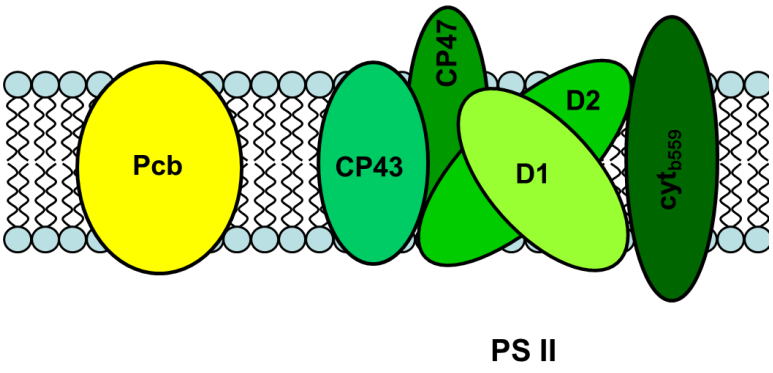

Figure 1.4: Reduced light-harvesting apparatus of *Prochlorococcus* strains.

Prochlorococcus strains possess a prochlorophyte Chl-binding (Pcb) antenna which binds divinyl-chlorophyll *a* and *b* for light-harvesting. In some strains like *Prochlorococcus marinus* MED4 a single β-subunit of PE III is attached onto the thylakoid (Steglich *et al.*, 2005). Pcb = prochlorophyte Chl-binding antenna; D1 = reaction center core protein 1, D2 = reaction center core protein 2, CP43 = core antenna protein, CP 47 = core antenna protein; cyt_{b559} = cytochrome b559 (taken from Wiethaus *et al.*, 2010)

For light-harvesting they use a divinyl-chlorophyll (DV-chl) *a*- and *b*-containing prochlorophyte binding protein (Pcb) as an adaptation to their LL environment (Ting *et al.*, 2001). In LL-strains this antenna is integrated into the thylakoid membrane connected to PS I and PS II (Fig. 1.4) (Goericke and Welschmeyer, 1993) but in HL strains only PS II is connected with the Pcb-antenna (Bibby *et al.*, 2003). As a further adjustment to their blue-light dominating environment, LL-strains increase the ratio of chlorophyll *b* to chlorophyll *a* in their photosystems (Goericke and Repeta, 1992).

In addition to the Pcb-antenna, *Prochlorococcus* strains possess a single phycoerythrin,PE III. This PE III is attached to the thylakoid membrane and its structure is similar to other cyanobacterial species, the typical (αβ)-heterodimer (Fig. 1.5) but no phycobilisome like structure is formed. Interestingly, the LL-strains possess a phycoerythrin III (PE III) and it is believed that this is a relic from an ancestral phycobilisome (PBS) (Hess *et al.*, 1992) whereas in HL strains only a single β-subunit of the PE III is attached to the thylakoid and the function of this degenerated PE remains unknown (Steglich *et al.*, 2005). The light-harvesting capability of PE III is rather low and the main light-harvesting is performed by the Pcb-antenna. Typical for PE III is the attachment of not only phycoerythrobilin (PEB) but also phycourobilin (PUB) which can absorb light with shorter wavelengths (Steglich *et al.*, 2005; Wiethaus *et al.*, 2010). The PUB content in this PE III with a ratio of 3:1 (PUB : PEB) is quite high in comparison to other cyanobacterial PEs (Hess *et al.*, 1996) but not surprising considering the water depth where these cyanobacteria occur (Wood, 1985). In contrast to *Prochlorochoccus* all *Synechococcus* strains employ phycobilisomes for optimal light-harvesting attached to the thylakoid membrane and their phycobilisomes are mostly composed of PC and some strains also add PE to this. They mostly appear in blue-green color but depending on the available light the color some *Synechococcus* strains can change their coloration to red or orange. This phenomenon is called “complementary chromatic acclimation (CCA)” and it provides the cyanobacteria with the ability to tailor the composition of the phycobilisomes for optimal light-harvesting efficiency (Tandeau de Marsac, 1977). There are four types of CCA mechanisms known (Type I – IV CCA) based on the changes in the light-harvesting antenna. Type I CCA shows no light dependent regulation of PC and PE expression. During Type II CCA green light (GL) and white light (WL) stimulates the PE expression, but not red light (RL) whereas during type III CCA the cyanobacteria can express PE or PC as an adaptation to GL and RL, respectively. And lastly, in Type IV CCA, even the chromophore content of PE II is modified to enhance the light-harvesting efficiency under green light conditions (Ho *et al.*, 2017). *Synechococcus sp.* WH8020 is classified as a Type IV chromatic adapter (Gutu and Kehoe, 2012).

1.3 Phycobiliproteins of cyanobacteria and their role in light-harvesting

The photosynthetic apparatus of cyanobacteria is located on the thylakoid membrane inside of the cyanobacterial cell. Where *Prochlorococci* utilize a single Pcb-antenna, other cyanobacterial species employ larger light-harvesting complexes attached to their thylakoid membrane, the phycobilisome. The phycobilisome forms rod-shaped structures and each implemented phycobiliprotein is connected with specific pigments for light-harvesting. In cyanobacteria the phycobiliproteins (PBP) are composed of (*αβ*)-heterodimers which consist of homologous *α*- and *β*- subunits (Fig 1.5 A). By connecting three (*αβ*)-heterodimers, a higher oligomeric state of a PBP is formed as a ring-like structure containing $(\alpha\beta)_3$-trimers (Fig 1.5 B). A fully assembled phycobiliprotein is achieved by connecting two $(\alpha\beta)_3$-trimers which then forms a $(\alpha\beta)_6$-hexamer (Fig. 1.5 C). The finally assembled PBP serves then as a module for PBS assembly and by stacking each PBP the rod-like structure is formed and can act as an energy funnel allowing the energy transfer from distal to proximal phycobiliproteins up to the reaction center of the photosynthetic apparatus where the chlorophyll acts as the terminal energy acceptor (Zilinskas and Greenwald, 1986). All cyanobacteria which employ phycobilisomes possess phycocyanin (PC) and allophycocyanin (APC) as their main PBS units but certain species can also employ phycoerythrin (PE) or phycoerythrocyanin (PEC) as an additional phycobiliprotein to their phycobilisome. (Fig. 1.4). Each phycobiliprotein carries covalently bound pigments, so called phycobilins, which belong to the class of open-chain tetrapyrroles (see section 1.7) and depending on the kind of phycobiliprotein, specific phycobilins are attached to the light-harvesting structure (Glazer, 1977; Grossman *et al.*, 1993).

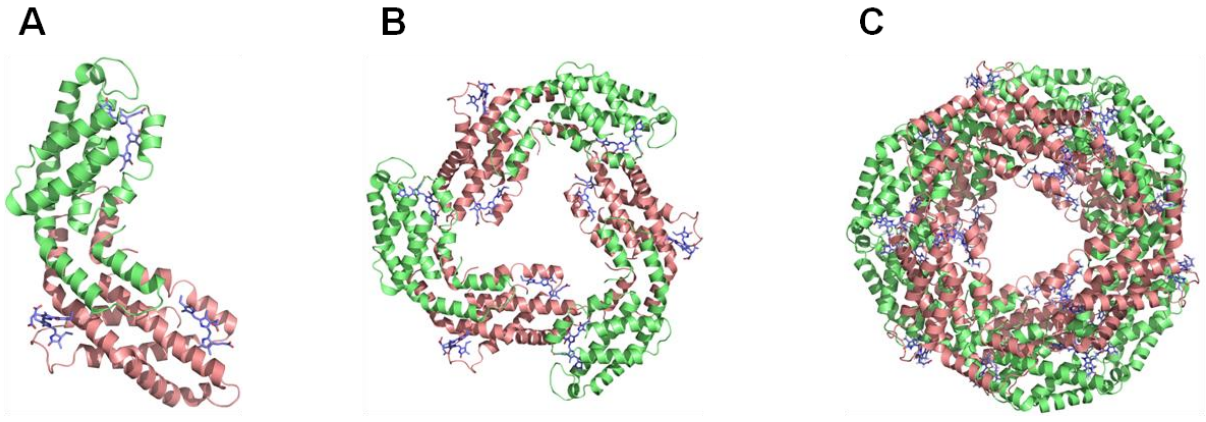

Figure 1.5: Structure and oligomerization states of a phycocyanin of the phycobilisome.

The crystal structure of the phycocyanin from *Synechocystis sp.* PCC 6803 is shown in cartoon representation, *α*-subunits are shown in green and *β*- subunits are colored in salmon. **(A)** The (*αβ*)-heterodimers of phycocyanin is assembled by homologues *α*- and *β*- subunits. **(B)** $(\alpha\beta)_3$-trimer of the phycocyanin of *Synechocystis sp.* PCC6803 (PDB 4F0T, (Marx and Adir, 2013). **(C)** The final $(\alpha\beta)_6$-hexamer possess a ring-like structure and is then built into the antennae rods of the phycobilisome of *Thermosynechococcus elongatus* BP-1 (PDB = 4ZIZ, (Fromme *et al.*, 2015)) (modified from Ledermann *et al.*, 2017).

PC contains phycocyanobilin (PCB) as its main chromophore molecule and PE contains mostly phycoerythrobilin (PEB) in addition to some phycourobilin (PUB). A PEC unit contains in addition to PEB also PCB attached to their binding sites (Kahn *et al.*, 1997). The different units of the phycobilisome (PC, APC, PE or PEC) possess different absorbance characteristics which are given in the table below.

Table 1.1 Absorbance ranges and pigmentation of the cyanobacterial phycobiliprotein types

Phycobiliprotein	Absorbance range [nm]	Color	Phycobilin
Phycocyanin	610 – 620	Blue	PCB
Allophycocyanin	650 – 655	Green-blue	PCB
Phycoerythrin	540 – 570	Orange-red	PEB
Phycoerythrocyanin	570 – 590	Violet	PEB & PCB

Phycobiliproteins obtain their absorbing characteristics from the composition of the covalently attached phycobilin chromophores. These linear tetrapyrrole molecules are posttranslationally attached via conserved cysteine residues to the apo-phycobiliproteins. Typically, up to three phycobilins are attached to the *α*- and *β*-subunits via the A-ring of these pigments (MacColl, 1998). Until today, four types of phycobilins are known which can serve as light-harvesting pigments in PBPs. The most common pigments are the blue pigment PCB (λ = 620 nm) and the pink pigment PEB (λ = 540 nm). Two less common phycobilin pigments are PUB (λ = 500 nm) and phycoviolobilin PVB (λ = 590 nm). The attachment of these phycobilins to the apo-phycobiliprotein can happen in two ways. It was shown *in vitro* that this attachment can occur spontaneously, leading to a heterogenic mixture of holo-PBPs with unspecific bound pigments (Fairchild and Glazer, 1994). In nature, the attachment of phycobilins occurs with a site- and stereospecific reaction which is mediated by a class of enzymes called phycobiliprotein lyases. Most of these lyases are specific for the phycobilin and it is also suggested that they are specific for the binding sites of the each apo-phycobiliprotein. Phycobiliprotein lyases ensure a correct binding of the pigments to the cysteine residue by forming a thioether bond between the phycobilin and the apo-phycobiliprotein. Mostly, the phycobilins are attached via the $C3^1$-atom to the PBP but in some cases a phycobilin forms a second bond with the $C18^1$-atom of the D-ring to a second cysteine residue (Scheer and Zhao, 2008).

1.4 The biosynthesis of light-harvesting pigments in cyanobacteria

The manifold colors of cyanobacteria and red algae are derived from the composition of the attached phycobilins to the phycobiliproteins. Phycobilins belong to the class of open-chain tetrapyrroles and are mostly involved in light-harvesting or light-sensing in these organisms. Furthermore, also plants utilize some phycobilins but they serve as light-sensing chromophores of the plant's phytochromes (Lagarias and Rapoport, 1980; Rudolf, 1928).

The biosynthesis of light-harvesting pigments in cyanobacteria is similar to that of red algae and cryptophytes. The open-chain tetrapyrroles are synthesized in subsequent oxidation steps starting with the ring opening reaction of heme to produce the green colored molecule biliverdin IXα (see section 1.4.1). Biliverdin serves then as a precursor for pigment formation for a class of enzymes called ferredoxin-dependent bilin reductases (FDBRs). These enzymes catalyze specific reduction steps of biliverdin to produce a various number of colorful pigments, including the two major phycobilins phycocyanobilin (PCB) and phycoerythrobilin (PEB).

1.4.1 Heme oxygenases and biliverdin formation

All functional members of the open-chain tetrapyrroles which are involved in light-harvesting processes derived from the ubiquitous molecule heme (Frankenberg *et al.*, 2001). Heme is a cyclic tetrapyrrole and therefore a ring-opening reaction is required to form the open-chain tetrapyrrole biliverdin IXα (BV IXα). Heme oxygenases are ubiquitous enzymes which are found for example in mammals, higher plants, insects and bacteria. They all mediate the ring opening reaction of heme but the typical HO products are distinguished depending on the cleavage position from BV IXα – β. From *Staphylococcus aureus* a novel HO is known (IsdG) which can degrade heme to staphylobilin and is so far the only HO yielding a different product than the previously described HOs (Reniere *et al.*, 2010). The different BVs fulfill several functions, e.g. heme catabolism, iron homeostasis, iron acquisition, antioxidants, chromophore synthesis or insect coloration (Abraham *et al.*, 1996; Cornejo *et al.*, 1998; Frankenberg-Dinkel, 2004; Paiva-Silva *et al.*, 2006; Richaud and Zabulon, 1997; Schmitt, 1997).

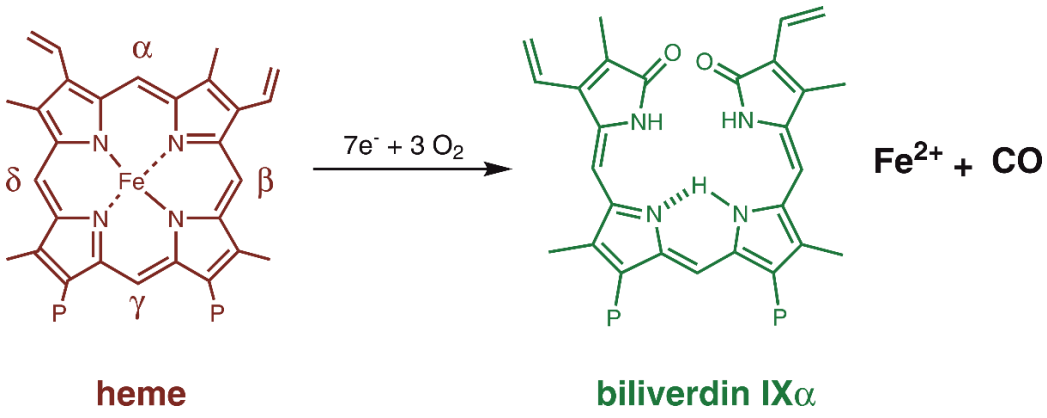

Figure 1.6: The heme oxygenase reaction.

The specific ring opening reaction of heme to produce biliverdin IXα (green) is mediated by heme oxygenase. For pigment biosynthesis the heme oxygenases are specific for the cleavage of the *α-meso* carbon bridge of heme (brown). The final products of the reaction are biliverdin IXα, Fe^{2+} and CO. The reaction requires seven electrons and three molecules of oxygen. P= propionate side chains.

For the pigment biosynthesis in cyanobacteria heme is taken from the heme synthesis pathway and the cleavage of the molecule's macrocycle is mediated by heme oxygenases (HO) (Cornejo and Beale, 1988; Rhie and Beale, 1992). This reaction is regio-specific for the position of the *α-meso* carbon bridge producing BV IXα (Montellano, 2000; Wilks, 2002).

There are other heme oxygenases known in bacteria with different regio-specificities. For example, the opportunistic pathogenic bacteria *Pseudomonas aeruginosa*, but also non-pathogenic *Pseudomonas* species, carry a gene for a second heme oxygenase (*hemO*) with a β- or δ-regio-specificity producing biliverdin IXβ or biliverdin IXδ, resp. (Gisk *et al.*, 2012; Ratliff *et al.*, 2001). These bacteria express those alternative HOs when they encounter iron starvation and use the released iron from the heme for their metabolism (Ratliff *et al.*, 2001). The heme oxygenase reaction requires three molecules of oxygen and seven electrons (Liu and Ortiz de Montellano, 2000). During this reaction several intermediate states are formed but with the final product formation the central iron is released together with CO (Fig. 1.6) (Wilks, 2002). In bacteria and photosynthetic eukaryotes, the required electrons for this reaction are preferably provided from ferredoxins with a [2Fe-2S]-cluster (Muramoto *et al.*, 1999; Rhie and Beale, 1992; Wilks and Schmitt, 1998). Mammals for example prefer the cytochrome P450 reductase as their electron donor for the heme oxygenase reaction (Schacter *et al.*, 1972).

1.4.2 Ferredoxin-dependent bilin reductases and phycobilin formation

The heme oxygenase reaction is the first instance in phycobilin formation and the HO product BV IXα serves as the precursor molecule for pigment biosynthesis. The first phycobilin was described in the early 1960's by isolating PCB from the filamentous cyanobacterium *Plectonema boryanum* and the structure was then confirmed by ^{1}H-NMR spectroscopy (Cole *et al.*, 1967). But the discovery of the PEB structure came shortly after by the isolation of R-PC (*Rhodophyta*-PC). Most phycobilins are synthesized by a class of enzymes called ferredoxin-dependent bilin reductases (FDBR). These enzymes have in common that they use biliverdin IXα as their substrate to produce manifold colored pigments for light-harvesting or light-sensing. The first FDBR activity was described in the early 1980's in cell-free extracts of the red algae *Cyanidium caldarium* where the conversion of biliverdin IXα to phycocyanobilin was observed (Beale and Cornejo, 1984b). Together with an observed HO activity, in this organism a connected pathway of phycobilin synthesis was postulated (Beale and Cornejo, 1984a). The early 1990's revealed the electron transfer of small ferredoxins to the FDBRs (Beale and Cornejo, 1991) and so the conclusion of a connected biosynthetic pathway for pigment formation was postulated. Another decade passed until the genes for phycobilin biosynthesis were identified, cloned and characterized (Cornejo *et al.*, 1998; Frankenberg *et al.*, 2001). The first described FDBR was the phytochromobilin - synthase (PΦB-synthase) (phytochromobilin:ferredoxin oxidoreductase; EC: 1.3.7.4; HY2) of *Avena sativa* L. cv Garry (McDowell and Lagarias, 2001). This FDBR catalyzes the reaction from BV to phytochromobilin (PΦB), the main chromophore of plant's phytochromes (Terry *et al.*, 1995; Terry *et al.*, 1993).

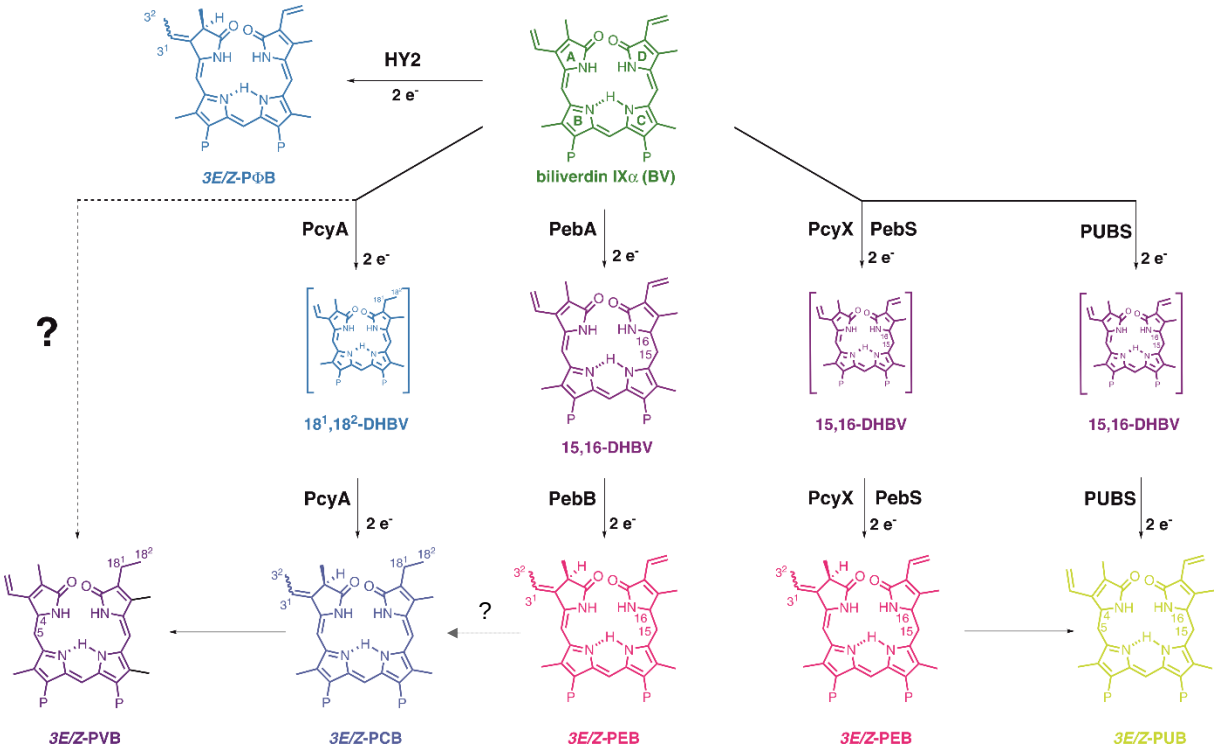

Figure 1.7: Overview of the phycobilin formation mediated by the FBDR family.

Biliverdin IXα (BV) is the substrate for all FDBRs with the exception of PebB, which uses 15,16-dihydrobiliverdin (DHBV) as its substrate to produce PEB. The pyrrole rings of BV are labeled from A to D. P = propionate side chains. The molecules inside the brackets represent protein bound intermediate states during pigment biosynthesis. The phycobilins are colored approximately as they appear in nature. The plant-based HY2, as well as the cyanobacterial enzymes PebA and PebB catalyze a formal two electron reduction of their substrate BV (or DHBV) to produce the specific products shown. In contrast, a four-electron reduction of BV is catalyzed by the FDBRs PcyA, PebS, PUBS and PcyX.

Reaction summary: HY2 catalyzes BV to the plant chromophore PΦB. The cyanobacterial BVR mediates the reaction from BV to bilirubin (BR). The blue pigment PCB is made by the reduction of BV by PcyA. PEB is formed by the subsequent reduction of two FDRBS: PebA and PebB. PebA converts BV to 15,16-DHBV which serves then as the substrate for PebB and is further converted to the pink pigment PEB. The phage encoded FDBRS PebS and PcyX are able to convert BV to PEB in a single step. PUBS converts BV to the yellow pigment PUB. Additionally, in the red algae *Galdieria sulphuraria* the conversion of PEB to PCB postulated based on biochemically data from cell-free extracts (Beale and Cornejo, 1991).

The identification of the gene related to FDBR activity cleared the way to identify several other genes encoding for FDBRs in cyanobacteria, red algae and plants (Frankenberg *et al.*, 2001). A second PΦB-synthase (HY2) was identified in *Arabidopsis thaliana* and after recombinantly production of the enzyme the identical reaction was observed (Kohchi *et al.*, 2001). The FDBR family was then expanded by the discovery of enzymes involved in PCB (PcyA) and PEB (PebA and PebB) formation, respectively (Frankenberg *et al.*, 2001). Interestingly, the latest discoveries of FDBRs were made from (cyano)-phages (e.g. cyanophage P-SSM2) with novel activities for PEB formation (PebS & PcyX). PebS was isolated from the cyanophage P-SSM2 which infects *Prochlorochoccus marinus* (Dammeyer *et al.*, 2008b). The origin of PcyX is still unclear since its gene was discovered in metagenomic data (Ledermann *et al.*, 2016).

Another interesting FDBR was found in the spreading earthmoss *Physcomitrella patens*, the model organism for several genetic and physiological processes, the phycourobilin synthase (PUBS). Until now, no known function of this phycobilin in the moss has been described yet (Y. R. Chen *et al.*, 2012). In cyanobacteria, PUB serves along with PEB as pigments in PEs but no PUB synthesizing enzyme was yet discovered in these organisms. Only the lyase/isomerase activity of the RpcG family was described for PUB formation in cyanobacteria (Blot *et al.*, 2009). In summary, six members of the FDBR family have been identified to date (Fig. 1.7). Additionally, in the red algae *Galdieria sulphuraria* the conversion of PEB to PCB was postulated in the early 90's. Cell-free extracts of *G. sulphuraria* were fractionated and PEB was added and the conversion to PCB was observed using HPLC (Beale and Cornejo, 1991). Over 20 years later the genome of *G. sulphuraria* was published (Schonknecht *et al.*, 2013) and by genomic investigation the only FDBRs found were homologs to PebA and PebB. After cloning these genes, first results showed the postulated activity of PEB formation by those enzymes as well as the previously observed conversion from PEB to PCB (Bachelor thesis Emma Eichler, Master thesis Jana Hartman; TU Kaiserslautern Microbiology). It is very obvious that a similar lyase or isomerase activity, as it occurs in some cyanobacteria, is present in *G. sulphuraria*, but it has not been discovered yet. All known members of the FDBR family can be divided into two functional groups, depending on the number of electrons they can transfer during the reaction. The first group consists of FDBRs which catalyze a two-electron reduction (e.g. HY2; PebA and PebB). The second group comprises FDBRs capable of a formal four-electron reduction of BV yielding the respective products (PcyA, PUBS, PebS and PcyX) (Fig. 1.7).

1.4.3 The biosynthesis of phycoerythrobilin in cyanobacteria

The main objective in this work covers the biosynthesis of the pink pigment phycoerythrobilin (PEB) via the cooperation of the two involved FDBRs PebA and PebB. For this reason, this biosynthesis pathway of PEB is described in detail. Interestingly, there are two different ways for PEB formation known to date (Fig. 1.8). PEB biosynthesis has been described in cyanobacteria, red algae, cryptophytes and phages (viruses that infect bacteria) (Dammeyer and Frankenberg-Dinkel, 2006; Dammeyer *et al.*, 2008b; Frankenberg *et al.*, 2001; Ledermann *et al.*, 2016; Tu *et al.*, 2004), while the conventional PEB formation in cyanobacteria, red algae and cryptophytes is identical and mediated by the cooperation of two FDBRs (PebA and PebB), those recently discovered in (cyano-)phages differs from that (PebS or PcyX). Interestingly, phage originated PEB biosynthesis requires only one FDBR enzyme to convert BV to PEB (Dammeyer *et al.*, 2008b; Ledermann *et al.*, 2016). The reaction mechanisms of all known FDBRs is quite similar since they all belong to radical enzymes.

To date, all FDBR reactions proceeds via a substrate radical mechanism where the required electrons are provided from small iron-sulfur proteins, the [2Fe-2S]-ferredoxins (Frankenberg and Lagarias, 2003). These ferredoxins can transfer one electron at a time leading to the formation of radical tetrapyrrole intermediates during product formation (Tu *et al.*, 2004). PebS, as a monofunctional enzyme for PEB synthesis shows a high structural similarity to PebA and most likely to PebB. Until now, the structure of several FDBRs were solved revealing a common pattern in their quaternary folding. Although their sequence identity is quite low the FDBRs prefer a similar structure of single α/β/α-sandwich folded globular proteins where two α-helices are flanking the central β-sheet (Busch *et al.*, 2011a; Dammeyer *et al.*, 2008b; Hagiwara *et al.*, 2006). In PebA and PebS the binding pocket is located between the proximal β-sheet and the C-terminal α-helix on the distal side. When the substrate BV IXα is bound to the active site, the A- and D-ring of the tetrapyrrole point towards the inside of the enzyme and the propionate side chains are facing to the outside (Fig. 1.9).

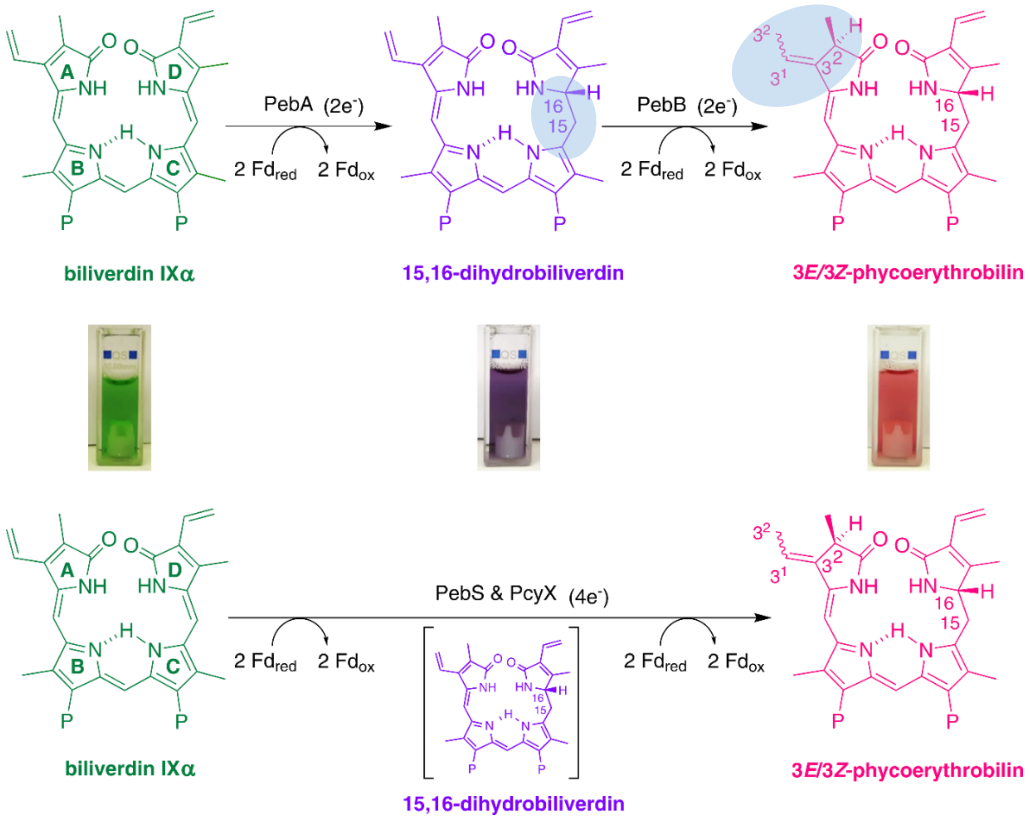

Figure 1.8: Two known pathways for phycoerythrobilin synthesis.

Overview of the two pathways known for phycoerythrobilin synthesis in cyanobacteria, red algae, cryptophytes and phages. BV serves as the natural substrate for all known FDBRs except PebB. The enzymatic conversion of BV to PEB is the result of a four-electron reduction step via the intermediate DHBV. While cyanobacteria require the two FDBRs PebA and PebB to produce phycoerythrobilin, phages possess enzymes that are able to perform both reaction steps. The FDBRs PebS and PcyX are able to convert BV to PEB as a single enzyme in a formal four-electron reduction step. The electrons needed for the reduction of BV and DHBV are provided from ferredoxins for both pathways. The change in color during pigment synthesis can be observed from green (BV) over violet (DHBV) to the final pink product (PEB). Fd = ferredoxin (reduced or oxidized). Chemical drawings were made with ChemDraw 14.

Determination of the charge at the protein surface around the binding pocket revealed a predominantly positive charge. This area seems most likely the region where the required electron donor for the catalysis, the ferredoxin, may interact (Dammeyer *et al.*, 2008b; Hagiwara *et al.*, 2006). Nevertheless, the structure of the FDBRs may be quite similar but they are able to catalyze different reactions and the structure does not reveal their specific activity. Both ways have in common that they catalyze the BV IXα reduction via a coupled electron transfer and the formation of tetrapyrrole-radical intermediates (Busch *et al.*, 2011a; Busch *et al.*, 2011b).

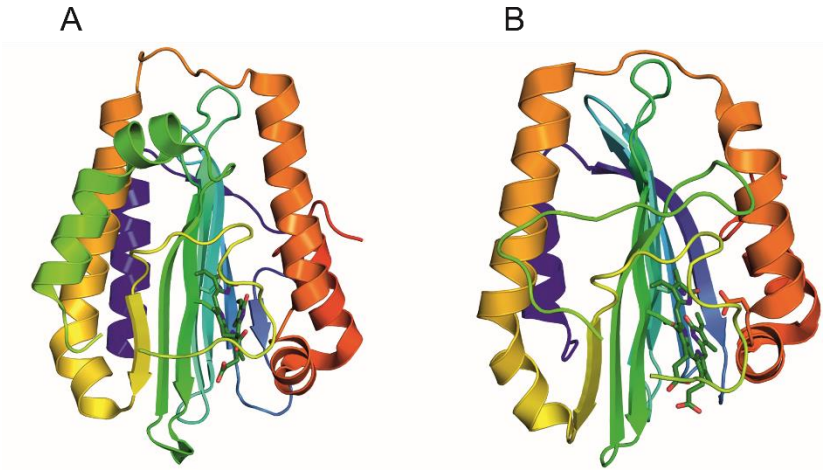

Figure 1.9 Comparison of the crystal structures of PebA and PebS.

Structural overview of the FDBRs PebA **(A)** from *Synechococcus sp.* WH8020 (PDB = 2XO9, (Busch *et al.*, 2011a)) and PebS **(B)** from the cyanophage P-SSM2 (PDB = 2VCK, (Dammeyer and Frankenberg-Dinkel, 2006)). The structures are shown in cartoon representation and the coloration goes from blue to red, starting with the N-terminus of each protein. Both FDBR crystal structures are solved with their substrate BV. Whereas the sequence identity is rather low (27%) their structure identity is much higher (modified from Ledermann *et al.*, 2017).

Interestingly, although PebA and PebS share a high structural similarity of (Fig. 1.9) (Busch *et al.*, 2011a), the reaction of PebA is terminated directly after DHBV formation whereas PebS keeps the intermediate DHBV and proceeds further to produce PEB (Dammeyer and Frankenberg-Dinkel, 2006). The cyanobacterial PEB biosynthesis is mediated by two members of the FDBR family, PebA and PebB. The 15,16-dihydrobiliverdin:ferredoxin oxidoreductase (PebA, EC: 1.3.7.2) reduces BV at the double bond position between C15–C16 to produce the intermediate molecule 15,16-dihydrobiliverdin (DHBV). BV is centered in the active site of PebA with the A- and D-ring located inwardly of the enzyme's binding pocket and the propionate side chains pointing towards the protein's outside. In the past the PebA structure was solved and compared with the already known structure of PebS. Here, several important amino acids for the catalysis have been identified since they are highly conserved in both enzymes.An important role in BV reduction plays the amino acid residue Asp84 (D84) which seems to stabilize the enzyme-substrate complex. An enzyme variant PebA_D84N was not able to convert BV to DHBV but rather seemed to stabilize the newly formed radical

intermediate. Another conserved amino acid residue is the Asp105 (D105) which is believed to be the initial proton donor for BV reduction. An exchange to D105N leads to the accumulation of BV radical intermediates. This aspartate is located on the proximal β-sheet in the active site of PebA (Fig 1.10). In contrast, the Asp205 (D205), which is an important catalytic amino acid residue in PebS, is rotated away from the substrate and is therefore not involved in any catalytic role in PebA. It rather seems to have an influence on the coordination of the resulting product 15,16-DHBV (Busch *et al.*, 2011a; Busch *et al.*, 2011b).

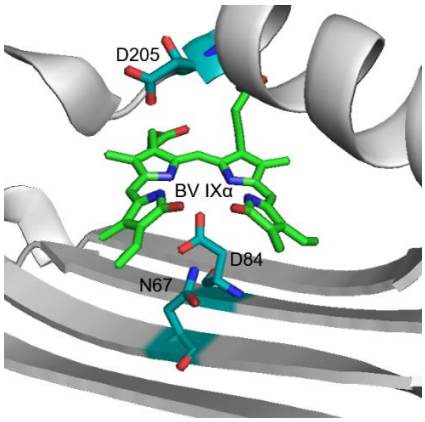

Figure 1.10: Overview of important catalytic amino acids residues of PebA.

The substrate BV is bound in the active site of PebA with the A- and D-ring oriented into the enzyme's binding pocket. The close-up view into the active site shows three important amino acid (N67, D84 and D205) residues which are important for BV reduction and stabilization of the enzyme-substrate complex. BV is shown as green sticks, the amino acids in teal sticks. The active site of PebA is shown in grey color. (*Synechococcus sp.* WH8020 PebA, 2X9O, (Busch *et al.*, 2011a).

When the PebA reaction is finished DHBV is then the substrate of the subsequently following enzyme PEB:ferredoxin oxidoreductase (PebB, EC: 1.3.7.3), which reduces the 2,3,3^1,3^2-diene system of the A-ring of the tetrapyrrole and the final product PEB is formed (Fig. 1.8). Since until now no crystal structure of PebB is solved, the reaction mechanisms can only be hypothesized. It is believed that the overall structure is similar to the previously solved FDBRs so the reaction mechanism is most likely similar to PebA or PebS with the difference that PebB possesses a strict substrate specificity to DHBV. This enzyme is not able to use BV IXα as a substrate. The protonated binding pocket of PebB binds DHBV the same way PebA binds BV IXα and elevates the substrate for the additional protonation steps (Busch *et al.*, 2011a). The electrons required for this reduction step are provided by ferredoxin and each reduction step requires two electrons (Dammeyer and Frankenberg-Dinkel, 2006). Recent studies revealed two alternative PEB biosynthesis pathways. One known from the cyanophage P-SSM2, a phage which infects cyanobacteria from *Prochlorococcus* species. This PEB-synthase (PebS, EC: 1.3.7.6) is able to perform the identical catalysis as the two-enzyme-system PebAB, which is established in cyanobacteria, as a single enzyme (Fig. 1.8). During infection the *pebS* gene is highly expressed to maintain the energy conservation of the host.

The second newly discovered PEB biosynthesis pathway also originates from phages but shows some differences to the PebS enzyme. This FDBR member PEB:ferredoxin oxidoreductase (BV), named PcyX (EC: 1.3.7.6), was found in metagenomics datasets during the “Global Ocean Sampling Expedition” (GOS) clustered with genes for heme oxygenases. Its suggested origin is believed to come from the group of α-proteobacteria, therefore a PEB biosynthesis in these organisms could be important for phytochrome assembly. Like PebS, PcyX belongs also to the group of four-electron using FDBRs. Interestingly, the reaction mechanism is more similar to PcyA but yields the same product and intermediate as PebS (DHBV & PEB) (Ledermann *et al.*, 2016). This is an interesting example of how different reaction mechanisms can result in a formally identical reaction (Fig 1.8).

1.5. The metabolic channeling of DHBV during PEB formation

In the marine cyanobacteria *Synechococcus sp.* WH8020 the genes *pebA* and *pebB* are located in an operon. Additionally, to these two genes this operon also contains the *cpeS* gene, which encodes for the PEB specific S-type lyase CpeS (Frankenberg *et al.*, 2001). Expression of this tricistronic operon leads not only to the cooperation of the two FDBRs but also to the lyase mediated attachment of PEB to the corresponding phycoerythrin. During chromatic acclimation a rapid switch to green-light absorbance is ensured. Interestingly, the FDBR genes *pebA* and *pebB* share an overlapping region of four nucleotides and their co-localization is the first hint of a common biosynthesis pathway. In our previous studies we postulated a metabolic channeling of the intermediate DHBV during PEB biosynthesis because both enzymes are required to yield the final product. Another hint of substrate channeling was the instability of the intermediate DHBV when it is not bound to protein. A direct channeling would ensure the stability of this molecule. It was also suggested that PebB seems to play an important role in taking over the DHBV from PebA because of the low substrate concentration *in vivo* (Dammeyer and Frankenberg-Dinkel, 2006). There are several types of protein-protein interaction known within a biosynthetic pathway. The process of a direct transfer of an intermediate between two enzymes involved in a pathway is called substrate (or metabolic) channeling. The channeling of an intermediate between two or more catalytic enzymes has several advantages during the whole process. The intermediate is prevented from loss by diffusion or in case of lability a direct channel can stabilize the product from the solvent (Ovadi, 1991). Furthermore, a correctly transfer of the intermediate is ensured to prevent side reaction on or within the molecule as well as the correct loading of a substrate is crucial for a proper conversion. For example, the δ-regio-specific heme oxygenase HemO from *Pseudomonads* is also able to cleave the heme at the β-position, but it is suggested to be an artificial product since the yield of biliverdin IXβ is much lower (Gisk *et al.*, 2012). The correct positioning of the substrate heme mediated by a metabolic channeling

process prevents this side reaction *in vivo*. *In vitro*, heme is added to the purified heme oxygenase and therefore the molecule can enter the active site of the HO in either orientation. The substrate channel can occur in three different ways – the direct channel, the proximity channeling or the enzyme clustering (Fig. 1.10) (Castellana *et al.*, 2014). During the direct channel of an intermediate from enzyme 1 (E_1) to enzyme 2 (E_2) both interaction partners come into physical contact to form a tunnel. The intermediate is funneled between both enzymes and is then further processed to the product (Fig. 1.10 a). In bacteria, an example of such an interaction is known from the tryptophane synthase of *Salmonella typhimurium* (Hyde *et al.*, 1988). Here, the *α*- and *β*- subunits of the tryptophane synthase are separate proteins that physically interact and form a tunnel between the active sites (Rhee *et al.*, 1998). An alternative channeling mechanism is called proximity channeling where two involved enzymes (E_1 and E_2) are positioned very close to each other to transfer the intermediate (Fig. 1.10 b). This can happen either by a high affinity to the interaction partner or the intermediate and forestalls the escape of the intermediate by diffusion (Bauler *et al.*, 2010). Interestingly, this kind of transfer is improved when the involved enzymes are colocalized on synthetic protein scaffolds (Dueber *et al.*, 2009; Lee *et al.*, 2012).

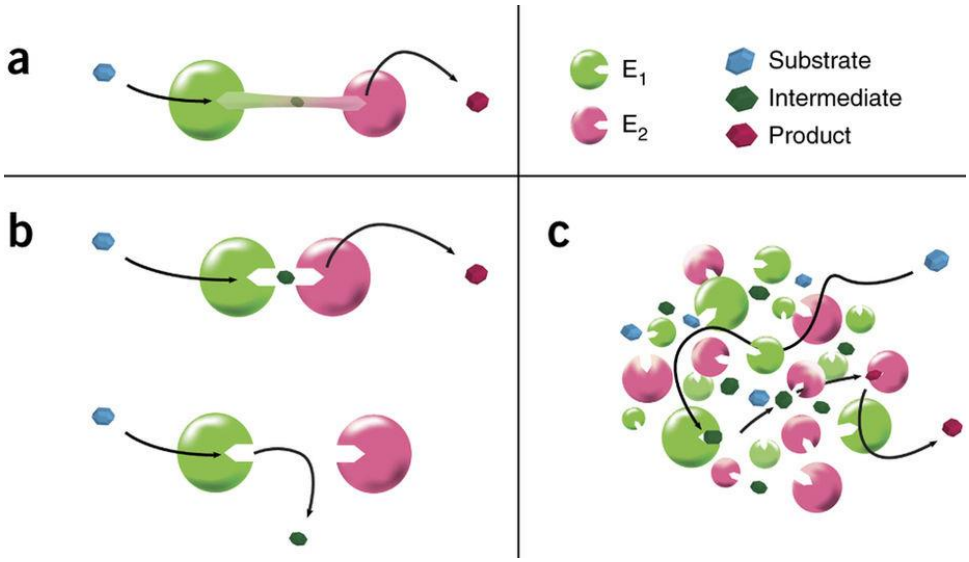

Figure 1.11: Different types of substrate channeling.

(a) *Direct channeling:* E_1 and E_2 physically interact to transfer the substrate via a tunnel formation before the product is released. **(b)** *Proximity channeling:* E_1 and E_2 come close to each other so the intermediate is channeled by diffusion before it is released to the bulk solvent. **(c)** *Enzyme clustering:* E_1 produces the intermediate and releases it to the environment. The chance of further processing of the intermediate is low, but it becomes higher if the subsequent following enzyme E_2 forms agglomerates (Castellana *et al.*, 2014). E_1 = enzyme 1, E_2 = enzyme 2.

The third transfer mechanism is mediated by a so-called enzyme clustering (Fig. 1.10 c). Here, the upstream enzyme E_1 produces the intermediate and releases it to the cytosol or a different environment. The probability of further processing is only high enough if the concentration of the downstream enzyme E_2 is high enough to form agglomerates.

Otherwise, the chance of product formation is rather low. Interestingly, this kind of enzyme clustering was found in several organisms. For example, in the baker's yeast *Saccharomyces cerevisiae* over 180 out of 800 GFP-tagged enzymes showed this form of clustering in the cytosol (Narayanaswamy *et al.*, 2009). Another example for such an enzyme clustering is the formation of carboxysomes in cyanobacteria forming bacterial microcompartments (BMCs). In these microcompartments the most abundant enzyme on earth, the ribulose 1,5-bisphopshate carboxylase/oxygenase (RuBisCO), and the carbonic anhydrase are localized (Shively *et al.*, 1973) which catalyze the carbon fixation in this mini organelle. During tetrapyrrole biosynthesis many examples of substrate transfers occur because the formation of such complex molecules is mediated by many enzymes involved in this process. But not every step is well researched in terms of transfer process. Recently discovered is the substrate channeling of two metabolites during the tricarboxylic acid cycle (TCA). Citrate and fumarate are directly channeled from citrate-synthase to aconitase respectively fumarate is directly channeled from succinate-dehydrogenase to fumarase (Zhang 2017). As a noteworthy example known from several bacteria like *E. coli*, *Rhodobacter capsulatus* or *Salmonella typhimurium*, the enzymes CobNST and CobH are involved in hydrogenobyrinic acid (HBA) formation, an intermediate molecule during the vitamin B_{12} pathway, also a molecule belonging to the tetrapyrroles (Roth *et al.*, 1993). Here, the substrate/intermediate HBA undergoes either a real channel or an enhanced transfer from CobH to CobNST which is caused by the higher affinity of the subsequent enzyme to its substrate (Deery *et al.*, 2012). A similar transfer was observed during the formation of 5-aminolevulinic acid (ALA), the precursor molecule for heme or chlorophyll biosynthesis. During this ubiquitous pathway ALA is made by the condensation of succinyl-CoA and glycine by the direct interaction of the involved enzymes, GluTR and GSAT. Both enzymes form a dimeric complex during their catalysis and a real substrate channel is facilitated (Richter and Grimm, 2013).

The given hints for protein-protein interaction during the PEB biosynthesis prefer the suggestion of a direct or a proximity channeling of the intermediate DHBV from PebA to PebB. The stability of DHBV is quite low when it is not bound to protein, which is known from earlier studies. Also, the transient interaction of both involved enzymes argues in favor of an at least close distance for the substrate transfer. The corresponding genes *pebA* and *pebB* are not only localized on the same gene cluster (Frankenberg *et al.*, 2001), but are also located in an operon and they are both involved in PEB biosynthesis (Dammeyer and Frankenberg-Dinkel, 2006). Since DHBV showed a low stability a rapid conversion to PEB is necessary and therefore a fast transfer is needed.

1.6 Objectives of this work

This work mainly focuses on the biosynthesis of the pink pigment phycoerythrobilin in the marine cyanobacteria *Synechoccocuss sp.* WH 8020. The cleavage of heme is the first step in phycoerythrobilin formation followed by two reduction steps performed by the cooperation of the two ferredoxin-dependent bilin reductases PebA and PebB. The intermediate molecule during phycoerythrobilin biosynthesis is 15,16-dihydrobiliverdin. In earlier studies, it was postulated that this intermediate is most likely transferred by means of a substrate channeling mechanism also called metabolic channeling (Dammeyer and Frankenberg-Dinkel, 2006). There are several hints for protein-protein interaction during the pigment biosynthesis and it is interesting to examine the postulated interaction in more detail with the aid of biochemical and spectroscopical methods. Furthermore, the binding affinities of PebA and PebB to their product/substrate 15,16-dihydrobiliverdin should be reevaluated with more sensitive techniques using microscale thermophoresis. The characterization of the already created gene fusion of *pebA* and *pebB* was also scheduled during this work. For this, the recombinantly production of PebAgB in *E. coli* will be performed and the produced protein will be characterized using the analytical methods established for FDBRs (Busch *et al.*, 2011a; Dammeyer and Frankenberg-Dinkel, 2006).

2 Materials and Methods

2.1 Chemicals and reagents

All chemicals and reagents used in this work were ACS grade or better unless stated otherwise. They were purchased from AppliChem (Darmstadt), Carl Roth (Karlsruhe), Merck (Darmstadt) and Sigma Aldrich (Munich). All FDBR assay chemicals were also purchased from Sigma-Aldrich except for BV, which was obtained from Frontier Scientific.

2.1.1 Equipment

Table 1: Used Instruments

Type of Instrument	Name	Manufacturer
Agarose gel electrophoresis	Com Phor L mini Com Phor L Midi	Biozym GmbH
Autoclave	VX 150	Systec GmbH
Blotting Equipment	Semidry Blot Trans-blot® SD	Bio-Rad Laboratories GmbH
Centrifuges	Centrifuge 5415D Centrifuge 5810R Z32HK Sorvall Lynx 6000	Eppendorf AG Hermle Labortechnik GmbH Thermo Fischer
Cell disruption	LM10 Microfluidizer	Microfluidics
Incubator Shaker	New Brunswick Innova® 44 Universal Shaker SM 30-control	Eppendorf AG Edmund Bühler GmbH
Fluorescence spectrometer	FP-8300 Monolith NT.115	Jasco Deutschland GmbH Nanotemper Technologies GmbH
FPLC	ÄktaPure	GE Healthcare
FPLC-columns	HiLoad™ 16/600 Superdex™ 75 pg GST-Trap FF 5 ml Strep-trap FF 5 ml Superdex 75 10/300 GL Superdex 200 10/300 GL	GE Healthcare
Gel documentation	GeliX20 Imager	Intas Science Imaging Instruments GmbH
HPLC	1100 series	Agilent Technologies
HPLC column	Luna 5 µm C18 (2) 100 Å, 250 x 4.6 mm	Phenomenex Inc.

pH meter	Basic pH Meter p-11	Sartorius AG
Photometers	8453 UV visible system	Agilent Technologies
	Nanodrop™ Lite	Thermo Scientific
	Novaspec III	Bio-Rad Laboratories GmbH
Pump	KNF LABOPORT® Series Laboratory Vacuum Pumps	KNF Neuberger Inc.
Power Supply	PowerPac 300	Bio-Rad Laboratories GmbH
Scales	AccuLab Research	Sartorius AG
SDS-PAGE	Mini-Protein® Tetra cell system	Bio-Rad Laboratories GmbH
Shaker	MR Hei-Standard	Heidolph Instruments GmbH & Co. KG
Thermocycler	T1 Thermocycler	Biometra GmbH
Ultrasonic homogenizer	UW 2200 with tip KE 76	Bandelin GmbH & Co. KG
Ultra-pure water system	MilliQ® Integral Water Purification System	Merck KGaA
Vortexer	Vortex Shaker	VWR International GmbH

2.1.2 Enzymes, kits, antibodies and special chemicals

Table 2: Special Chemicals and materials

Product	**Name**	**Manufacturer**
Column material for affinity chromatography	Protino® Glutathione Agarose 4B	Macherey - Nagel GmbH & Co. KG
	Strep-Tactin® Sepharose®	IBA Lifesciences GmbH
Concentrator	Vivaspin 6 10.000 MWCO	Sartorius AG
	Vivaspin 6 50.000 MWCO	
Dialysis tubular membranes	Visking MWCo 10.000	Carl Roth GmbH
DNA loading dye	DNA Gel Loading Dye (6x)	Thermo Scientific
DNA stains	GelRed®	Biotium Inc.
Fluorescence capillaries	Monolith NT.115 Capillaries	Nanotemper Technologies GmbH
HPLC sample filter	Phenex™ Teflon® (PTFE) Filter Membranes, 0.45um	Phenomenex Inc.
Protein standards	PageRuler™ Prestained Protein Ladder	Thermo Scientific

Protein labeling kit	Monolith Protein Labeling Kit RED-NHS (Amine Reactive) Monolith Protein Labeling Kit BLUE-NHS (Amine Reactive)	Nanotemper Technologies GmbH
PVDF membrane	Roti®-PVDF-Membrane	Carl Roth
Solid phase sample extraction	Sep-Pak C18 Plus Light Cartridge	Waters Corporation
Sterile filter	Rotilabo® 0.20 µm Rotilabo® 0.45 µm	Carl Roth

Table 3: Enzyme and kits

Product	Name	Manufacturer
DNase I		Applichem
DNA ligase	T4-DNA Ligase	Thermo Scientific
DNA polymerase	Phusion High-Fidelity DNA polymerase Pfu DNA polymerase, recombinant	Thermo Scientific
Gibson Assembly®	HiFi DNA Assembly Cloning Kit	New England Biolabs Inc.
Lysozyme	Lysozyme	Carl Roth
PCR clean-up kit	NucleoSpin® Gel and PCR Clean-up	Macherey - Nagel GmbH & Co. KG
Plasmid miniprep kit	NucleoSpin® Plasmid EasyPure	Macherey - Nagel GmbH & Co. KG
Protease	PreScission Protease	GE Healthcare
Restriction endonucleases	FastDigest restriction endonucleases High Fidelity restriction endonucleases	Thermo Scientific New England Biolabs Inc.

Table 4: Antibodies

Antibody	Antigen	Manufacturer
6x-His Tag Monoclonal Antibody (1:3.000)	*his*-tag	Thermo Scientific
Goat anti-GST antibody (1:10.000)	GST-tag	Pharmacia Biotech
Rabbit anti-goat IgG alkaline phosphatase (1:30.000)	Goat IgG	Immuno research
Strep-Tactin® AP conjugate (1:4.000)	Strep-tag	IBA Lifesciences GmbH

2.1.3 Microbial strains

All cloning steps were conducted in *E. coli* JM83 or *E. coli* DH5α unless otherwise stated. The heterologous protein production was performed in *E. coli* BL21 (DE3). The bacterial two-hybrid system was employed in *E. coli* BTH101 and *E. coli* JM109.

Table 5: Microbial strains

***E. coli* strain**	**Genotype**	**Reference**
E. coli BL21 (DE3)	F⁻ *ompT gal dcm lon hsdS$_B$*($r_B^-m_B^-$) λ(DE3 [*lacI lacUV5-T7p07 ind1 sam7 nin5*]) [*malB*$^+$]$_{K-12}$(λ^S)	(Studier and Moffatt, 1986)
E. coli BTH101	F-, *cya-99*, *araD139, galE15, galK16, rpsL1 (Str r)*, *hsdR2, mcrA1, mcrB1*	(Karimova *et al.*, 1998)
E. coli DH5α	F$^-$ endA1 glnV44 thi-1 recA1 relA1 gyrA96 deoR nupG Φ80d*lacZ*ΔM15 Δ(*lacZYA-argF*)U169, hsdR17(r_{K^-} m_K^+), λ–	(Sambrook *et al.*, 1989)
E. coli JM83	F⁻ *ara Δ(lac-proAB) rpsL* (Str^R)*[φ80 dlacΔ(lacZ)M15] thi*	(Vieira and Messing, 1982)
E. coli JM109	endA1 glnV44 thi-1 relA1 gyrA96 recA1 mcrB$^+$ Δ(lac-proAB) e14- [F' traD36 proAB$^+$ lacI^q lacZΔM15] hsdR17($r_{K^-}m_K^+$)	(Yanisch-Perron *et al.*, 1985)

2.1.4 Plasmids

All plasmids used in this study were constructed by ligating an amplified and appropriately digested PCR product into the vector of interest. The cloning was confirmed by DNA sequencing of the constructed plasmids (GATC-Biotech AG).

Table 6: Plasmids

Plasmids	**Description**	**Tag**	**Origin**
pACYC_Duet-1	Duet vector with two MCS designed for co-expression of two target genes; Cm^R, T7-promoter	*His$_6$*-tag S-tag	Novagen
pACYC_pebAB_*ho 1*6803	pACYC-derivate, encoding *ho1* from *Synechocystis sp.* PCC6803 and *pebAB* from *Synechococcus sp.* WH8020	N-*Strep*-tagII-*pebA* C-*His$_6$-pebB* C-*S-ho1*	This study

pACYC_pebAB_*ho 1*-P-SSM2	pACYC-derivate, encoding *ho1* from cyanophage P-SSM2 and *pebAB* from *Synechococcus sp.* WH8020	N-*Strep*-tagII-*pebA* C-*His*$_6$-*pebB* C-*S*-*ho1*	This study
pASK-IBA45$^+$	Expression vector, *tet*-promoter, amp^R	N-*Strep*-tag II C-*His*$_6$-tag	IBA Lifesciences GmbH
pASK-IBA45$^+$-*pebA*	pASK-IBA45$^+$-derivate; *pebA* from *Synechococcus sp.* WH8020	N-*Strep*-tag II	This study
pASK-IBA45$^+$-*pebB*	pASK-IBA45$^+$-derivate; *pebB* from *Synechococcus sp.* WH8020	C-*His*$_6$	This study
pASK-IBA45$^+$-*S*-*pebB*	pASK-IBA45$^+$-derivate; *pebB* from *Synechococcus sp.* WH8020	N-*Strep*-tag II	This study
pASK-IBA45$^+$-*pebAgB*	pASK-IBA45$^+$-derivate; *pebAB* from *Synechococcus sp.* WH8020	N-*Strep*-tagII-*pebA* C-*His*$_6$-*pebB*	Master thesis Maximilian Klosowski
pASK-IBA45$^+$-*pebAgB*	pASK-IBA45$^+$-derivate; *pebAgB* from *Synechococcus sp.* WH8020	N-Strep-tag II C-*His*$_6$	Master thesis Maximilian Klosowski
pGro7	pACYC-derivate; encodes for *groES* and *groEL*, araB promoter; Cm^R		Takara Clontech Inc.
pGEX-6P-1	Expression vector, *tac*-promoter, *amp*^{R}	N-GST-tag	GE Healthcare
pGEX-6P-1_*pebA*	pGEX-6P-1-derivate; *pebA* from *Synechococcus sp.* WH8020	N-GST	Frankenberg and Lagarias, 2003
pGEX-6P-1_*pebB*	pGEX-6P-1-derivate; *pebB* from *Synechococcus sp.* WH8020	N-GST	Frankenberg and Lagarias, 2003
pGEX-6P-3_*pebS*	pGEX-6P-1-derivate; *pebS* from cyanophage P-SSM2	N-GST	Dammeyer et. al, 2008
pGEX-6P-1_*pebAgB*	pGEX-6P-1-derivate; *pebAgB* from *Synechococcus sp.* WH8020	N-GST	This study
pGEX-6P-1_*pcyA*	pGEX-6P-1-derivate; *pcyA* from *Anabaena sp.* PCC7120	N-GST	Frankenberg and Lagarias, 2003
pKD13	Template plasmid for gene disruption, *amp*^{R}; *FRT*-sites flanking a *kan*^{R}-cassette		Datsenko *et al.*, 2000

pKD46	Lambda Red recombinase expression plasmid; *amp*^{R}; encodes for *gam*, *beta* and *exo* from Phage λ, *araC*-promoter		(Datsenko and Wanner, 2000)
pKT25	Bacterial-Two-Hybrid vector; N-terminal T25 fragment of adenylate cyclase, *kan*^{R}; *lac*-promoter		(Karimova *et al.*, 1998)
pKT_*pebA*	pKT25-derivate; *pebA* from *Synechococcus sp.* WH8020	N-T25	This study
pKT_*pebB*	pKT25-derivate; *pebB* from *Synechococcus sp.* WH8020	N-T25	This study
pKT_*pcyA*	pKT25-derivate; *pcyA* from *Anabaena sp.* PCC7120	N-T25	This study
p25N	Bacterial-Two-Hybrid vector; C-terminal T25 fragment of adenylate cyclase, *kan*^{R}; *lac*-promoter	C-T25	
p25N_*pebA*	p25N-derivate; *pebA* from *Synechococcus sp.* WH8020	C-T25	This study
p25N_*pebB*	p25N-derivate; *pebB* from *Synechococcus sp.* WH8020	C-T25	This study
p25N_*pcyA*	p25N-derivate; *pcyA* from *Anabaena sp.* PCC7120	C-T25	This study
pUT18	Bacterial-Two-Hybrid vector; C-terminal T18 fragment of adenylate cyclase, *amp*^{R}; *lac*-promoter		
pUT18_*pebA*	pUT18-derivate; *pebA* from *Synechococcus sp.* WH8020	C-T18	This study
pUT18_*pebB*	pUT18-derivate; *pebB* from *Synechococcus sp.* WH8020	C-T18	This study
pUT18_*pcyA*	pUT18-derivate; *pcyA* from *Anabaena sp.* PCC7120	C-T18	This study
pUT18C	Bacterial-Two-Hybrid vector; N-terminal T18 fragment of adenylate cyclase, *amp*^{R}; *lac*-promoter		
pUT18C_*pebA*	pUT18C-derivate; *pebA* from *Synechococcus sp.* WH8020	N-T18	This study
pUT18C_*pebB*	pUT18C-derivate; *pebB* from *Synechococcus sp.* WH8020	N-T18	This study
pUT18C_*pcyA*	pUT18C-derivate; *pcyA* from *Anabaena sp.* PCC7120	N-T18	This study

pYPRUB168	pUC_Sma_only Derivat, *amp*^{r}	
pUC_*ho1_kan*	pYPRUB168_derivate; integration cassette *frt-ho1-kan-frt; ho1* from *Synechocystis sp.* PCC6803	This study
pUC_*ho1_pebS_kan*	pUC_*ho1_kan* _derivate; integration cassette *frt-ho1-pebS_kan-frt*; *pebS* from cyanophage P-SSM2	This study
pUC_*ho1_pcyA_kan*	pUC_*ho1_kan* _derivate; integration cassette *frt-ho1-pcyA_kan-frt*; *pcyA* from *Anabaena sp.* PCC7120	This study

2.1.5 Oligonucleotides

The primer used in this study were all synthesized by Eurofins Genomics GmbH.

Table 7: Oligonucleotides

No.	Name	Sequence 5‘ – 3‘	Constructed plasmid
1	S-PebB_EcoRI_fw	CGT GAA TTC CAT GAC AAA TCA AAG ATT CAA AAG C	pASK-IBA45$^+$-*S-pebB*
2	S-PebB_XhoI_rv	GCT CTC GAG TTA TAG ATC AAA AAG CAC AG	pASK-IBA45$^+$-*S-pebB*
3	pebABSacI_fw	GCG AGC TCA TGG CTA GCT GGA G	pACYC_pebAB_*ho1*6803 pACYC_pebAB_*ho1*-P-SSM2
4	pebAbNotI_rev	CGC GGC CGC TTA GTG ATG GTG AT	pACYC_pebAB_*ho1*6803 pACYC_pebAB_*ho1*-P-SSM2
5	pebA_pUT18_fwd	GCG GTA CCA TGT TTG ATT CAT TTC TC	pUT18_*pebA*
6	pebA-pUT18-rev	GCG AAT TCG CTT TGT GAG AGG AGG A	pUT18_*pebA*
7	pebA_pUT18C_fwd	GCG GTA CCG ATG TTT GAT TCA TTT CT	pUT18C_*pebA*
8	pebA-pUT18C-rev	GCG AAT TCT TTG TGA GAG GAG GAG G	pUT18C_*pebA*
9	pebB_pUT18_fwd	GCT CTA GAA TGA CAA ATC AAA GAT TC	pUT18_*pebB*
10	pebB-pUT18-rev	GCG GTA CCG CTA GAT CAA AAA GCA C	pUT18_*pebB*
11	pebB_pUT18C_fwd	GCT CTA GAG ATG ACA AAT CAA AGA T	pUT18C_*pebB*
12	pebB-pUT18C-rev	GCG GTA CCT AGA TCA AAA AGC ACA G	pUT18C_*pebB*
13	pebA_pKT25_fwd	GCG GTA CCG ATG TTT GAT TCA TTT CT	pKT_*pebA*

14	pebA_pKT25_rev	GCG AAT TCT TTG TGA GAG GAG GAG GC	pKT_*pebA*
15	pebA_p25N_fwd	GCG GTA CCA TGT TTG ATT CAT TTC TC	p25N_*pebA*
16	pebA_p25N_rev	GC GAA TTC GCT TTG TGA GAG GAG GAG	p25N_*pebA*
17	pebB_pKT25_fwd	GCT CTA GAG ATG ACA AAT CAA AGA TT	pKT_*pebB*
18	pebB_pKT25_rev	GCG GTA CCT AGA TCA AAA AGC ACA GT	pKT_*pebB*
19	pebB_p25N_fwd	GCT CTA GAA TGA CAA ATC AAA GAT TC	p25N_*pebB*
20	pebB_p25N_rev	GCG GTA CCG CTA GAT CAA AAA GCA CA	p25N_*pebB*
21	pcyA_ATG_fwd	GCG GTA CCA TGA TCT CAC TTA CTT CCA	pUT18_*pcyA*
22	pcyA_ATG_rev	GCG AAT TCG CTT CTG GG AGA TCA AAT A	pUT18_*pcyA*
23	pcyA_stop_fwd	GCG GTA ACG ATG ATC TCA CTT ACT TCC	pKT_*pcyA*
24	pcyA_stop_rev	GCG AAT TCT TAT TCT GGG AGA TCA AAT	pKT_*pcyA*
25	Ho1_6803_fwd	ATG AGT GTC AAC TTA GCT TCC CAG TTG CGG	pUC_*ho1_kan*
26	Ho1_6803_rv_rbs	ATG GAT CCA T*TC CTC* TTT AAC TAG CCT TCG GAG GTG GC	pUC_*ho1_kan*
27	Kan_frt_fwd	ATG GAT CCG AAT TCC TGC AGT TCG AAG TTC CTA	pUC_*ho1_kan*
28	Kan_frt_rev	GCG ATT GTG TAG GCT GGA GCT GCT TC	pUC_*ho1_kan*
29	pcyAPCC7120_fwd_NEB	GTT AAA GAG GAA TGG ATC CGA TGT CAC TTA CTT CCA TTC	pUC_*ho1_pcyA_kan*
30	pcyAPCC7120_rev_NEB	TAG GAA CTT CGA ACT GCA GGT TAT TCT GGG AGA TCA AAT AAC	pUC_*ho1_pcyA_kan*
31	pebS_fwd_NEB	GTT AAA GAG GAA TGG ATC CGA TGA CTA AAA ACC CAA GAA ATA AC	pUC_*ho1_pebS_kan*
32	pebS_rev_NEB	TAG GAA CTT CGA ACT GCA GGT CAT TTG TAT GAA AAA AGG AAA TC	pUC_*ho1_pebS_kan*
33	LacZ_ho1kan_fwd	GCT CGT ATG TTG TGT GAA ATT GTG AGC GGA TAA CAA TTT CAC ACA GGA AAC AGC TAT GAG TGT CAA CTT AGC TTC	Construction of BL21_*ho1_kan_frt*

34	LacZ_ho1kan_rev	GCC CGG TTA TTA TTA TTT TTG ACA CCA GAC CAA CTG GTA ATG GTA GCG ACC GGC GGC GAT TGT GTA GGC TGG AGC	Construction of BL21_ho1_kan_frt
35	Ho1_intern_rev	CTG CAG GAA TTC GGA TCC ATT CCT	Strain screening
36	Kan_intern_fwd	AGG AAT GGA TCC GAA TTC CTG CAG	Strain screening
37	lacZ_fwdneu	TTC CGG CTC GTA TGT TGT GTG	Strain screening
38	lacZ_revneu	CGG GAA GTA GGC TCC CAT GAT	Strain screening

2.2 Microbial methods

2.2.1 Sterilization

All buffers and media used for cell cultivation were sterilized ahead of use for at least 15 minutes with 121 °C and 1 bar by autoclaving. Heat sensitive supplements were sterilized by filtration with a pore size of 0.2 µm and added after media sterilization.

2.2.2 Media and supplements

Liquid cultures of *E. coli* were grown in Luria Bertani (LB) or in 2YT medium with the appropriate antibiotics and supplements. In order to prepare solid media for the cultivation of *E. coli* 1.5 % Agar-Agar was added to the media prior to the media sterilization (Sambrook, 2001).

LB-medium		2YT-medium	
NaCl	10 g/l	NaCl	5 g/l
Tryptone	5 g/l	Tryptone	16 g/l
Yeast extract	5 g/l	Yeast extract	10 g/l

Supplements were added to the media prior to the inoculation with *E. coli* strains or before induction, when the cells reached the desired optical density (OD).

Table 8: Media supplements

Supplement	Stock concentration	Final concentration
Anhydrotetracycline (AHT)	2 mg/ml	200 µg/ml
Ampicillin (Amp)	100 mg/ml	100 µg/ml
L-Arabinose	100 mg/ml	0.5 mg/ml
Chloramphenicol (Cm)	34 mg/ml	34 µg/ml
Isopropyl-β-D-thiogalactopyranosid (IPTG)	1 M	0.25 – 0.5 mM
Kanamycin (Kan)	50 mg/ml	50 µg/ml
X-Gal	100 mg/ml	80 µg/ml

2.2.3 Cultivation of *E. coli* cells

To prepare a starter culture of *E. coli* cells an appropriate volume of LB media was supplemented with the respective antibiotic (see table 8) and inoculated with a single colony from a freshly transformed *E. coli* plate or with a sterile loop from a glycerol stock. The starter – culture was incubated over night with constant shaking at 37 °C and 180 rpm (SM30 Control, Edmund Bühler; Innova®44 New Brunswick, Eppendorf). The main culture was prepared by inoculating LB- or 2YT media containing the appropriate supplement with 1:100 dilution of a starter – culture. Then the main culture was incubated at 37 °C and 100 rpm (Innova®44 New Brunswick, Eppendorf) until an OD_{578} ~ 0.5 – 0.8 was reached. The cell density was determined by extracting 1 ml of cells followed by a photometrical measurement of the OD at 578 nm. The cultivation media was used as the reference sample. The Induction of gene expression was conducted after the incubator reached 17 °C for overnight incubation of the main culture at 100 rpm (Innova®44 New Brunswick, Eppendorf).

2.2.4 Preparation of chemically competent *E. coli* cells

An overnight culture of *E. coli* strains was inoculated with a dilution of 1:00 in 100 ml LB media and cultivated until an OD_{578} = 0.5 was reached. After sedimentation by centrifugation at 4000 rpm and 4 °C (Centrifuge 5415D, Eppendorf) the cells were then re-suspended in 50 ml $CaCl_2$-buffer and incubated for 1 h on ice. Then another centrifugation step was conducted and the sedimented cell were then re-suspended in 5 ml 50 mM $CaCl_2$/15 %-glycerol. Aliquots of 200 µl in reaction tubes were then stored at -80 °C.

2.2.5 Preparation of electro-competent *E. coli* cells

An overnight culture of *E. coli* strains was inoculated 1:00 in 100 ml LB media and cultivated until an OD_{578} = 0.5 was reached. The cells were collected by centrifugation at 4000 rpm and 4 °C (Centrifuge 5415D, Eppendorf) the cells were then washed three times with 50 ml ice-cold H_2O. Then the cells were again collected by centrifugation and re-suspended in ice-cold H_2O/10 %-glycerol. Aliquots of 50 µl in reaction tubes were then stored at -80 °C.

2.2.6 Transformation of chemically competent *E. coli* cells

To chemically competent *E. coli* cells, 1 µl of plasmid DNA or 10 µl of ligation product was added and the cells were then incubated for 30 min on ice. Afterwards, the cells were heat shocked for 90s and allowed to recover on ice for another 2 min. After the addition of 700 µl LB media the cells were incubated by shaking at 180 rpm and 37 °C (SM30 Control, Edmund Bühler) for 45 min followed by plating on agar plates containing the appropriate antibiotic. The petri dishes were then incubated over night at 37 °C.

2.2.7 Transformation of electro-competent *E. coli* cells

For the phage λ mediated gene disruption, electro-competent *E. coli* BL21 (DE3) cells were transferred to a precooled electroporation cuvette and 3 µl of linear integration DNA was added to the cells. After an electrostatic shock the cells were rapidly re-suspended with 1ml SOC media and incubated for 1-12 h at 180 rpm and 30 °C. After this regeneration phase the cells were plated on LB-media containing the appropriate antibiotic and incubated over night at 37 °C. The transformed plasmid DNA was removed by the cells after increase in cultivation temperature and cells with the newly integrated cassette were cultivated.

2.3 Molecular biological methods

2.3.1 Preparation of plasmid DNA

For the preparation of plasmid DNA from freshly transformed *E. coli* JM83 or *E. coli* DH5α cells single colonies of these cells were inoculated in 5 ml LB media containing the appropriate antibiotic and incubated over night at 37 °C and 180 rpm (SM30 Control, Edmund Bühler). The plasmid DNA was isolated by using the NucleoSpin® EasyPure Kit (Macherey-Nagel) according to the manufacturer's instructions.

2.3.2 Determination of the concentration of nucleic acids

Immediately after the isolation of nucleic acids the concentration was determined by measuring the absorbance of the DNA solution at 260 nm (NanoDrop™ Lite). The purity of the isolated nucleic acids was determined by the calculation of the ratio of the absorbance at 260 nm and 280 nm. For sufficiently pure double stranded DNA solution the absorption ratio is A_{260}/A_{280} is ~ 1.8 – 2.0.

2.3.3 Analysis of nucleic acids by agarose gel electrophoresis

Agarose gel electrophoresis of nucleic acids was performed to separate and identify DNA molecules according to their size (Aaij and Borst, 1972). Analytical approaches were set up by dissolving 1 % (w/v) of agarose in boiling 1x TAE buffer. For gel extraction of DNA fragments a concentration of 0.8 % (w/v) of agarose was used the same way. Once the solution was cooled down the DNA stain reagent GelRed™ was added to the liquid agarose and the whole solution was filled into prepared gel chambers. During the polymerization of the gel the DNA samples were prepared by adding 6x DNA loading dye (Thermo Fisher). The samples were then loaded into the wells of the gel and the separation of the DNA fragments was performed in 1x TAE buffer at a constant current of 100V.

TAE buffer (1x)	
Tris/acetate pH 8.0	40 mM
EDTA	1 mM

As a reference of size, the GeneRuler™ DNA ladder mix (Thermo Fisher) was used for comparison. After separation the DNA was visualized by the fluorescence ability of the DNA staining reagent at 312 nm using the gel document station (Intas). For gel extraction the desired fragment was cut out from the gel and prepared using the NucleoSpin® Gel and PCR Clean-up Kit (Macherey-Nagel) according to the manufacturer's instructions.

2.3.4 The polymerase chain reaction (PCR)

The specific amplification of DNA fragments which were used during this work were conducted by the polymerase chain reaction (Mullis and Faloona, 1987). For the amplification process the Phusion® High-Fidelity DNA Polymerase (Thermo Fisher) was used. For the analytical verification of newly generated *E. coli* strains the PCR was performed with *Pfu*-polymerase (Thermo Fisher). All generated PCR products were analyzed via agarose gel electrophoresis (see section 2.2.3). Amplified DNA fragments for cloning into plasmid were purified using the NucleoSpin® Gel and PCR Clean-up Kit (Macherey-Nagel) according to the manufacturer's instructions.

Table 9: PCR reaction with Phusion® High-Fidelity DNA polymerase (50 µl)

Component	Final concentration
Phusion® High-Fidelity DNA Polymerase	0.02 U/µl
5x HF Phusion Buffer	1x
10mM dNTPs	200 µM each
Primer forward	100 pmol
Primer reverse	100 pmol
Template DNA	5-10 ng
H_20	ad 50 µl

Table 10: Reaction step using Phusion® High-Fidelity DNA polymerase

Reaction step	Temperature	Time	
Initial Denaturation	98 °C	30 s	
Denaturation	98 °C	10 s	
Annealing	Primer specific	15 – 20 s	x 30 cycles
Elongation	72 °C	15 s / kb	
Final elongation	72 °C	5 min	

Table 11: PCR reaction with *Pfu*-DNA polymerase (50 µl)

Component	Final concentration
Pfu-DNA Polymerase	0.05 U/µl
10x *Pfu* Buffer with 20 mM $MgSO_4$	1x
10mM dNTPs	200 µM each
Primer forward	100 pmol
Primer reverse	100 pmol
Template DNA	5-10 ng
H_20	ad 50 µl

Table 12: Reaction step using *Pfu*-DNA polymerase

Reaction step	Temperature	Time	
Initial Denaturation	95 °C	3 min	
Denaturation	95 °C	30 s	
Annealing	Tm-5	30 s	x 30 cycles
Elongation	72 °C	2 min/kb	
Final elongation	72 °C	10 min	

2.3.5 Restriction Endonuclease digestion of nucleic acids

Digestion of plasmid DNA or PCR products was carried out by FastDigest restriction endonucleases (Thermo Fisher) in a total volume of 20 µl. The buffers and enzymes for the digestion were used as recommended by the manufacturer's instructions. After digestion the enzymes were thermally inactivated at 80 °C and in case of plasmid DNA the restriction process was validated by agarose gel electrophoresis (see section 2.2.3).

2.3.6 Ligation of DNA molecules

For conventional cloning, vector DNA and PCR products were digested with the appropriate restriction endonucleases (see section 2.2.5) and ligated using T4 DNA ligase (Thermo Scientific) in a volume of 20 µl according to the manufacturer's instructions. Vector to insert DNA of a 3:1 (insert:vector) was used as recommended and ligated for 30 min at room temperature. The ligation process was then thermally inactivated by incubating the solution at 65 °C for 10 min. Then, 10 µl of the ligation sample were transformed into *E. coli* JM83 resp. *E. coli* DH5α and plated on LB agar plates containing the appropriate antibiotic.

2.3.7 Gibson Assembly® of DNA molecules

As an alternative to the conventional cloning technique the Gibson Assembly® was used for efficient cloning where the conventional methods did not work. Gibson Assembly® employs a 5'- exonuclease, a 3'-extension and also a DNA-ligase activity in a single tube reaction (Gibson *et al.*, 2009). For this, the NEBuilder® Assembly Tool (http://nebuilder.neb.com/) was used to

design the primer and for the selection of the right restriction enzyme for the assembly. Target genes were then amplified using the primer generated this way and the designated vector was digested with the appropriate restriction enzyme. Both vector DNA and PCR product were prepared as described (see sections 2.2.4 & 2.2.5) and then used for the assembly using the Gibson Assembly Cloning Kit Manual (New England Biolabs) according to the manufacturer's instruction.

2.3.8 Construction and validation of expression plasmids

All expression vectors constructed during this work were assembled in an identical process. The genes for *pebA* and *pebB* (*Synechococcus sp.* WH8020), *pebAgB* (artificial gene fusion), *pebS* (cyanophage P-SSM2) or *pcyA* (*Anabaena sp.* PCC7120) were amplified as described (2.3.4) using the introduced restriction sites via the primers listed in Table 7. The amplified DNA fragments were then cloned conventionally (see section 2.3.5) or via Gibson Assembly® (see section 2.3.6) into the corresponding expression plasmids and then transformed into *E. coli* JM83 resp. *E. coli* DH5α cells (see section 2.2.7). The cells were then plated on selective LB agar media and transformed cells were then analyzed if the obtained plasmid was correctly assembled. For this, single colonies were picked and the plasmid DNA was isolated as described (see section 2.3.1) and linearized with restriction enzymes. These isolated plasmids were analyzed using agarose gel electrophoresis (see section 2.3.3) using the linearized empty vector as a reference for size. Samples with a shift in size indicating a successful ligation event were validated using DNA sequence analysis at MWG Eurofins (Ebersberg) or GATC Biotech (Konstanz). Correctly assembled expression vectors were then stored at -20 °C.

2.3.9 Site-directed mutagenesis and construction of a fusion protein

The previously constructed fusion protein played a big role during this work, so the construction of PebAgB is shortly reproduced in this chapter. From genomic DNA of *Synechococcus sp.* WH8020 only the overlapping genes *pebA* and *pebB* genes were amplified via PCR (see section 2.3.4) and ligated (see section 2.3.6) into the pASK-IBA45$^+$ (IBA Lifesciences GmbH) expression plasmid. This resulted in a 5'-*Strep*-tag being fused to *pebA* and *pebB* fused to a 3'-*His*$_6$-tag. For the insertion of a guanine base the QuikChange® Lightning Kit (Agilent) was used following the manufacturer's instructions. As a template the previously generated plasmid pASK-IBA45$^+$-pebAB was used (Masterthesis Max Klosowski). The sequence of the primer used for the site-directed mutagenesis (for clarity only the forward primer is shown; the reverse primer is complementary to the forward primer) is shown here:

5'– CCGCCTCCTCCTCTCACAAAGTGACAAATCAAAGATTCAAAAGC – 3'.

The site of mutation is shown underlined. Positive clones were checked via sequence analysis (MWG Biotech, Munich).

2.3.10 λ – Red recombineering – a phage mediated gene disruption

As a side project, an *E. coli* BL21 (DE3) strain with integrated genes for phycobilin synthesis was planned and conducted. For the introduction of new genes into *E. coli* this recombination system of the *E. coli* specific phage λ was used, which is capable of integrating genes into any chromosomal location. Using the *recET* recombinase system was described as a simple and reliable method for bacterial chromosomal gene integration (Albermann *et al.*, 2010).

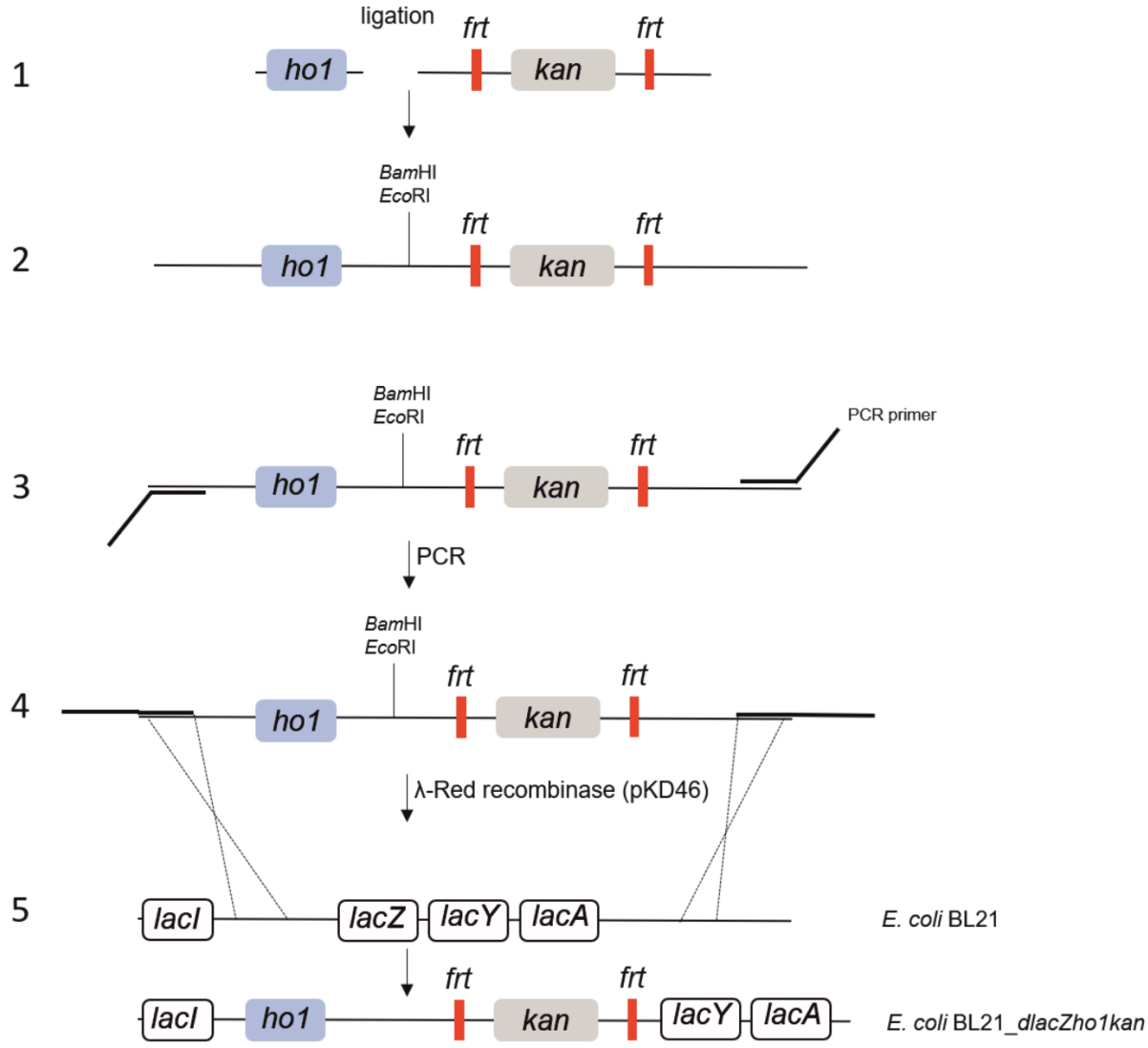

Figure 2.1: Integration strategy for the introduction of recombinant gene expression into chromosomal DNA of *E. coli* BL21 (DE3).

(1) Amplification and ligation of the genes ho1 from *Synechocystis sp.* PCC6803 and the selection marker *kan* flanked by *frt*-sites. **(2)** Linear ligation product with introduced mini MCS containing restriction sites for *Bam*HI and *Eco*RI. Via these restriction sites the genes for the FDBRs *pcyA* from *Anabaena sp.* PCC7002 and *pebS* from the cyanophage P-SSM2 should be integration into this position. **(3)** Amplification of integration cassette with primers containing homologues sequences of the target integration locus *lacZ*. **(4)** λ-Red recombination mediated by the already transformed expression plasmid pKD46. *(5)* The desired *E. coli* mutant strain *E. coli* BL21_*dlaczho1kan*. (modified after (Albermann *et al.*, 2010))

The introduction of genes for the cyanobacterial heme oxygenase *ho1* from *Synechocystis sp.* PCC6803 and the FDBRs *pcyA* from *Anabaena sp*. PCC7002 and *pebS* from cyanophage P-SSM2 were obtained and cloned together with the selection marker as described below into the pYBRUB168 vector for interim storage. The integration cassette should contain FRT-sites and a *kan*-gene as a selection marker. First, the assembly of the integration cassette *ho1-FRT-kan-FRT* was started with the amplification of the *ho1* and the *FRT-kan-FRT* cassette with the appropriate primer containing sequences for specific restriction sites (Step 1, Fig. 2.1). The primer also contained sequences for a mini multiple cloning site specific for *Bam*HI and *Eco*RI. After amplification both fragments were ligated as described (see section 2.3.6), the obtained integration cassette was purified from the agarose gel by gel purification. Afterwards, this ligation product was then cloned into pYBRUB168 via blunt end integration (Step 2, Fig. 2.1). Then, another amplification of this fragment was performed using special primers with homologues DNA sequences for the chromosomal integration locus *lacZ* (Step 3, Fig. 2.1). The advantage of using *lacZ* as the target of integration was the rapid analysis of mutants via the β-galactosidase activity (Step 4, Fig. 2.1). The linear integration cassette was then introduced into *E. coli* BL21_pKD46 via electroporation (see section 2.2.7). The already transformed vector pKD46 contained the genes *gam*, *beta* and *exo* from Phage λ which are responsible for the integration event. Since these genes were under the control of a p_{Bad}-promotor, 1 mM L-arabinose was added to the freshly transformed cells. After shaking for 1-12 h at 30 °C the cells were plated on LB agar containing kanamycin as the selective antibiotic and 50 µg/ml X-Gal for blue/white selection of mutant cells. Obtained mutants were then screened via PCR and sequence analysis (Step 5, Fig. 2.1).

2.4. Protein biochemical and analytical methods

2.4.1 Production of recombinant proteins in *E. coli* BL21 (DE3)

All recombinant proteins used during this study were produced heterologous in *E. coli* BL21 (DE3). For the production of GST-PebA, GST-PebB, GST-PebS and GST-PcyA the freshly transformed *E. coli* cells were grown in LB media containing the right antibiotic (see table 8). The production of Strep-PebA, Strep-PebB, Strep-PebAgB-His and GST-PebAgB was made in 2YT media since LB media yielded a lower amount of these proteins. The growing conditions for both types of media was identical. The main culture was set up as described (see section 2.2.3) and incubated at 37 °C and 100 rpm in Innova®44 New Brunswick (Eppendorf) until the OD_{578} reached 0.5 – 0.8. Right after a shift in temperature to 17 °C, the protein expression was induced with the appropriate inductor (IPTG for *lac*- or *tac*-promoter, L-Arabinose for p_{BAD}-promoter and AHT for *tet*-promoter; see table 8). For an optimal yield of GST-PebA and/or GST-PebB a co-expression of GroES and GroEL mediated by the pGro7 helper plasmid was performed. Therefore, the main culture was treated with L-Arabinose (see table 8) to induce

the chaperone expression prior to the protein expression. The cells were then incubated overnight at 17 °C with constant shaking at 100 rpm. The next morning the cells were harvested by centrifugation for 10min at 4 °C and 9.000 rpm (Sorvall Lynx™ 6000 Centrifuge) and transferred into 50 ml centrifuge tubes (Falcon™). The cells were either directly lysed for protein purification or stored at -20 °C.

2.4.2 Purification of recombinant proteins

Affinity chromatography of GST-tagged or Strep-tagged proteins using FPLC

Harvested cells containing GST-tagged proteins were re-suspended in 50-100 ml PBS buffer (137 mM NaCl, 2.7 mM KCl, 10 mM Na_2HPO4, 1.8 mM KH_2PO_4, pH 7.4) and 1 mg / ml of each lysozyme and DNAse I (Applichem) was added to the re-suspended cells. Cell disruption was conducted by passage through a microfluidizer cell disruption system (Microfluidics Corporation) at 15.000 psi. This process was repeated twice under iced conditions. Then the cell debris were sedimented by centrifugation for 1h at 19.000 rpm and 4 °C (Sorvall™ LYNX™ 6000 centrifuge, rotor T29-8) and the supernatant was filtered with 0.45 µM RC syringe filters (Carl Roth) for the following affinity chromatography.

The cells containing the Strep-tagged proteins were lysed the identical way as described above, but only the lysis buffer was exchanged to Buffer W (150 mM NaCl, 100 mM Tris/HCl, 1 mM EDTA, pH 8.0) according to the manufacturer's instruction. Filtered lysate was loaded on a 5 ml GST-trap FF column resp. 5 ml Strep-trap FF column and affinity chromatography was performed according to the manufacturer's instructions (GE Healthcare, Äkta Pure). The flow rates of the equilibration (10 CV), washing (10 CV) and elution steps of the columns was set to 5 ml / min. The samples were loaded at a lower flow rate of 1 ml / min from a 150 ml superloop. The proteins were eluted with 6 CV of the appropriate elution buffer (see below). Fractions with GST-tagged proteins were pooled and used for PreScission Protease cleavage (2 Units / mg protein) for tag removal in cleavage buffer overnight. On the next day the protein solution was loaded on a 5 ml GST-trap FF column to separate the tag from the protein by using the manufacturer's instructions (GE Healthcare ÄktaPure) and then verified via SDS-PAGE. For "on-column" experiments the GST-tag of PebA and/or PebB was not removed. After successful verification the proteins were dialyzed against the desired buffer over night at 4 °C for further analysis. For Strep-tagged proteins the dialysis was set up immediately after the purification against the desired buffer over night at 4 °C. After dialysis the proteins were then concentrated using Vivaspin® 6 concentrator with a molecular weight cut off of 10.000 Da or 50.000 Da according to the size of the proteins.

Affinity chromatography of His-tagged proteins

Harvested cells containing His-tagged PebB were re-suspended in lysis buffer (see below) and 1 mg/ml of each lysozyme and DNAse I (Applichem) was added to the re-suspended cells. The cell disruption process was identical as described above. After lysis, the cells were centrifuged to remove cell debris and the supernatant was filtered afterwards through a 0.45 µm RC syringe filter (Carl Roth). For affinity chromatography, a 5 ml column of TALON® column material was prepared by removing the storage buffer with 10 CV of H_2O and equilibration with 10 CV of 20 mM Na_3PO_4 buffer (binding buffer without imidazole). After equilibration the lysate was loaded onto the column and migrated through the column by gravity flow. Immediately after the lysate passed through the column was washed with 10 CV of 20 mM Na_3PO_4 and afterwards again with 10 CV of Na_3PO_4, 50 mM imidazole (binding buffer) to remove unspecific bound proteins from the column. The target His6-tagged protein was eluted with 3 CV of 60 mM Na_3PO_4, 200 mM imidazole (His-tag elution buffer) and fractions of 1 ml each were collected and analyzed via SDS-Page. Protein containing fractions were pooled and dialyzed against the desired buffer over night at 4 °C. After buffer exchange the protein was concentrated using Vivaspin® 6 concentrator with a molecular weight cut off of 10.000 Da.

Buffers used for affinity chromatography:

10x PBS buffer, pH 7.4	
NaCl	1.4 M
KCl	27 mM
Na_2HPO_4	100 mM
KH_2PO_4	18 mM

GST-elution buffer	
Tris/HCl, pH 8.0	50 mM
red. glutathione	10 mM

Buffer W	
Tris/HCl	100 mM
NaCl	150 mM
EDTA	1 mM

Buffer E
Buffer W + 2.5 mM desthiobiotin

PreScission Protease cleavage buffer	
Tris/HCl, pH 7.5	50 mM
NaCl	150 mM
EDTA	1 mM
DTT	1 mM

Binding buffer	
Na_2HPO_4/NaH_2PO_4	20 mM
Imidazole	50 mM
NaCl	300 mM

Lysis buffer	
Tris/HCl, pH 7.5	50 mM
NaCl	300 mM
Glycerin	10 % (v/v)

His-tag elution buffer
Binding buffer + 150 mM Imidazole

Purified proteins were further purified from impurities using gel filtration (see section 2.4.6) and a following concentration step as described above was carried out.

2.4.3 SDS-polyacrylamide gel electrophoresis (SDS-PAGE)

Synthesized proteins were analyzed using SDS-polyacrylamide gel electrophoresis (SDS-PAGE) by separation according to their molecular weight. The separation of the proteins was conducted in a discontinuous system (Laemmli, 1970) which consisted of a stacking gel (pH 6.8) with an acrylamide concentration of 5.25 % and a separation gel (pH 8.8) with an acrylamide concentration of 12.5 %. Sodium dodecyl sulfate (SDS is a denaturing detergent which masked the charge of the proteins and replaced them by a negative charge to separate the proteins in an electric field. The acrylamide concentration determined the resolution of the separation, larger proteins migrate slower through the acrylamide matrix than smaller proteins. Protein samples were prepared by adding 4x Laemmli buffer, boiled for 10 min and centrifuged (Centrifuge 5810R, Eppendorf) for another 1 min and loaded on the gel for separation. The electrophoresis was performed by applying 200 V for 45 min or until the loading dye reached the bottom of the gel.

4x Stacking gel buffer	
Tris/HCl pH 6.8	0.5 M
SDS	0.4 % (w/v)

4x Separation gel buffer	
Tris/HCl pH 8.8	1.5 M
SDS	0.4 % (w/v)

4x Loading Dye	
Tris	100 mM
SDS	8 % (w/v)
Glycerol	40 % (v/v)
β- Mercaptoethanol	10 % (v/v)
Bromophenol blue	1 % (w/v)

10x SDS PAGE running buffer	
Tris/HCl pH 8.8	250 mM
Glycine	1.92 M
SDS	1 % (w/v)

Staining solution	
Acetic acid	10 % (v/v)
Ethanol	30 % (v/v)
Coomassie Brilliant Blue	0.25 % (w/v)

Unstaining solution	
Acetic acid	10 % (v/v)
Ethanol	30 % (v/v)

Stacking gel (5.25 %, 4 gels)	
Rotiphorese Gel 30	1.4 ml
4x Stacking gel buffer	2 ml
A. dest	4.6 ml
10 % APS	30 µl
TEMED	20 µl

Separation gel (12.5 %, 4 gels)	
Rotiphorese Gel 30	5.3 ml
4x Separation gel buffer	4 ml
A. dest	6.7 ml
10 % APS	80 µl
TEMED	8 µl

For visualization of the proteins the gel was incubated in Coomassie staining solution for 10 min. Afterwards the gels were unstained using the same solution without Coomassie until excess dye was removed. The proteins were then detected by blue bands on the gel. As a reference, the PageRuler Prestained Protein Ladder (Thermo Scientific) was used to identify the proteins of interest.

2.4.4. Immuno-detection of immobilized proteins (Western Blot)

Western blotting is an analytical method to detect a specific protein in a sample with the use of specific antibodies after SDS-PAGE and transfer the proteins from the gel onto a membrane (Towbin *et al.*, 1979). Protein samples were first separated by SDS-PAGE (see section 2.4.3) and subsequently transferred onto a PVDF membrane using a semidry blotting system for 20 min at 15 V. Before the transfer process, the gel and two sheets of blotting paper (Whatman, 3 mm) were incubated in Towbin buffer for 10 min. The membrane was activated in 100 % methanol for 1 min and then equilibrated in Towbin buffer together with the gel. For the transfer of the proteins the gel and the membrane were stacked together surrounded by the blotting paper in a sandwich formation and placed between anode and cathode of the semidry blot system. After 15 min the unspecific binding sites of the membrane were saturated by incubation in blocking solution for 1 h at room temperature or overnight shaking at 4 °C. Then the membrane was washed 3x with PBS-T to remove the blocking solution. The saturated membrane was then incubated with the appropriate primary antibody (see table 8) for 1h under slow shaking conditions. For Strep-tagged proteins the membrane was also incubated with 2 µg/ml avidin before the primary antibody was added. After removal of the primary antibody the membrane was washed again 3x with PBS-T buffer.

Towbin transfer buffer		10x PBS buffer	
Tris	25 mM	See section 2.4.2	
Glycine	192 mM		
Blocking solution		PBS-T buffer	
1x PBS		1x PBS	
Albumin fraction V	3 %	Tween-20	0.1 %
AP-buffer		NBT solution	
Tris/HCl pH 9.5	100 mM	NBT	10 % (w/v) in DMF
NaCl	100 mM		
$MgCl_2$	5 mM	BCIP solution	
		BCIP	5 % (w/v) in DMF

Detection solution	
AP buffer	10 ml
NBT solution	33 µl
BCIP solution	66 µL

For the detection of GST- or His_6-tagged proteins the membrane was incubated with the appropriate secondary antibody (see table 8) for 1h under shaking followed by an additional washing step with PBS-T buffer. Before detection the membrane was washed 2x with PBS buffer to remove the Tween-20 followed by an incubation of the membrane in AP buffer. Afterwards, the chromogenic reaction was mediated by adding BCIP/NBT solution to the membrane. The proteins were detected by blue bands on the membrane.

2.4.5 Determination of protein and phycobilin concentrations

Purified protein concentrations were determined by measuring the absorbance A_{280} and using the molar extinction coefficient ε_{280} of the proteins calculated by the online available protein calculator (http://protcalc.sourceforge.net/) for the respective protein. This calculation is based on the absorbance ability of the aromatic amino acids tryptophan (Trp, W), tyrosine (Tyr, Y) and cysteine (Cys, C) at a wavelength of 280 nm (Gill and von Hippel, 1989).

$\varepsilon_{280} = (n_{Trp} \times 5690 + n_{Tyr} \times 1280 + n_{Cys} \times 120)\ M^{-1}cm^{-1}$

n_x = number of amino acids per molecule of protein

According to Lambert-Beer's law the concentration is calculated as followed:

$$c = \frac{A_{280}}{\varepsilon_{280}} \cdot d$$

$$c = concentration\ in\ mol/l$$

$$A_{280} = absorption\ at\ 280\ nm$$

$$\varepsilon_{280} = molar\ extinction\ coefficient\ at\ 280\ nm$$

$$d = path\ length\ of\ the\ cuvette\ in\ cm$$

The concentration of phycobilins were also determined by using Lambert-Beer's law with molar extinction coefficients known from the literature (see table 13). The molar extinction coefficient of the proteins used in this work are listed below (see table 14):

Table 13: Molar extinction coefficients to determine phycobilin concentration

Phycobilin	Extinction coefficient ε_{280}	Solvent	Reference
BV	ε_{698} = 32.6 [$mM^{-1}cm^{-1}$]	2.5 % HCl in MeOH	(Heirwegh *et al.*, 1991)
DHBV	ε_{564} = 46.9 [$mM^{-1}cm^{-1}$]	5 % HCl in MeOH	
3*(E)*-PEB	ε_{594} = 46.9 [$mM^{-1}cm^{-1}$]	5 % HCl in MeOH	(Gossauer and Klahr,
3*(Z)*-PEB	ε_{571} = 46.9 [$mM^{-1}cm^{-1}$]	5 % HCl in MeOH	1979)

Table 14: Molar extinction coefficients to determine protein concentration

Protein	Extinction coefficient ε_{280} [$M^{-1}cm^{-1}$]
PebA	51470
PebB	50190
PebS	35110
PcyA	26390
GST-PebA	92390
GST-PebB	91110
Strep-PebB	55880
Strep-PebAgB	107350
PebAgB	107660

2.4.6 Gel permeation chromatography (GPC)

Gel permeation chromatography was used as a further purification step for already purified proteins with affinity chromatography. This method ensured the removal of impurities or aggregates from a protein solution by separation on a gel filtration column according to the molecular radius of the proteins. The GPC was performed automatically on an ÄktaPure FPLC-system (GE Healthcare) with a HiLoad Superdex™ 75 16/600 pg column for PebA, PebB and PebS. For these proteins carbonic anhydrase was used as a size reference (29 kDa, Sigma Aldrich). Proteins still fused to the GST-tag were separated on a Superdex™ 200 10/300 GL. Here, albumin was used as a size reference (66 kDa, Sigma Aldrich). The proteins were loaded onto the applicable column and the separation was performed using the manufacturer's instruction at a constant flow rate of 1 ml / min. Depending on the following analysis different buffers were used for column equilibration. For FDBR assays, the columns were equilibrated in TES-KCl buffer (see section 2.4.7). For affinity determination the columns were equilibrated with NaP_i-buffer (see section 2.4.10). The protein elution was followed by measuring the absorbance at 280 nm during the separation and it was collected in 5 ml fractions during the run. Those fractions containing the desired FDBRs were pooled and concentrated with a Vivaspin® concentrators (Sartorius).

2.4.7 Anaerobic bilin reductase assay (FDBR assay)

The anaerobic bilin reductase assay was employed to test the activity of purified FDBRs (Tu *et al.*, 2004) or to produce a specific bilin in a larger scale (→ feeding assay, modified after (Busch *et al.*, 2011a)). The enzyme-substrate complex was incubated for at least 10 min in the dark. The required electrons for the reduction of BV IXα were provided from an NADPH-regenerating system (NRS) consisting of glucose-6-phosphate and glucose-6-phosphate-dehydrogenase. This reaction required $NADP^+$ as a co-factor and the electrons were transferred to the provided ferredoxin from Cyanophage P-SSM2($Fd_{P\text{-}SSM2}$) in the sample.

To regenerate the ferredoxin the FNR PetH from *Synechocystis sp.* PCC7002 was used (Fig. 2.2). To ensure an anaerobic condition the whole reaction mixture was constantly gassed with nitrogen. Residual oxygen or uprising oxygen during the reaction was removed by adding an oxygen-scavenging-system (OSS) to the assay solution. At first, all assay components (see table 14) were premixed in a gas-tight anaerobic quartz cuvette and the residual oxygen was removed by a nitrogen gas flow with constant stirring for 20 min. During this step the enzyme-substrate complex was mixed. For activity assays an equimolar amount of FDBR and substrate of 10 µM was used, for feeding assays 10 µM of FDBR and 20 µM of BV IXα was used. The total volume of a standard or feeding assay was 2 ml. Time-coursed FDBR assays were performed in a 3ml volume. The reaction was initiated by the addition of the NRS and then monitored via UV-Vis spectroscopy. A single spectrum was taken automatically every 30s for a whole reaction time of ten minutes (20 minutes for feeding assays).

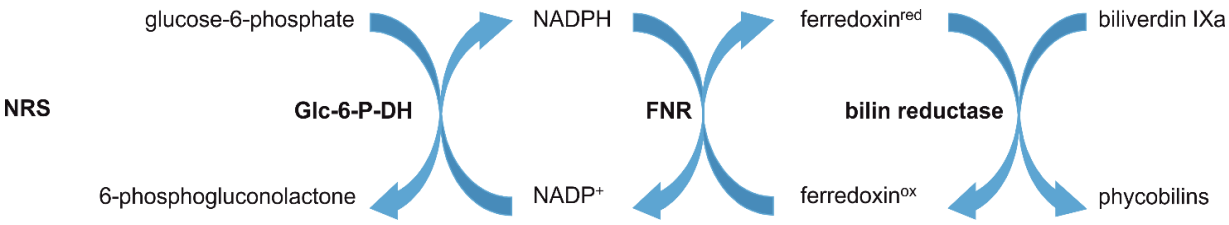

- Glc-6-P-DH = glucose-6-phosphate dehydrogenase
- FNR = ferredoxin-NADP^{+} reductase
- NADPH = nicotinamide adenine dinucleotide phosphate
- NRS = NADPH regenerating system

Figure 2.2: Schematic overview of the anaerobic bilin reductase assay

Overview of the electron transfer chain during the anaerobic FDBR assay. The NADPH-regenerating system (NRS) is given in excess to the solution to ensure a constant electron flow for the whole reaction time. The $Fd_{P\text{-}SSM2}$ transferred the electron to the FDBR to reduce BV IXα to the specific bilin (e.g. DHBV, PEB). The ferredoxin is regenerated by an FNR ($PetH_{SynPCC7002}$) which also required NADPH as a cofactor.

Production of DHBV via PebA feeding experiments

For the Microscale thermophoresis and FDBR:DHBV titration experiments, a quite high amount (~ 4-5 mM / µl) of DHBV had to be produced and purified. The production of DHBV was conducted via the PebA feeding experiment where 20 µM of BV IXα is added at every given time point to increase the yield of the DHBV formation up to 4 times (Fig. 2.3). The production of DHBV was observed via UV-Vis spectroscopy. During this reaction the same determinants were detected as in the standard PebA assay. For these planned experiments at least 3-4 feeding assays were performed and combined after purification. Produced DHBV was purified via HPLC using the identical column (Luna 5 µm reversed phase C18 column, Phenomenex) but the outlet which comes directly after the DAD detector was opened to collect the fraction which was eluted with a retention time of ~ 9.5 min.

This fraction contained pure DHBV which was further lyophilized and stored for later experiments.

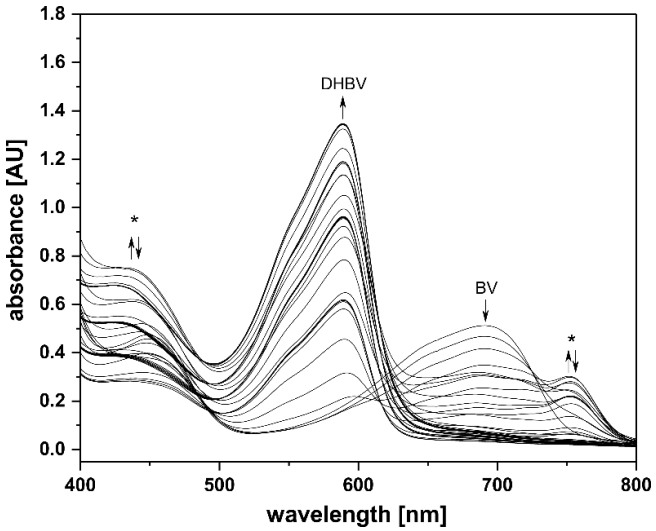

Figure 2.3: PebA feeding assay for DHBV production.

Similar to the standard PebA assay the feeding assay differs only in the extra addition of 20 µM of BV IXα every 3 min. The rise in absorbance at ~ 580 nm is clearly higher than in the standard assay. DHBV was processed after the reaction and purified using HPLC (see section 3.1.2).

FDBR assay components	
BSA	10 µM
Glucose	100 mM
Glucose oxidase	50 U/ml
Catalase	5 µM
$Fd_{P\text{-}SSM2}$	1 µM
$PetH_{SynPCC7002}$	0.01 µM
NRS	100 µl
FDBR:BV IXα	10 µM each
TES-KCl buffer	ad 2 ml or 3ml

NADPH-regenerating system		TES-KCl buffer	
NADP+	8.2 mM	TES/KOH pH 7.5	25 mM
Glucose-6-phosphate	65 mM	KCl	100 mM
Glucose-6-phosphate dehydrogenase	11 U/ml		

Time-coursed FDBR assays and peak integration

With the construction of the fusion protein PebAgB there was now a third way of PEB biosynthesis *in vitro*. To put the reaction mechanism as well the velocity in relation to the already described enzymes for PEB formation time-coursed FDBR assay experiments were performed.

The time-coursed experiments were a modified FDBR assay as described above but with a slightly larger scale to draw several samples (each 500 µl) at different time points (T0 = 0 min, T1 = 1 min, T2 = 3 min, T3 = 5 min, T4 = 7 min). The reaction products of each time point were processed as described above and then analyzed via HPLC (see section 2.4.9). The velocity of product formation is indicated by the increase or decrease of the specific peaks areas of the bilins while eluting from the HPLC column. Therefore, the obtained peaks corresponding to BV, DHBV and PEB were integrated using the Open Lab CDS Chemstation Edition (Agilent Technologies) integration tool. At each time point the percentage area of these peaks were compared for each enzyme and the bilin formation is then visualized by plotting the time points against the area using the software Origin® 2017.

2.4.8 Development of "on-column" FDBR assays with immobilized enzymes

Based on our previous research we suggested a transient interaction of both examined enzymes PebA and PebB. To get deeper insights into this interaction process we developed an adapted FDBR assay (see section 2.4.7) approach with one interaction of the partner immobilized on chromatography columns. Since this was the first time our established FDBR assay would be performed in an immobilized form we also check if the used enzymes retain their activity in this state. Here, we mostly used GST-sepharose (MACHEREY-NAGEL GmbH & Co. KG, Germany) for the protein binding to the column. For this study PebA was produced using the pGEX-6P1_*pebA* construct providing a GST-fusion with this enzyme. In contrast to the manufacturer's protocol, no PreScission-protease cleavage was performed and therefore the GST-PebA fusion protein was just further purified via gel filtration (see section 2.4.6). The required PebB for this experiment was produced via the pASK-IBA45*-*pebB* construct providing an N-terminally Strep-tag fusion with this enzyme. Due to the different tag, this protein will not bind to the column and like GST-PebA this fusion protein was also further purified via gel filtration. The reaction time for the "on-column" assay was calculated by a previously performed GST-PebA assay to until a full substrate conversion was detected (see section 2.4.7). This control assay was performed ahead of each "on-column" assay. Based on this calculation a reaction time of ten minutes was set up for all "on-column" assays. The so called "on-column" assay was performed by binding 10 µM of GST-PebA:BV complex on500 µl GST-sepharose, equilibrated with assay buffer (TES-KCl buffer, see section 2.4.7). Then all required assay components were dissolved as described above and added to the column which was closed via the provided column cap (Bio-Rad Laboratories GmbH, Germany). After then minutes the column cap was removed and the column was washed with 2 CV of assay buffer and following by the elution of GST-PebA with elution buffer (see section 2.4.2). Each fraction was collected and diluted 1:10 with 0.1%-TFA. Produced bilins were then isolated according to the standard purification process (see section 2.4.9) and analyzed via HPLC.

The following “on-column” experiment was performed identically to the previous one but after the first washing step another washing step was conducted with 3 CV assay buffer containing 10 µM PebB. The subsequent bilin purification and analysis was performed as before. Here, these fractions were also analyzed via UV-Vis spectroscopy to verify the typical FDBR:bilin complex formation.

A coupled enzyme assay was also performed by setting up the “on-column” assay as in the previous experiments but after five minutes of reaction time an equimolar amount of GST-PebB (produced and purified identically to GST-PebA) was added to the column material. Then, after ten minutes the column was washed with 2 CV assay buffer followed by the elution of the proteins with 3 CV elution buffer (see section 2.4.2). Bilin purification and analysis were made identically to the previous experiments.

2.4.9 HPLC analysis and phycobilin extraction

High-performance liquid chromatography (HPLC) was used to determine and identify produced phycobilins from FDBR assays by separating the enzyme’s substrates and products according to their polarity. The reaction products of the bilin reductase activity assays were analyzed on a Luna 5 µm reverse phase C18-column (Phenomenex) performed on the Agilent 1100 series HPLC. Before analysis the column was equilibrated with the mobile phase consisting of degassed and filtered 50 % (v/v) acetone and 50 % (v/v) 20 mM formic acid. The isocratic elution was performed with a constant flow rate of 0.6 ml/min. To isolate the DHBV of the PebA-feeding assay, the reaction product was collected directly after the outlet of the DAD detector and immediately frozen at -80 °C for lyophilization as described above.

Sample preparation for HPLC analysis

Preparation of phycobilins were made under dim-light to prevent photo-damage of the pigments. Directly after FDBR assays the reaction mixture was diluted 1:10 with 0.1 %-TFA. These samples were then used for a solid phase extraction process with SepPak® C18 light cartridges (Waters) to remove residual salt and assay components from the mixture. Before sample loading the cartridges were prepared by flushing twice with the following chemicals.

Acetonitrile	3 ml
A. dest	3 ml
0.1 %-TFA	3 ml
10 % MeOH in 0.1 % TFA	3 ml

Using a syringe, the samples were loaded on the cartridges and afterwards washed with 5 ml 0.1 % - TFA. Then, with 1 ml of acetonitrile the bound phycobilins were eluted and immediately frozen at -80 °C for lyophilization. The lyophilization process was performed for approximately 24 h (Alpha 2-4 LSC plus, Martin Christ GmbH) until the samples were dry.

Dried samples were dissolved in 15 µl DMSO and diluted 1:10 with the mobile phase. Before injection the samples were filtered using a PTFE filter (Phenomenex). For bilin determination standard bilins were used and prepared the same way.

Extraction of phycobilins

To isolate the DHBV of the PebA-feeding assay, the reaction product was collected directly after the outlet of the DAD detector and immediately frozen at -80 °C for another lyophilization process as described above.

HPLC mobile phase	
Acetone	50 % (v/v)
Formic acid (20 mM)	50 % (v/v)

2.4.10 Fluorescence titration and Microscale Thermophoresis (MST)

The following experiments were performed in cooperation with PD Dr. Marc Nowaczyk (AG Cyanobacterial Membrane Protein Complexes, Dep. of Plant Biochemistry, Ruhr-University Bochum). In order to reevaluate the binding constant of FDBRs to DHBV a more sensitive technique was used than in previous studies (Dammeyer and Frankenberg-Dinkel, 2006). The FDBRs PebA and PebB were produced and purified as described (see section 2.4.2).

Fluorescence titration to determine binding affinity constants

To determine the affinity (K_d-value) of the indicated proteins PebA and PebB to DHBV, fluorescence titration experiments were performed. Thus, a dilution series of either PebA or PebB in a micromolar (140 µm starting concentration) range in NaP_i-buffer was created and a constant concentration of DHBV was added in a micromolar range (13 µM) to each sample. Protein-bilin affinity was then measured using MonolithTM NT.115 Standard Capillaries in a Monolith NT.115 instrument (Nanotemper Technologies GmbH, Munich). The measurements were performed at MST power 20 % and 40 % and LED power 20 % and 40 % using the “red” filter of the instrument to detect the intrinsic fluorescence of the FDBR:bilin complex. The fluorescence titration experiments were done in triplets and the evaluation was made using the MO.Affinity Analysis Software (NanoTemper Technologies GmbH, Munich, Germany).

Microscale thermophoresis to determine binding affinity constants

The affinity of either PebA or PebA:DHBV complex to PebB was measured via microscale thermophoresis using the identical instrument as described above. PebB was labelled using the Monolith™ NT.115 Protein Labeling Kit BLUE-NHS (Amine Reactive) according to the manufacturer’s instructions (labelled protein is marked with “*”). A dilution series in NaP_i-buffer of either PebA or PebA:DHBV was created, whereas the PebB* concentration was kept constant.

The thermophoretic movement were measured and performed identically as described above. The MST experiment was performed twice and the obtained data were also analyzed using the MO.Affinity Analysis Software (NanoTemper Technologies GmbH, Munich, Germany) to calculate the K_d-value.

Na-P_i buffer	
Na_2HPO_4/NaH_2PO_4 pH 7.5	60 mM
NaCl	150 mM

2.4.11 Bacterial Two-Hybrid System (BacTH)

The Bacterial Two-Hybrid system (BacTH) was used to detect and analyze protein-protein interaction *in vivo* using an appropriate *E. coli* strain as a host. This system is based on the reporter gene activity of the β-galactosidase whose expression is induced by the availability of lactose and the absence of glucose. For expression of the β-galactosidase signal molecule cAMP is required which is converted by two molecules of ATP by the adenylate cyclase (AC) of *Bordetella pertussis* during the signal transduction pathway of the lactose utilization. The catalytic domain of the AC consists of the T25 and the T18 fragment (Fig. 2.4). For this system, each of those fragments were cloned into the BacTH plasmids (see table 6). Using standard cloning techniques, the FDBR genes of interest (*pebA*, *pebB*, *pcyA*) were cloned in various orientation into these expression plasmids providing each fragment either on the N- or C-terminus of the enzymes (Karimova *et al.*, 1998). As a second negative control the non-FDBR MsrF from *Methanosarcina acetivorans* was used which was provided by Anna Scherhag (Bachelorthesis 2017). MsrF is a regulator protein involved in the expression of the methyltransferase MtsD and served as a negative control (Fig. 2.5). Putative interacting proteins lead to the reconstitution of the adenylate cyclase activity and therefore also in β-galactosidase activity. A pair of plasmids with putative interacting proteins were co-transformed into *E. coli* BTH101 (see section 2.2.6) and plated on agar plates with the right antibiotics over night at 30 °C. Those *E. coli* strains lack the natural adenylate cyclase by a deficiency in the *dcyA* gene. On the next day, colonies of each combination were picked and resuspended in 100 µl LB. Then a drop of each combination was dripped on either agar plates containing 0.5 mM IPTG, 50 µg/ml X-Gal and the corresponding antibiotics or on MacConkey agar plates containing 20 % lactose and the appropriate antibiotics.

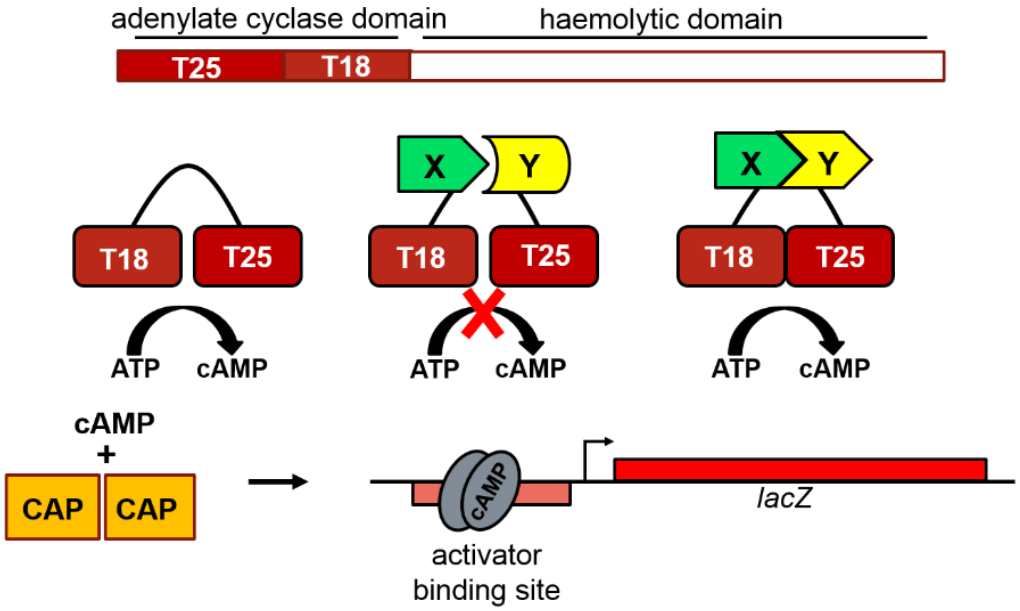

Figure 2.4: The principle of the Bacterial Two-Hybrid system

The adenylate cyclase of *Bordetella pertussis* consists of two catalytic domains which can be separated into the fragments T25 & T18. Putative interacting proteins can be genetically fused with one of the domains. If the proteins interact *in vivo* the two fragments will come in close contact which leads to the reconstitution of the AC-domains and cAMP can be formed. The accumulation of cAMP leads to the expression of the natural *lacZ* gene and therefore to the activity of the reporter gene β-galactosidase. The used *E. coli* strain dcyA deficient lacking the natural adenylate cyclase (Karimova *et al.*, 1998). (T18 & T25 = adenylate cyclase domains; X & Y = proteins of interest; cAMP = cyclic adenosin monophosphate; CAP = catabolite activator protein)

MacConkey medium	
MacConkey agar	50 g/l
10 % Lactose	1 % (v/v)

These plates were incubated up to 48 h at 30 °C in the incubator until a coloration of the colonies appeared. Empty vectors were used as negative controls and the pKT25zip & pUT18Czip plasmids were used as a positive control. These plasmids encode for the leucine-zipper domains of the transcription factor Gcn4P from the baker's yeast *Saccharomyces cerevisiae*. Protein interaction was determined by coloration of the resulted colonies. On X-Gal plates blue colored colonies indicated a reporter gene activity and on MacConkey plates the colonies turned red.

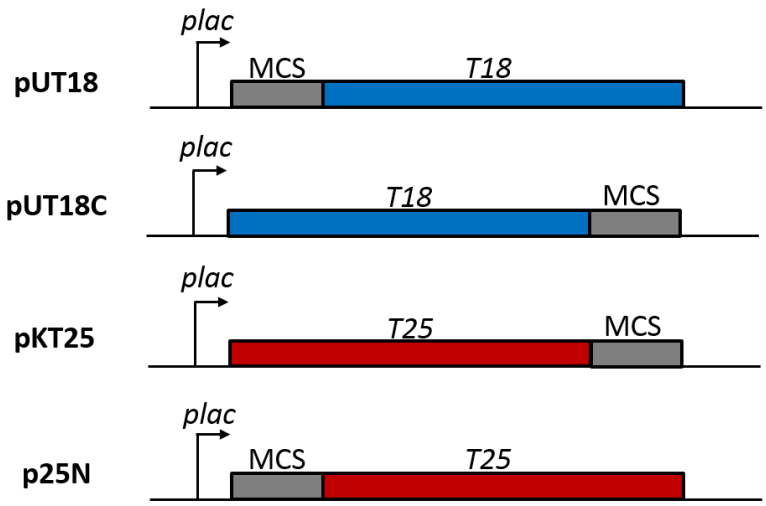

Figure 2.5: Different expression plasmids for BacTH

The genes *pebA* and *pebB* from *Synechococcus sp.* WH8020 and *pebS* from the cyanophage P-SSM2 were cloned into the MCS of these plasmids providing different orientations of the adenylate cyclase fragments T25 and T18. Each plasmid contains a *plac* promoter for inducible gene expression (Karimova *et al.*, 1998).

2.4.12 *In-vivo* crosslinking with Strep-protein interaction experiments (SPINE)

The Strep-protein interaction experiment (SPINE) was described as a rapid method to analyze and detect protein-protein interaction *in vivo* (Christina *et al.*, 2007). The most-likely interacting FDBRs PebA and PebB were co-produced in *E. coli* BL21 (DE3) using the expression plasmid pASK-IBA45+_*pebAB* providing Strep-tagged PebA and His_6-tagged PebB. The protein production was performed as described (see section 2.4.1) in 100 ml culture volumes but after induction with AHT the cells were shaken for 2.5 h at 30 °C and 100 rpm (Innova®44 New Brunswick, Eppendorf). During this incubation time a formaldehyde stock solution was prepared (4 % *para*-formaldehyde in PBS, pH 7.4). For an optimal solving of the crosslinking reagent the buffer was preheated to 60 °C. After 2.5 h of incubation of the cells the crosslinking solution was added to the cells in different final concentrations (0 %; 0.2 %; 0.4 %; 0.6 %) to determine the efficiency and the influence of the cross linker. After addition of formaldehyde the culture were further incubated for another 30 min at 30 °C.

Crosslinking buffer		CL-washing buffer	
para-formaldehyde	4 g	Tris/HCl pH 7.5	50 mM
PBS (see section 2.4.2)	100 ml	NaCl	200 mM

Cells were then harvested as described (see section 2.4.1) and washed once with 50 ml CL-washing buffer to remove residual formaldehyde from the cells. Cells were then stored at -20 °C or directly lysed with a following proteins purification via Streptactin agarose (see section 2.4.2). The detection of crosslinked proteins was performed by Western Blot analysis using antibodies against the Strep-tag (PebA evidence) resp. the His_6-tag (crosslinked PebB proof).

3 Results

In marine cyanobacteria, the biosynthesis of phycoerythrobilin is mediated by the cooperation of two enzymes from the class of ferredoxin-dependent bilin reductases, PebA and PebB. PebA uses BV IXα as a substrate and catalyzes the reduction of the C15 – C16 double bond position to yield 15,16-dihydrobiliverdin. This violet pigment serves as the substrate for the subsequent FDBR PebB which reduces the vinyl group of the A-ring to produce the final product PEB. This pink pigment is then transferred and connected to the light-harvesting complex, the phycobiliproteins, via phycobiliprotein lyases. In *Synechococcus sp.* WH8020 the genes for *pebA* and *pebB* are located on an operon which indicates an involvement in the same biosynthetic pathway. In earlier studies it was postulated that DHBV is transferred via metabolic channeling from PebA to PebB. In this study we wanted to achieve deeper knowledge of this protein-protein interaction to find out whether there is a physical interaction between PebA and PebB or, the transfer happens by proximity channeling, without any physical contact.

3.1 Substrate affinities of FDBR:DHBV complexes

3.1.1 New evaluation of affinity binding constants of FDBRs to DHBV

The binding affinities of PebA and PebB to DHBV were re-evaluated with a more sensitive technique using the intrinsic fluorescence of the FDBR:bilin complex. Both proteins were overproduced heterologously and affinity purified as GST-fusion proteins in *E. coli* BL21 (DE3) (Fig. 3.1).

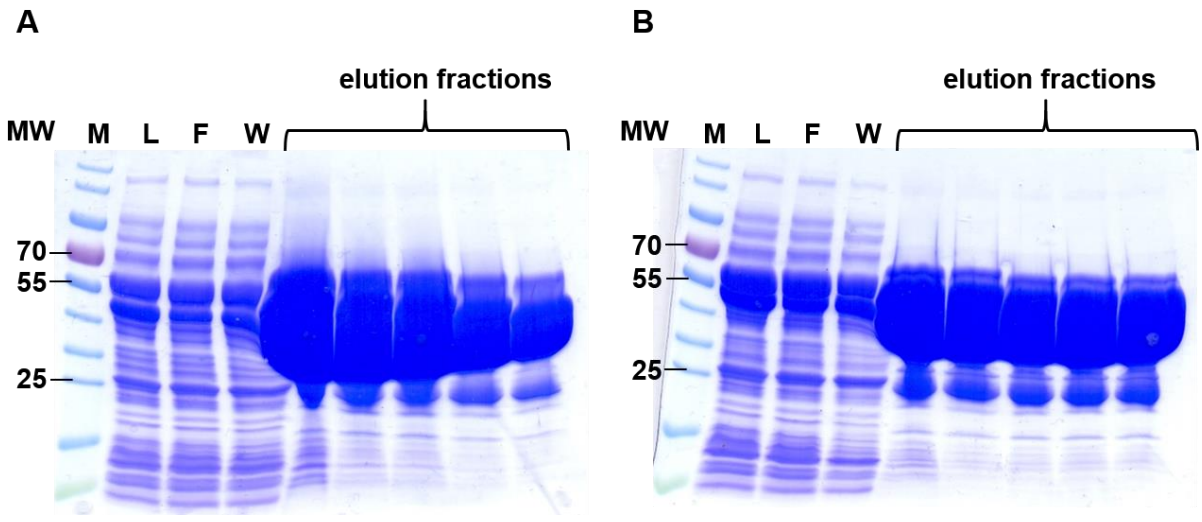

Fig. 3.1: SDS-PAGE of the purification of GST-PebA (A) and GST-PebB (B).

M = protein ladder (PageRuler™ Prestained, Thermo Scientific); MW = molecular weight; L = lysate; F = flow-through fraction; W = washing fraction. The elution fractions were collected in 2 ml volumes. The estimated protein sizes of the fusion proteins were 54,4 kDa (GST-PebA) and 56,6 kDa (GST-PebB).

The obtained concentration of both overproduced proteins was high enough (The yield is related to 1 l *E. coli* culture: GST-PebA: Ø 8 mg / ml; GST-PebB: Ø 13 mg /ml) (Fig. 3.1) and after tag-removal by PreScission® protease (for GST-tagged proteins) cleavage followed by a second affinity chromatography on an ÄktaPure (Ge Healthcare) using a GST-trap FF 5 ml column these proteins were further purified via GPC.

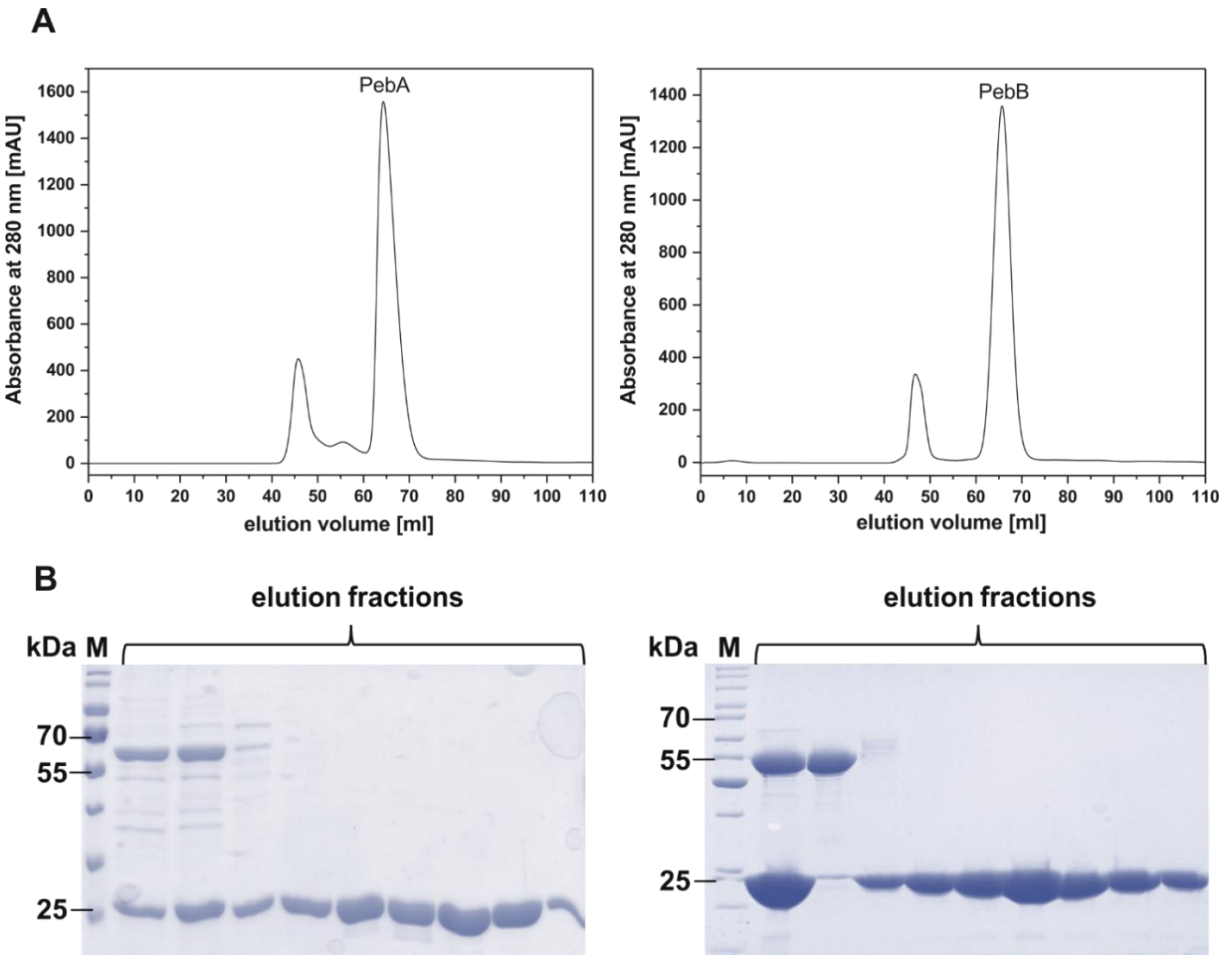

Fig. 3.2: Gel permeation chromatography and SDS-PAGE of PebA and PebB purification.

(A) After PreScission™ protease digestion and a subsequent purification by a second affinity chromatography both enzymes PebA (MW = 27.2 kDa) and PebB (MW = 29.2 kDa) were further purified via gel permeation using HiLoad Superdex 75 pg 16/600 GL (GE Healthcare). The column was equilibrated with NaP_i-buffer pH 7.5. To identify the FDBRs from the elution profile carbonic anhydrase with a similar molecular weight of 29 kDa was used as a reference (not shown) **(B)** Samples from the second affinity chromatography and gel permeation chromatography were analyzed via SDS-PAGE to check the purity of both proteins. For further experiments, only the pure fractions were pooled.

The oligomeric state of both PebA and PebB was already characterized and described as soluble monomers (Dammeyer and Frankenberg-Dinkel, 2006). The proteins showed both an elution volume of ~ 65 ml on a HiLoad Superdex® 75 pg 17/600 (Fig. 3.2 A). The FDBRs were identified by a reference protein with a similar size (carbonic anhydrase, MW = 29 kDa) which also eluted at ~ 65 ml.

Each fraction was collected and a sample was taken for SDS-PAGE to check the purity of the produced proteins (Fig. 3.2 B). The elution fractions containing only pure PebA or PebB proteins were pooled and concentrated for later experiments.

3.1.2 Analysis of the activity of purified PebA and PebB

All purified FDBRs were tested for their activity before they underwent further analytical experiments. For this the well-established anaerobic bilin reductase assay was employed to test the activity of PebA and PebB. Here equimolar amounts of FDBR:BV IXα were used and the reaction was monitored via time-resolved UV-Vis spectroscopy.

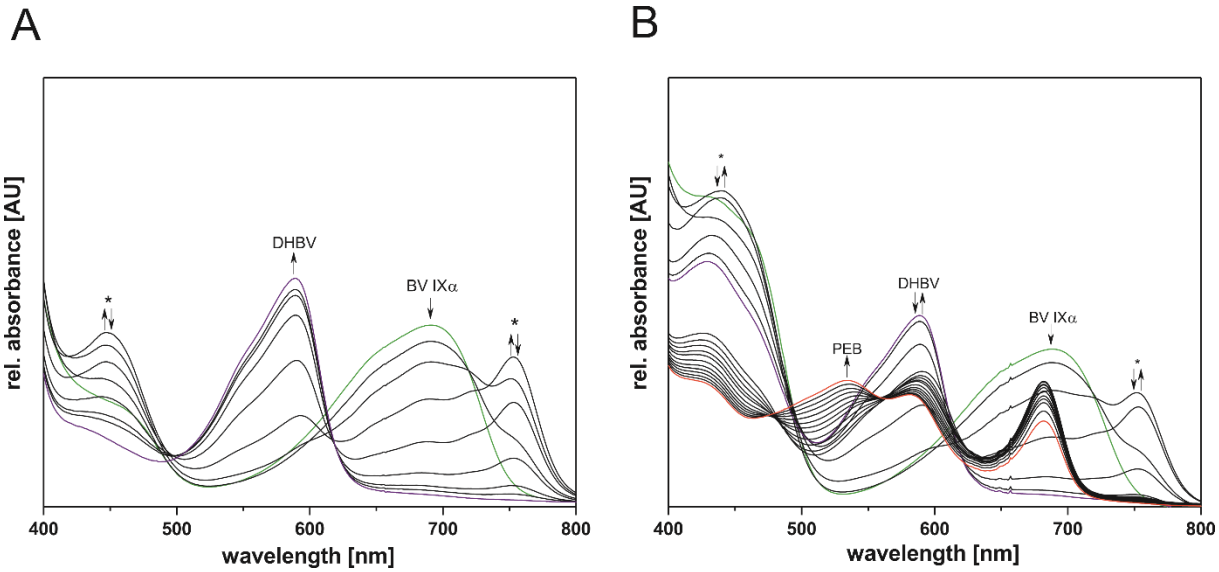

Fig. 3.3: Enzyme activity assay of purified FDBRs PebA and PebB.

Produced and purified PebA **(A)** was tested for activity and also a coupled assay of PebA and PebB **(B)** was tested for activity using the anaerobic FDBR assay. Equimolar amounts of FDBR:bilin (10 µM) were used and the assays were started by the addition of the NADPH-regenerating system (NRS). Spectra were recorded every 10 s during a whole reaction time of 10 min. For more clarity the absorbance spectra at the start of the reaction is colored green (FDBR:BV complex) and the end of the reaction is colored in red (FDBR:PEB complex). The violet color is used to show the formation of the intermediate DHBV (BV = biliverdin IXα; DHBV = 15,16-dihydrobiliverdin; PEB = 3 *E/Z*-phycoerythrobilin). The arrows indicate the decrease and increase of substrate and/or product formation whereas the asterisks mark upcoming radical intermediates during the reaction.

Both PebA and PebB showed their expected activity after purification. PebA converted BV IXα to DHBV rapidly, indicated by an increasing absorbance at ~ 580 nm. The typical peak of the FDRB:BV complex with an absorbance maximum at ~ 680 nm declined fast as well. Also, the typical radical intermediates were detectable at 450 nm and 750 nm which subsequently disappeared over the reaction time (Fig. 3.3 A). The occurrence of radical intermediates during the FDBR reaction were previously described (Busch *et al.*, 2011b; Tu *et al.*, 2004). The PebB activity was also validated by an additional FDBR assay similar to the PebA assay. After the PebA reaction was completed, an equimolar amount of PebB was added to the cuvette and the conversion of DHBV to PEB was observed by an increase in absorbance at ~ 540 nm with a simultaneous decrease of absorbance at ~ 580 nm (Fig 3.3. B).

The reaction products of both FDBR assays were verified via HPLC analysis (Fig. 3.4) and compared to previously described standards (Frankenberg and Lagarias, 2003; Tu *et al.*, 2004). The produced phycobilins showed their typical elution profile with a retention time of ~ 9.5 min for DHBV, ~ 8 min for 3[*E*]-PEB and ~ 12 min for 3[*Z*]-PEB. Some residual DHBV was observed after the PebB assay because the assay was stopped after 10 min with the addition of 0.1 % TFA and so a full conversion to PEB was not finished yet. This indicated that the reaction time of PebB was slower than the PebA reaction since there was no BV IXα detectable at the end of the reaction suggesting a rapid conversion to DHBV by PebA. BV IXα had a retention time of ~ 25 min (Data not shown, (Frankenberg and Lagarias, 2003; Tu *et al.*, 2004)).

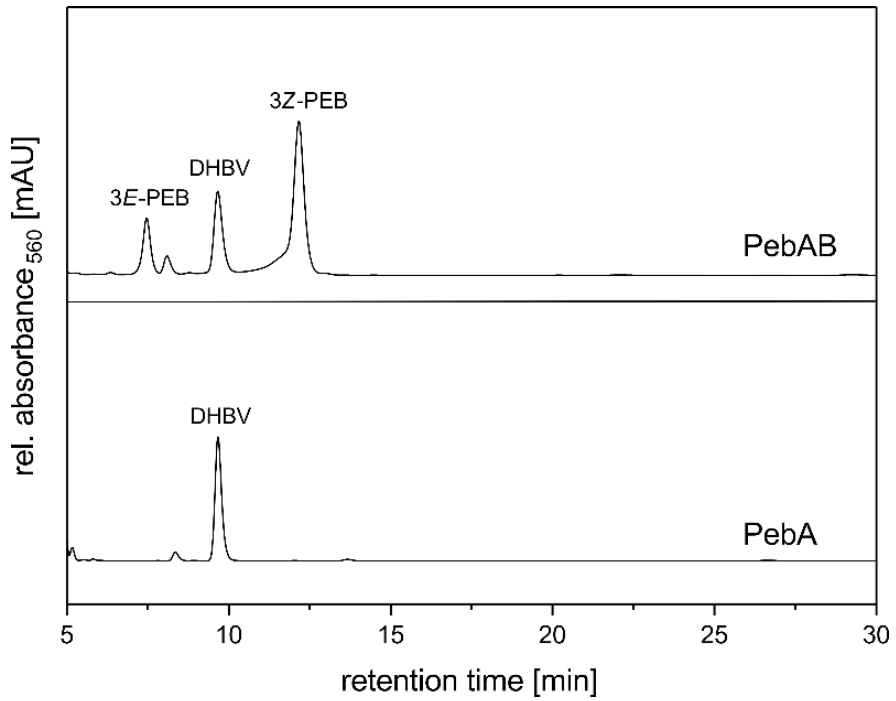

Figure 3.4: HPLC analysis of FDBR reaction products.

The reaction products of both PebA and PebB assays were processed ahead and analyzed on a Luna 5 µm reversed phase C18 column (Phenomenex) as stationary phase. The mobile phase was composed of 50 % (v/v) acetone and 50 % (v/v) 20 mM formic acid. Using a diode array detector (DAD) at a wavelength of 560 nm the produced bilins were detected. The identity of the phycobilins DHBV and PEB was cleared up by comparison to the literature (Frankenberg and Lagarias, 2003; Tu *et al.*, 2004).

3.1.3 The FDBRs PebA and PebB form a fluorescent complex with DHBV

As already described, during the formation of PEB the intermediate DHBV forms a fluorescent complex with both PebA and PebB. The fluorescence of the FDBR:bilin complex was excited at 570 nm for PebA:DHBV and at 605 nm for PebB:DHBV as stated in the literature (Dammeyer et al., 2006). The respective emission maximum for both FDBR:bilin complexes were determined at 606 nm (PebA:DHBV) and 633 nm (PebB:DHBV). Interestingly, the intensity in fluorescence of the PebB:DHBV was 5 times higher than the PebA:DHBV complex (Fig. 3.6). This is in contrast to the previously determined data where the intensity of the fluorescence from these two complexes was in a similar range. Free DHBV was also tested for fluorescence but showed only a very weak emission (Data not shown).

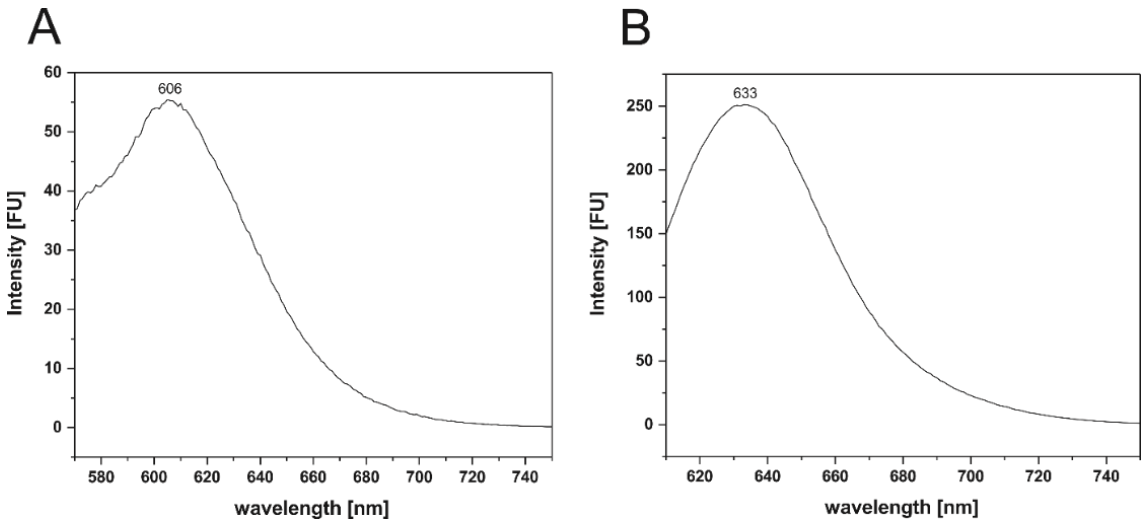

Figure 3.6: Fluorescence emission spectra of FDBR:DHBV complexes.

The fluorescence emissions of the complexes PebA:DHBV **(A)** and PebB:DHBV **(B)** were excited at their individual long wavelength absorbance maximum (PebA:DHBV: λ = 570 nm; PebB:DHBV: λ = 605 nm). Before the excitation 10 µM of proteins were pre-incubated for 10 min on ice with 5 µM of previously purified DHBV.

3.1.4 Binding affinities of FDBRs to DHBV point to metabolic channeling

Binding affinity of the recombinantly produced enzymes to the intermediate DHBV were re-evaluated by employing a more sensitive technique. In earlier studies, the binding affinities of either PebA or PebB to DHBV were estimated via the fluorescent properties of the resulting enzyme:bilin complexes (see section 3.1.4). Here, the binding affinities of either PebA:DHBV or PebB:DHBV were also assessed using fluorescence titration experiments. However, a more rigorous analysis was performed using the MO.Affinity Analysis Software (NanoTemper Technologies GmbH, Munich, Germany). To do so, unlabeled proteins were used and GPC was performed prior to the fluorescence measurements to avoid non-specific binding of the ligand DHBV to impurities. Therefore, an increasing amount of DHBV was mixed with a constant concentration of each enzyme (up to 140 µM each). The complex formation of the enzymes with the bilins affected the fluorescent properties of this complex.

By measuring this intrinsic fluorescence of the FDBR:DHBV complex with an emission wavelength of 670 nm, the dissociation constant of the bilin to the FDBRs via the initial fluorescence of this complex was calculated (Fig. 3.7 A). A dissociation constant (K_d) in the lower micro-molar range was determined for both PebA and PebB (PebA to DHBV = 1.70 µM ± 1.30 µM; PebB to DHBV = 0.27 µM ± 0.20 µM). In contrast to earlier observations, the calculated affinity of PebB to DHBV was higher than before displayed by a lower K_d-value (PebB:DHBV: K_d = 1.48 µM, (Dammeyer and Frankenberg-Dinkel, 2006)). This result supported the suggestion of a metabolic channeling of the intermediate DHBV. Based on the K_d-determination of either PebA or PebB to DHBV the next step was to investigate whether the binding of DHBV to PebA enhanced the affinity to PebB. Therefore, the affinity of PebA (with and without bound DHBV) to the subsequent FDBR PebB was determined using microscale thermophoresis. For this experiment PebB was labeled ahead with the NHS-NT495 dye (NanoTemper Technologies GmbH, Munich, Germany). The fluorescence emission maximum of this dye is in the range of 500 – 570 nm, therefore it will not interfere with the intrinsic fluorescence of the FDBR:bilin complex. Here, an increasing amount of either PebA or the pre-incubated PebA:DHBV complex was added to a constant concentration of labeled PebB and the thermophoretic movement was monitored. The calculated K_d displayed a higher affinity of PebA to PebB when DHBV is bound to this enzyme (PebA:DHBV – PebB* = 0.18 µM). In the absence of bound DHBV, the affinity to PebB was five times lower (Fig. 3.7 B).

Based on the K_d-determination of either PebA or PebB to DHBV the next step was to investigate whether the binding of DHBV to PebA enhanced the affinity to PebB. Therefore, the affinity of PebA (with and without bound DHBV) to the subsequent FDBR PebB was determined using microscale thermophoresis. For this experiment PebB was labeled ahead with the NHS-NT495 dye (NanoTemper Technologies GmbH, Munich, Germany). The fluorescence emission maximum of this dye is in the range of 500 – 570 nm, therefore it will not interfere with the intrinsic fluorescence of the FDBR:bilin complex. Here, an increasing amount of either PebA or the pre-incubated PebA:DHBV complex was added to a constant concentration of labeled PebB and the thermophoretic movement was monitored. The calculated K_d displayed a higher affinity of PebA to PebB when DHBV is bound to this enzyme (PebA:DHBV – PebB* = 0.18 µM). In the absence of bound DHBV, the affinity to PebB was five times lower (Fig. 3.7 B).

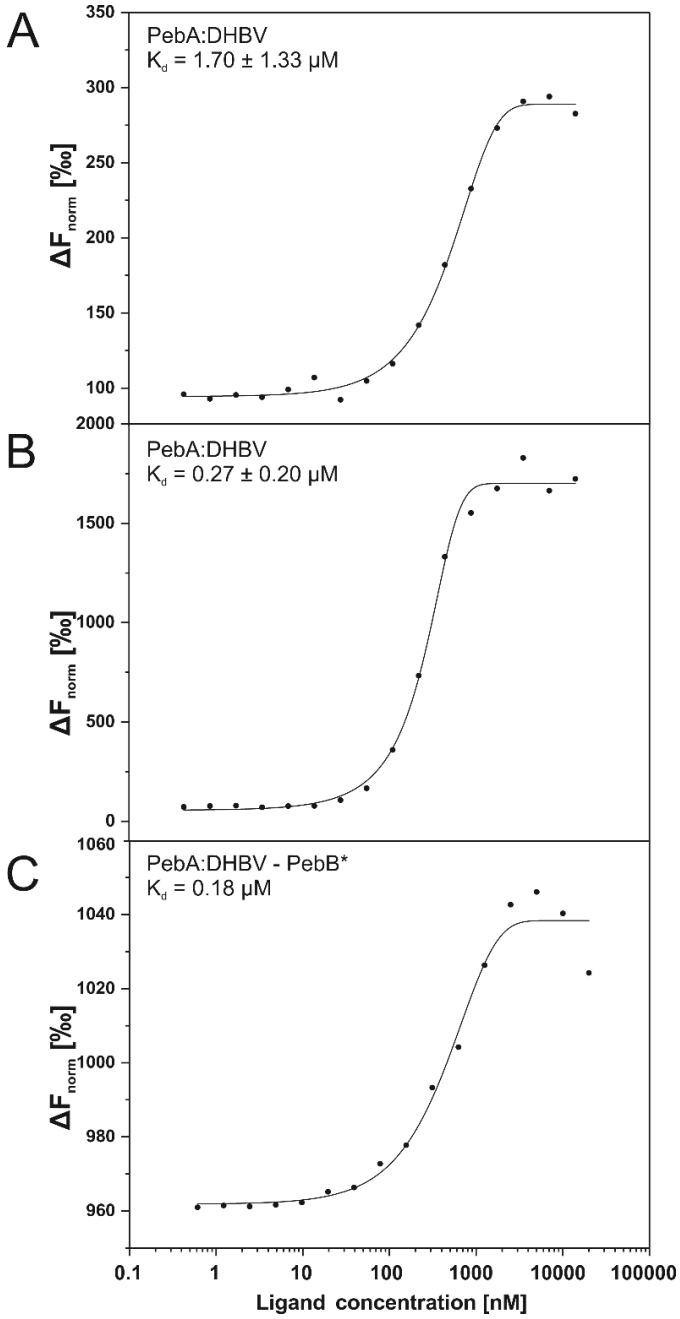

Figure 3.7: Substrate binding affinity of the PebA:DHBV/PebB:DHBV complexes and determination of the PebA-PebB affinity using microscale thermophoresis.

(A) Analysis of the substrate binding affinity of DHBV to the FDBRs PebA and PebB using fluorescent titration experiments with unlabeled proteins. The intrinsic fluorescence of DHBV was used to calculate the dissociation constant (K_d) with an excitation at 647 nm. DHBV concentration was kept constant at 13 µM, the concentration of either PebA or PebB was titrated in a micromolar excess up to 75 µM. **(B)** The enzyme-product complex PebA:DHBV was used to determine the affinity to the subsequent enzyme PebB. PebB was labeled with NHS-NT495 dye (indicated by an asterisk) to avoid interference with the intrinsic fluorescence of DHBV. The PebB concentration was kept constant at 200 nM, the concentration of the PebA:DHBV complex was added in a micromolar excess up to 20 µM.

The difference in normalized fluorescence [‰] was plotted against the ligand concentration [nM]. All measurements were repeated at least twice and all the results as well as the K_d calculation were evaluated using the MO.Affinity Analysis Software (NanoTemper Technologies GmbH, Munich, Germany).

3.2 Development of “on-column” FDBR assays

3.2.1 FDBRs show activity after immobilization on chromatography beads

Based on earlier experiments, a metabolic channeling of the intermediate DHBV from PebA to PebB was postulated. To gain more insight into this process and to test, whether direct protein-protein interaction is involved the so-called “on-column” assay (OCA) was established. In contrast to the standard FDBR assay, with the “on column” assay the tested FDBRs were bound to an affinity chromatography resin via the corresponding tag and an enzyme assay was conducted with immobilized proteins. The first test was to check whether immobilization of GST-tagged PebA on column material retained the enzymatic activity. Therefore, the complex of GST-tagged PebA and BV IXα was bound on GST-sepharose and an FDBR-assay was performed as described. The initial green color of the bound complex turned into a violet color after a couple of minutes, indicating the formation of DHBV (Figure 3.8 A). Interestingly, the conversion to DHBV was only observed when the on-column assay was performed under micro-oxic conditions (Data not shown), i.e. when an oxygen scavenging system (OSS) was present. Although the OSS is also part of our regular FDBR assay in solution, the conversion of the substrates is also observed in assays lacking this system (Frankenberg and Lagarias, 2003). As substrate turnover of the “on-column” assay cannot be monitored using UV-Vis spectroscopy, a control FDBR assay was performed ahead in solution and monitored via UV-Vis spectroscopy. This was used to calculate the time for full substrate conversion. The product of this conventional assay was also used as the bilin standard for the following HPLC analysis of the reaction products directly after the “on-column” experiment. The reaction time of all “on-column” assays was set to 10 minutes based on the control assays. Performing an “on-column” assay with 10 µM GST-tagged PebA:BV showed marginal amounts of DHBV in the wash fraction after washing with two CV of assay buffer. DHBV eluted together with PebA right after treating the GST-sepharose with three CV of elution buffer. HPLC analysis confirmed the identity of DHBV (Figure 3.8 B).

3.2.2 The intermediate DHBV is transferred from PebA to PebB on the column

In order to test whether the substrate bound DHBV can be directly transferred to PebB, the following set-up was chosen: After performing an OCA of PebA and subsequent washing steps, 3 CV of assay buffer containing 10 µM of His-tagged PebB were run over the column. Here the release of the majority of bound DHBV from PebA was observed and HPLC analysis confirmed the elution of DHBV together with PebB (Figure 3.8 C). At last, GST-tagged PebA was eluted from the GST-sepharose with only a minor amount of DHBV being detectable (Figure 3.8 C). These results confirmed the data obtained with fluorescence titration (Figure 3.7) indicating a higher affinity of DHBV towards PebB.

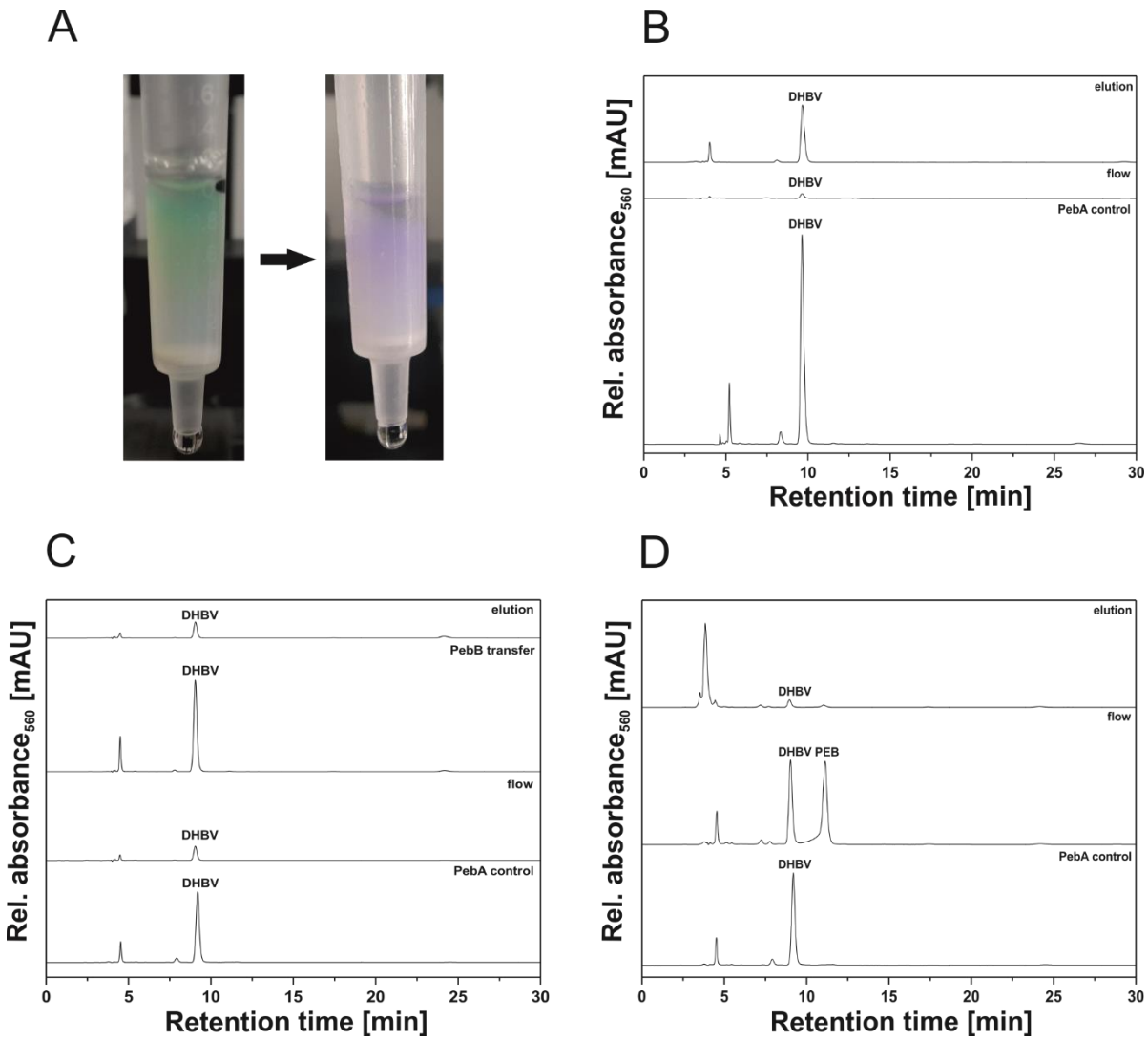

Figure 3.8: Establishment of an "on-column"- bilin reductase assay to investigate the transient substrate interaction between PebA and PebB.

(A) 10 µM GST-tagged PebA with an equimolar concentration of BV was bound to 0.5 mL GST-sepharose and a FDBR assay was performed by adding all required components (including the oxygen scavenging system) to the column. After approximately five minutes a change in color from green to violet was observed. Without the oxygen scavenging system, no product formation was detectable (data not shown). **(B)** Assay as described in (A). After ten minutes the column was washed with two CV washing buffer and the tagged PebA was then eluted with three CV elution buffer. Fractions were collected and bilins were purified as described. **(C)** Assay as described in (A). After ten minutes the column was washed with two CV washing buffer followed by an additional washing with three CV washing buffer containing 10 µM PebB. Finally, the tagged PebA was eluted with three CV elution buffer. Fractions were collected and bilins were purified as described. **(D)** Assay as described in (A). After ten minutes the column was washed with two CV washing buffer and the tagged proteins were eluted with three CV elution buffer. Fractions were collected and bilins were purified as described.

The bilins in all collected fractions were analyzed using HPLC on a Luna 5 µm RP C18-column (Phenomenex) with acetone and 20 mM formic acid (50:50 (v/v)) as the mobile phase at a flow rate of 0.6 ml/min. All reaction products were monitored at 560 nm.

3.2.3 Column immobilized PebA and PebB are still functional and show activity

In addition to a single enzyme assay on the column, the next test was to check whether it is also possible to perform a coupled FDBR assay on the column, with both PebA and PebB each fused to the GST-tag. For this set up, 10 µM of PebA:BV complex was added first to the column as described before and the reaction was performed as described above. The whole reaction time was also set to ten minutes but after five minutes 10 µM of GST-tagged PebB was added to the column. The collected wash fraction contained the majority of the produced DHBV and all produced PEB. The final elution of both FDBRs in this fraction contained just minor amounts of free DHBV and no PEB (Figure 3.8 D).

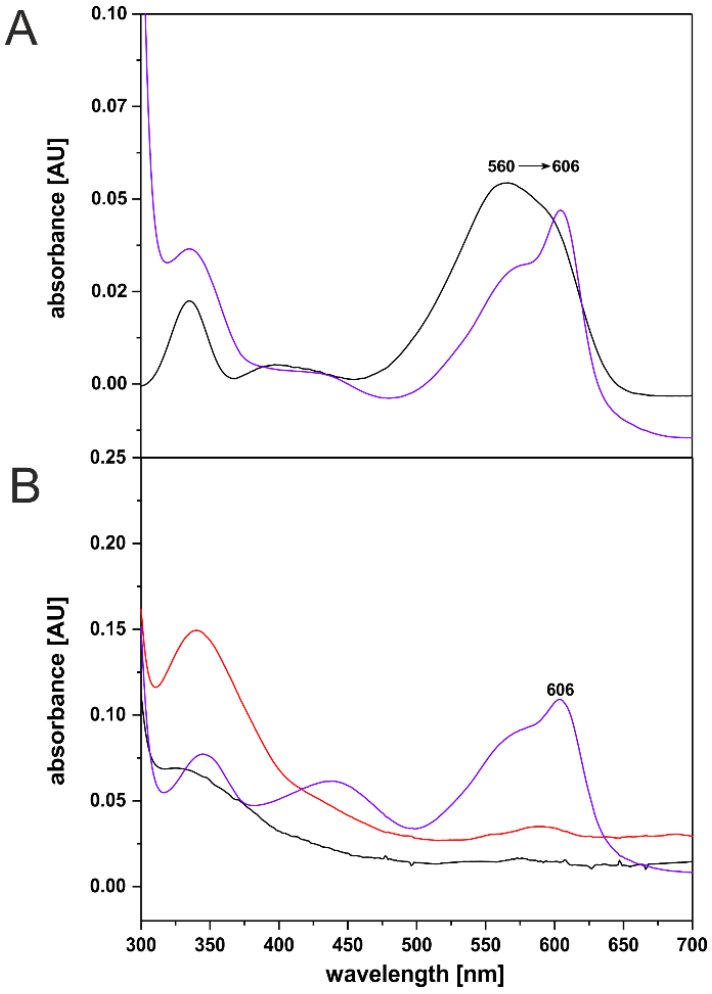

Fig. 3.9: Interaction between PebA and PebB results in the direct transfer of DHBV.

(A) Binding spectra of PebB:DHBV complex in comparison to the protein free bilin via UV-vis spectroscopy. 10 µM PebB was incubated with an equimolar amount of DHBV in TES/KOH buffer, pH 7.5 (violet line). The black line shows protein free DHBV with a concentration of 10 µM in TES/KOH buffer, pH 7.5. **(B)** UV-Vis spectra of the transferred reaction product from an OCA with Strep-*tagged* PebA and His-*tagged* PebB. The OCA-column were prepared as described by adding 10 µM Strep-tagged PebA with an equimolar amount of BV to 0.5 mL streptactin-agarose and a FDBR assay was employed by adding all required components (including the oxygen scavenging system) to the column. After ten minutes the column was washed with two CV washing buffer (red line) and an additional washing with three CV washing buffer containing His-*tagged* PebB (violet line). The black line shows the absorbance of the flow right after the column cap was removed.

All spectra were smoothed with Origin® 2017.

These results indicated that both enzymes can interact on the column and strengthen the observation of a DHBV channeling from PebA to PebB. Earlier studies showed a lower affinity of PebB to PEB (5.8 µM) than PebB to DHBV, and this result fits to this previous observation.

3.2.4 UV-Vis spectroscopy confirmed the FDBR:bilin complex

The transfer of the intermediate DHBV was not only tracked via HPLC analysis but due to the alteration of the spectral absorbance properties of the bilins in their free and in their complexed form together with FDBRs, the collected OCA fractions (wash, PebB-wash and elution, Fig 3.8 C) were also monitored via UV-Vis-spectroscopy. As a reference, 10 µM of free DHBV was dissolved in assay buffer and a whole spectrum was taken. The free bilin DHBV showed an absorbance maximum at 560 nm, as described previously. The addition of 10 µM PebB to the free bilin led to a typical shift of the absorbance maxima from 560 nm to 606 nm, indicating the FDBR-bilin complex formation (Figure 3.9 A). These three fractions were analyzed via UV-Vis spectroscopy. As expected, DHBV was not present in the washing fraction. The majority of DHBV co-eluted with the PebB-washing fraction. Here, the formation of the PebB:DHBV complex with its typical spectral properties resulting in an absorbance maximum of 606 nm was observed (Figure 3.9 B).

3.3 Creating a fusion protein of PebA and PebB

3.3.1 A simple base insertion leads to the fusion of PebA and PebB

In cyanobacteria, the formation of PEB requires the activity of two sequential FDBRs, PebA and PebB. Often, the encoding genes are located next to each other in either a bi- or a tricistronic operon, together with a gene encoding for a heme oxygenase. In *Synechococcus sp.* WH8020 the genes encoding for *pebA* and *pebB* share an overlapping region. The *pebA* stop codon TGA is part of the *pebB* start codon *ATG* (Figure 3.10, upper half). The artificial fusion of these two genes was then mediated by the insertion of a guanine into the start-stop-region of the *pebAB*-operon generating a direct translational fusion of both proteins, termed PebAgB. The newly generated codon *GTG* encodes for a valine residue, which now serves as a diminutive linker between PebA and PebB (Figure 3.10, upper half).

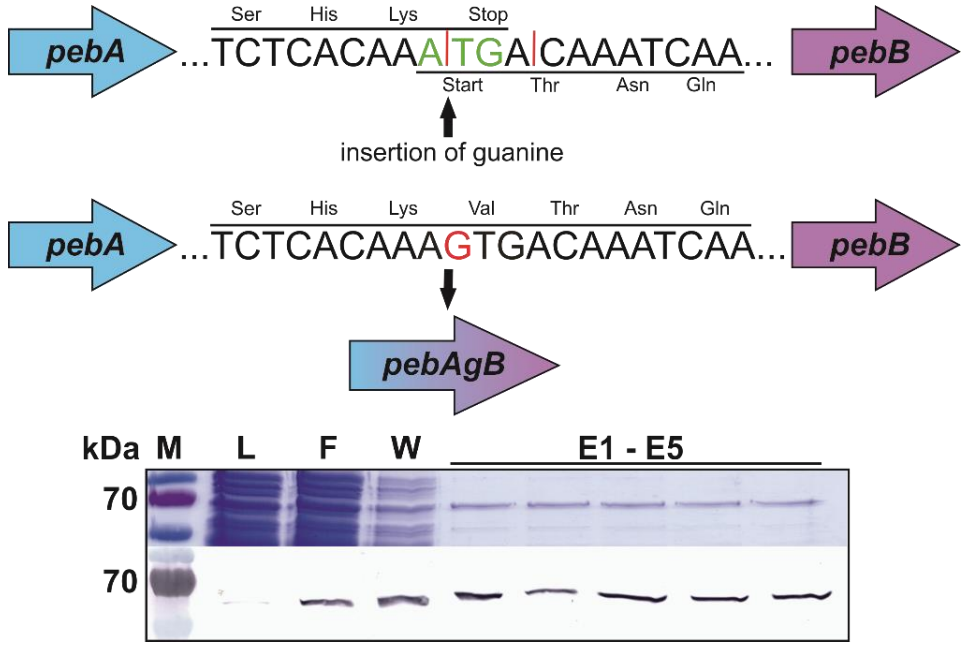

Figure 3.10: Construction of the fusion protein PebAgB.

The construction of the translational fusion protein PebAgB was mediated by an insertion of a guanine base into the start-stop (green color = start codon for *pebB*, red bars = stop codon for *pebA*) codon of the *pebAB*-operon via QuikChange®-mutagenesis. This insertion resulted in a frameshift of the *pebB* (violet arrow) into the translational frame of *pebA* (blue arrow) creating a codon for valine as a diminutive linker between both genes. The derived fusion gene *pebAgB* (blue-violet arrow) was created in the pASK-IBA-45^{+}-vector (IBA Life Science GmbH) creating a N-terminal *strep*-tag fusion as well as a C-terminal *his*-tag fusion. Production of the fusion protein was followed by SDS-PAGE and Western Blot analysis (Strep-Tactin® AP conjugate). M = protein ladder (PageRuler™ Prestained, Thermo Scientific), L=lysate, F=flow, W=wash, E=elution.

3.3.2 The PebAgB translational fusion protein shows PebS-like activity

PebAgB was heterologously produced and purified using affinity chromatography (Fig. 3.10, lower half) via Streptactin agarose. The yield of this protein production was quite low, even when tested several growing conditions and/or media to improve the amount of purified protein (concentration of purified PebAgB per 1 l *E. coli* culture = Ø 1-3 mg / ml). The Western blot analysis did show produced fusion protein (Fig 3.10, lower half). The activity of the fusion protein PebAgB was checked and the established anaerobic bilin reductase assay was performed in comparison to the cyanophage-encoded bifunctional FDBR PebS. The enzymatic turnover was monitored for ten minutes via UV-Vis spectroscopy (Figure 3.11 A). The initial absorbance (Figure 3.11 A, green line) of the FDBR:BV complex with an absorbance at 660 nm decreased during the first few minutes of the reaction. Shortly thereafter, the formation of substrate radical intermediates was monitored indicated by an increase in absorbance at 450 nm and 750 nm (1972; Busch *et al.*, 2011a; Tu *et al.*, 2004). Next, the formation of DHBV was then observed, indicated by a simultaneously decrease of the radical absorbance and an increasing absorbance maximum at 580 nm (Figure 3.11 A, violet line).

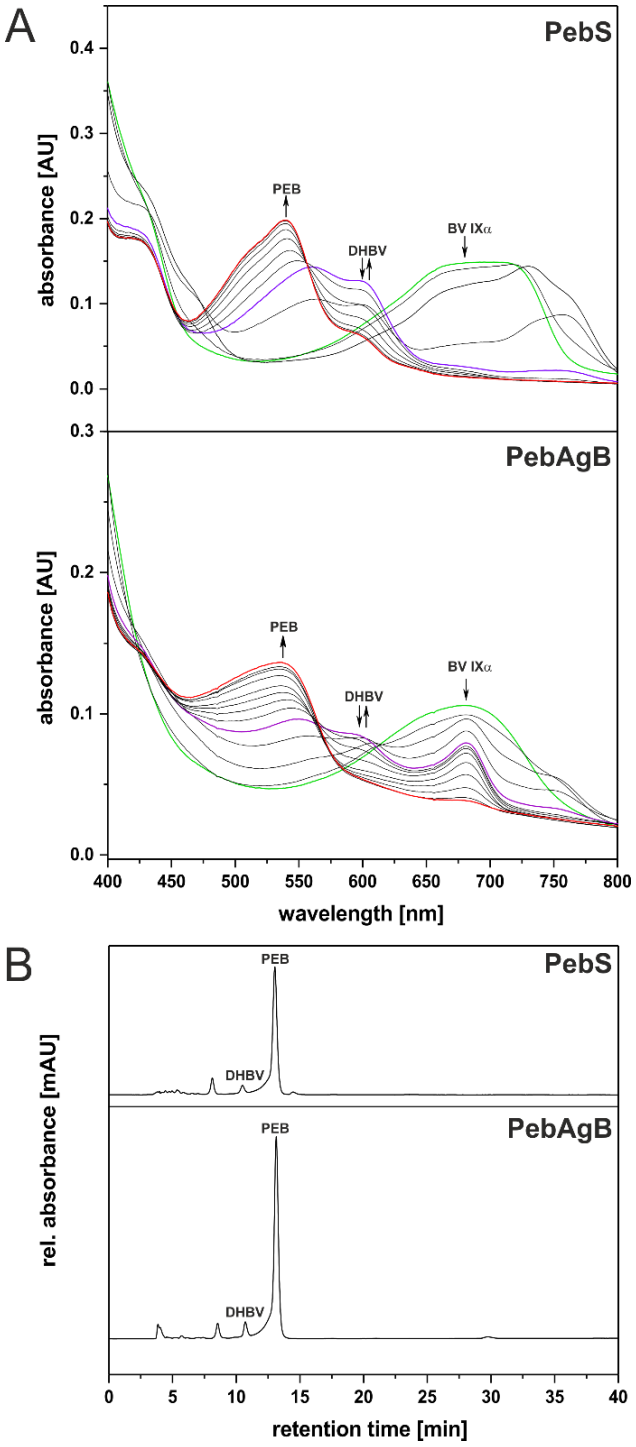

Figure 3.11: The fusion protein PebAgB shows PebS-like activity.

(A) Time-resolved UV-Vis spectra of an anaerobic bilin reductase assay using 10 µM of PebS respectively PebAgB with equimolar amounts of BV. The PEB formation was tracked every 30 s for a maximum reaction time of 10 minutes. The starting absorbance of the FDBR:BV complex is indicated with a green line, the maximal absorbance of the derived intermediate DHBV is shown as the violet line. The red line displays the end of the PEB formation with the maximal product absorbance. Peak maxima are indicated with the corresponding bilin name. For further investigation the reaction products were purified for HPLC analysis. **(B)** The reaction products were analyzed with HPLC on a Luna 5 µm RP C_{18}-column (Phenomenex) with acetone and 20 mM formic acid (50:50/v/v) as the mobile phase at a flow rate of 0.6 ml/min. All reaction products were monitored at 560 nm. The PebS reaction products were used as a standard for bilin identification.

The last steps of the reaction showed a shift of the absorbance maxima from 580 nm to 540 nm (Fig. 3.11 A, red line) which indicated the further reduction of DHBV to PEB. The observed reaction steps of the PebAgB assay fit well within the reaction pattern of the PebS reaction. Based on the spectroscopical properties of the PebAgB reaction, the newly constructed fusion enzyme catalyzes the reaction from BV IXα to PEB via the intermediate DHBV. Final verification of the reaction product was performed via HPLC analysis with known standard bilins produced by the PebS reaction. The elution profile of the produced bilins from the PebAgB reaction matched the elution profile of the PebS reaction products. The main product of the PebAgB reaction is 3*Z*-PEB, but 3*E*-PEB is also produced during this reaction (Fig. 3.11 B).

3.4 Time-coursed experiments of different FDBRs to produce PEB

Time-resolved FDBR assays were employed to get further insights into PEB formation and moreover the postulated metabolic channeling of the intermediate 15,16- DHBV. The FDBRs PebA & PebB, PebS (originated from the cyanophage P-SSM2) and the fusion protein PebAgB were produced and purified as described (see sections 2.4.2 & 2.4.6). The product or intermediate formation of the tested FDBRs were analyzed in a time-course experiment where samples were taken from the assay solution at different time points during the reaction followed by a subsequent analysis of the bilins via HPLC. PebA and PebB were employed simultaneously in this experiment. The comparison of these now three different pathways of PEB formation should reveal more insights into the reaction mechanisms. Using this method, the course of the bilin formation during each enzyme's reaction was visualized by integrating the obtained peaks of each corresponding product and setting these data in relation to the total peak areas. The calculated peak areas were then plotted against the reaction time (Fig. 3.12).

The time-resolved assays revealed that the amount of BV IXα decreased when catalyzed by the FDBRs PebS and PebAgB. The reduction to 15,16-DHBV proceeded more rapidly by these proteins (60 – 75 % at minute 3) whereas the double enzyme system PebAB seemed to stall BV IXα over a longer time period. Here, the intermediate formation reached a similar amount of DHBV in the later phase of the reaction (60 % at minute 5). Interestingly, all three different PEB producing enzymes seemed to form the final product in the later stages of this reaction period. The PEB formation during the PebAgB reaction was detectable from minute 3 and in later stages. PebS as well as PebAB proceeded later with the conversion of 15,16-DHBV to PEB. The first peak of PEB emerged at minute 5 and increased slowly.

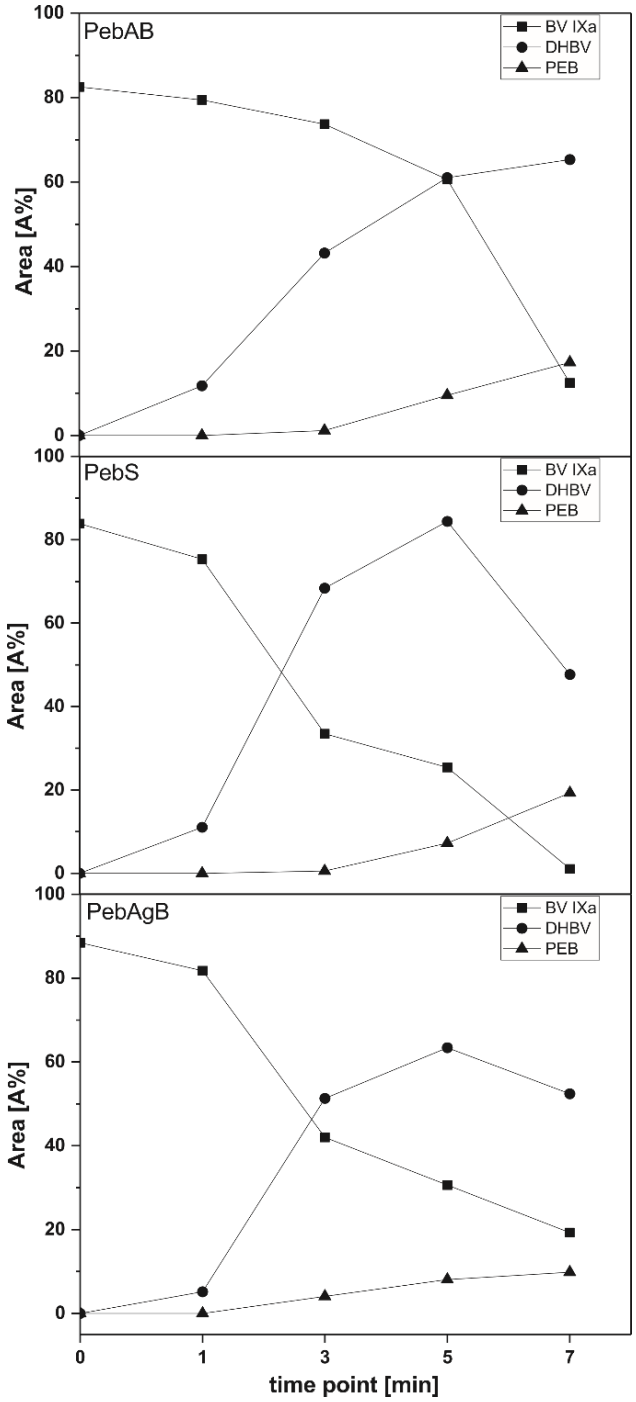

Figure 3.12: Comparison of the PEB formation velocity of PebAB, PebS and the fusion protein PebAgB by time-course experiments.

A standard FDBR assay was employed for the tested FDBRs PebAB, PebS and the newly created fusion protein PebAgB in a 3 ml volume for ten minutes. The reaction was monitored via UV-Vis spectroscopy and at each given time point (0 min, 1 min, 3 min, 5 min and 7 min) a sample of 500 µl was taken out and added immediately to 0.1 % TFA solution to stop the reaction in the sample. Each sample was then prepared for HPLC analysis (see section 2.4.9) to evaluate the amount of product formation during the assays. Therefore, the obtained peaks corresponding to BV, DHBV and PEB were integrated using the Open Lab CDS Chemstation Edition (Agilent Technologies) integration tool. At each time point the percentage area of these peaks were compared for each enzyme and the bilin formation is then visualized by plotting the time points against the area in Origin® 2017.

The fusion protein PebAgB seemed to have the reaction characteristics of both other PEB formation systems. On the one hand, PebAgB is able to convert BV IXα to 15,16-DHBV as rapidly as PebS. On the other hand, the fusion protein reduced the intermediate molecule to PEB as a similar rate to the coupled enzymes PebAB, which displayed the original characteristic of the protein fusion. This result confirmed that the protein fusion of PebA & PebB enhanced DHBV formation, which was similar to PebS, but the formation of terminal product PEB was not enhanced. In earlier studies it was shown that the phage enzyme PebS is able to convert BV IXα to PEB in a rapid manner, but during this time-course experiment the velocity of this FDBR was reduced for unknown reasons. The postulated metabolic channeling was not clearly proven by this method since there was still room for speculation whether a single molecule of PebAgB performs the whole reduction from BV IXα to PEB, or if a second protein molecule enters upside down and the intermediate was then channeled to that partner.

3.5 Bacterial Two-Hybrid system shows slight interactions

Another quick and easy method to detect and characterize protein-protein interactions *in vivo* is the Bacterial Two-Hybrid system (BacTH). The complementation of the lacking adenylate cyclase (AC) was used to determine protein interaction in *E. coli* BTH101 by introducing two plasmids with each fragment (T18 and T25) of the catalytic domains of the AC from *Bordetella pertussis*. Each fragment was fused with proteins with a predicted interaction, here with PebA and PebB. If there is an interaction of both enzymes, the β-galactosidase is expressed and the activity of this enzyme indirectly displayed the intensity of the interaction. Using PebA and PebB in different orientation in the BacTH-vectors led to a similar result. An interaction was detected in all combinations including the controls but not every colony showed the same color intensity of either red or blue color depending on detection methods used. On MacConkey agar plates, some of the colonies formed a strong red halo (No. 4; No. 5; No. 6 & No. 8) around the center. By comparison of these colonies to the positive control, this strong color intensity suggested an interaction event in these cells, whereas other colonies formed no or very small halos (No 3; No. 7 and No. 9). The coloration was not as strong in those colonies and by comparing these colonies to the controls the assumption of an interaction was uncertain (Fig. 3.13 A). The same outcome was true when the cells were dripped on LB-agar plates containing X-Gal giving blue colored colonies when an interaction occurred (Fig. 3.13 B). The orientation of the fusion proteins might have had an influence on the interaction but no pattern was observed. The complex signal cascade of this detection system combined with the indirect detection of the interaction could lead to variations in the output signals and therefore the creation of false-positives cannot be excluded.

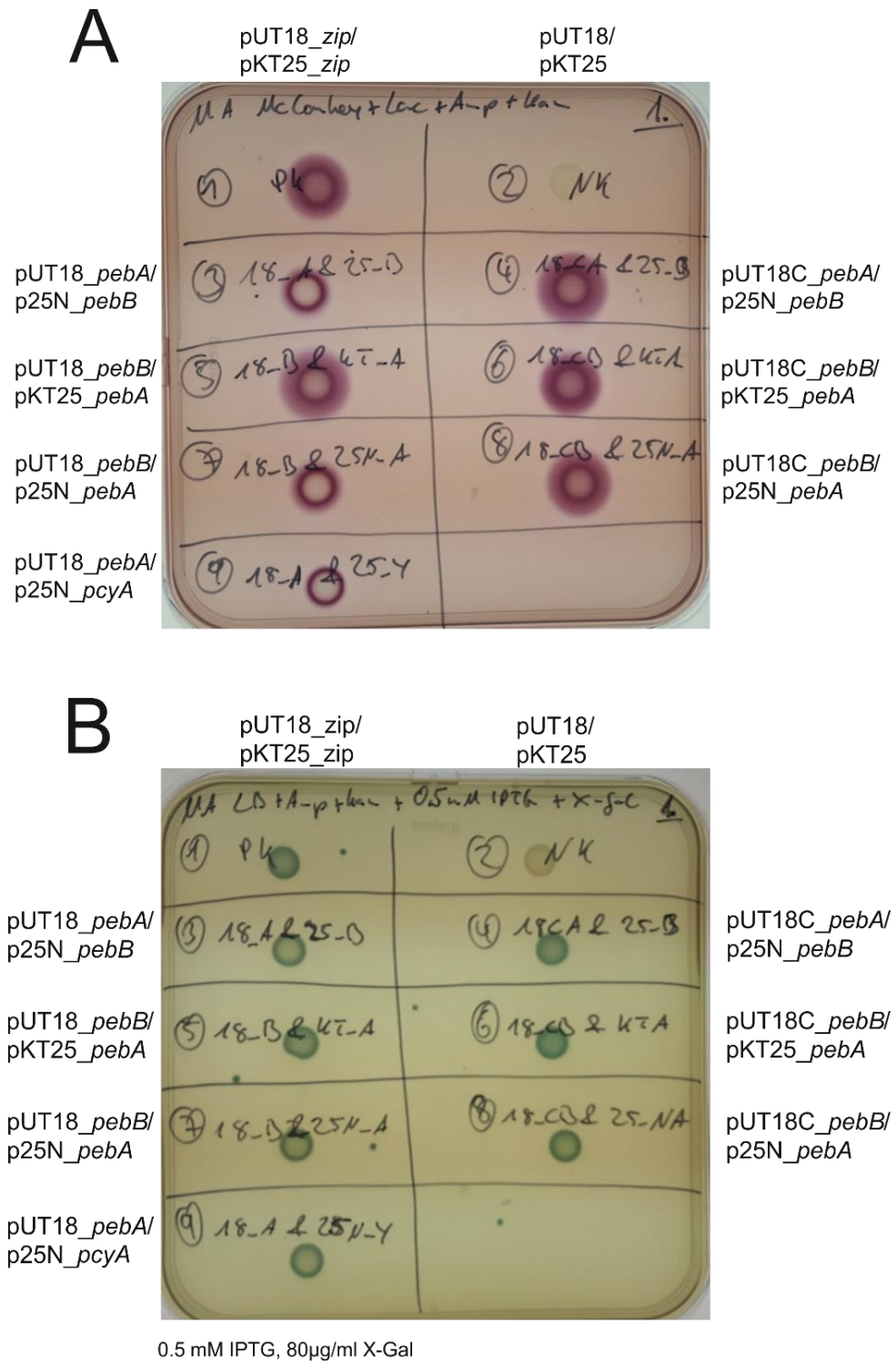

Figure 3.13: Confirmation of PebA and PebB interaction via Bacterial Two-Hybrid

E. coli BTH 101 cells were transformed with two plasmids each carrying one part of the catalytic domain of the adenylate cyclase from *Bordetella pertussis* fused with *pebA* and *pebB*, respectively. The cells were incubated at 37 °C overnight and then each transformant was resuspended in fresh LB media and dripped on two different agar plates which induced reporter gene activity of the β-galactosidase. Drop-plates were then incubated up to 24 h at 30 °C until a change in color was visible. **(A)** Different combinations of PebA and PebB (No.1 – No. 9) of *E. coli* BTH 101 transformants carrying BacTH plasmids dropped on MacConkey Agar containing 1 % Lactose. **(B)** Same procedure as in (A) but dripped on LB agar + 80 µg/ml X-Gal + 0.5 mM IPTG.

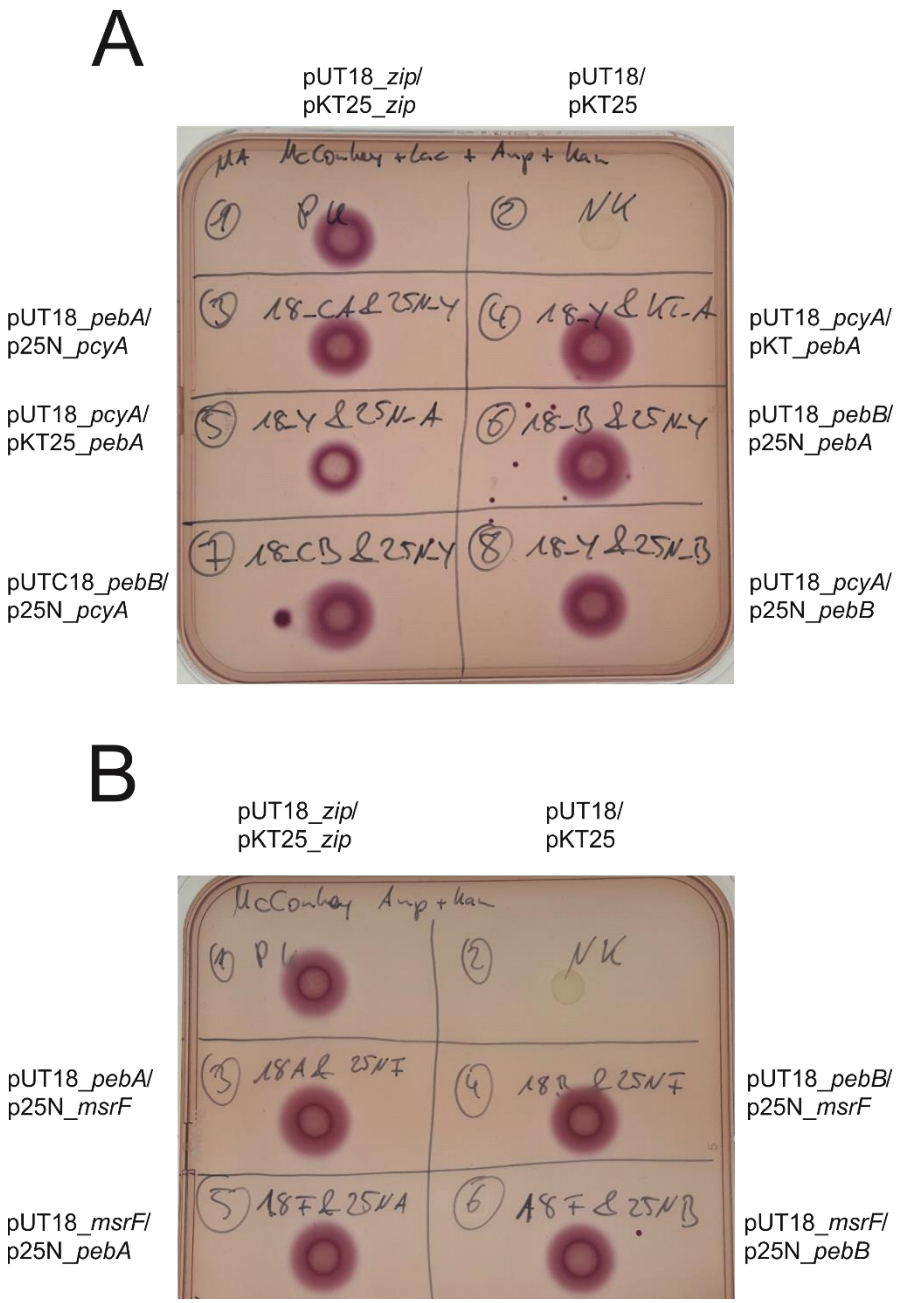

Figure 3.14: Control interaction of the BacTH system.

E. coli BTH 101 cells were transformed with two plasmids each carrying one part of the catalytic domain of the adenylate cyclase from *Bordetella pertussis* fused with *pebA* and *pebB*, respectively. The cells were incubated at 37 °C overnight and then each transformant was resuspended in fresh LB media and dripped on two different agar plates which induced reporter gene activity of the β-galactosidase. Drop-plates were then incubated up to 24 h at 30 °C until a change in color was visible. **(A)** Different combinations of PebA or PebB co-produced with the FDBR PcyA from *Anabaena sp.* PCC7120 (No.1 – No. 8) of *E. coli* BTH 101 transformants carrying BacTH plasmids dropped on MacConkey Agar containing 1 % Lactose. **(B)** Different combinations of PebA and PebB co-produced with the regulator protein MsrF from *Methanosarcina acetivorans* (No.1 – No. 6) of *E. coli* BTH 101 transformants carrying BacTH plasmids dropped on MacConkey Agar containing 1 % Lactose.

To test whether the interaction is specific or artificial, two additional control proteins were used in combination with PebA and PebB separately. On the one hand PcyA was used because it is also a FDBR and similar in structure and sequence to PebA/PebB.

The second protein used as a control was MsrF, which is an archaeal regulator protein and involved in the expression of the methyltransferase MtsD from the anaerobic archaeon *Methanosarcina acetivorans* (Bose *et al.*, 2009). Based on the prediction, control proteins should interact with neither PebA nor PebB.

Interestingly, the coproduction of either PebA or PebB together with PcyA (Fig 3.14 A) as well as their coproduction with MsrF (Fig 3.14 B) exhibited also strong interactions based on the β-galactosidase activity on the plates. The halos arounds the colonies from both MacConkey agar plates were mostly large and similar to the positive control. So far, this method proved no specific interaction of the tested FDBRs PebA and PebB because both proteins seem to interact with the control proteins. The possibility of false-positives is not excluded, but this part of the project was not further pursued.

3.6 PebA and PebB can be crosslinked with formaldehyde

The protein-protein interaction of PebA and PebB was also investigated *in vivo* in *E. coli* cells with the Strep-protein interaction experiment (SPINE). This method combined the Strep-tag protein purification with a reversible cross-linking via formaldehyde inside the *E. coli* cells. Crosslinked proteins were supposed to be examined to identify the interaction sites on the peptide surface via mass spectrometry analysis. An increasing concentration of formaldehyde (0 %, 0.2 %, 0.4 % and 0.6 %) was used to start the cross-linking event. Cross-linked proteins were detected via Western Blot analysis with antibodies against the Strep-tag as well as the His_6-tag (Fig. 3.15 A). Staining of the SDS-PAGE revealed PebA production in all fractions as expected (~28 kDa). Interestingly, with increasing concentration of the cross-linking reagent formaldehyde the protein pattern of the gel got more and more diffuse. This strongly toxic reagent somehow had also an influence on the gel matrix or even on the protein structure itself so the staining solution was not able to bind completely. However, the optimal concentration for crosslinking experiments should not exceed 0.4 % in the growth media. With the addition of formaldehyde more protein bands appeared with an estimated size of double the size of PebA (~55 - 60 kDa) shown by the Western Blot performed with Strep-tag antibody (Fig. 3.15 B). Here, the presence of PebA is clearly shown in all fractions at ~ 28 kDa. The newly appeared signals of crosslinked proteins with the greater molecular sizes suggested that PebA interacted with a protein of similar size. It was probably the co-produced PebB or another molecule of PebA which were crosslinked and caused the size shift on the gel. To prove whether PebB is crosslinked to PebA another Western Blot with anti-His_6 antibody was performed. This experiment revealed that PebB was crosslinked to PebA because it co-eluted together with PebA in all elution fractions independent of the formaldehyde concentration. Additionally, the bands of ~ 55 – 60 kDa in each elution fraction overlapped with the Strep-tag Western Blot, therefore these fractions contained both FDBRs PebA and PebB.

Additionally, more signals appeared with molecular sizes beyond 100 kDa, indicating crosslinking events of more than two molecules of PebB (Fig. 3.15 C). To figure out if there is a stronger interaction when the natural substrate of PebA is present in the cells, a coproduction of PebAB together with the heme oxygenase HO1 from *Synechocystis sp.* PCC 6803 provided from the expression plasmid pTD_*ho1* was conducted. This experiment gave inconclusive results. For unknown reasons, neither PebA nor PebB was not produced or the expression of the heme oxygenase did not work confirmed by Western Blot analysis (Data not shown). Therefore, this experiment was not further followed up.

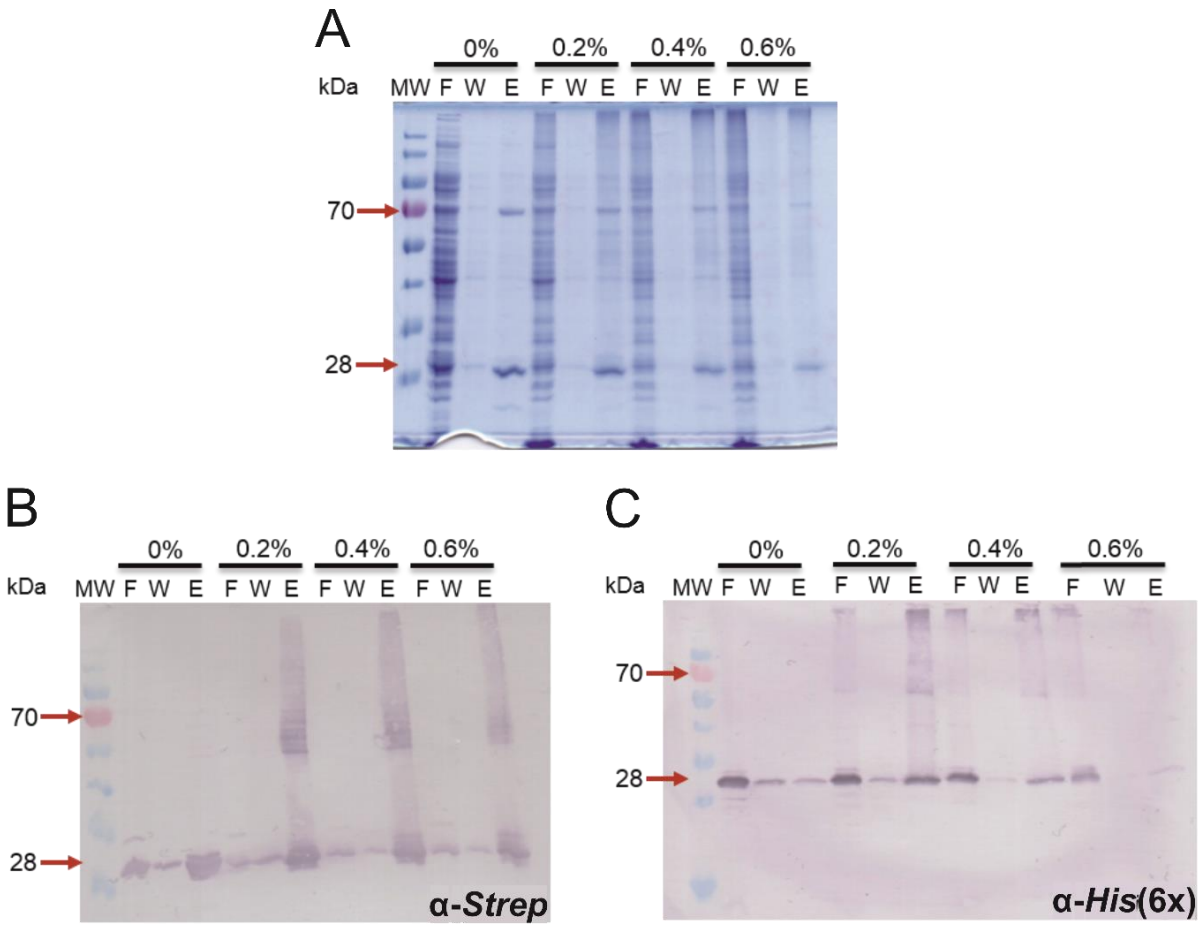

Figure 3.15: Evaluation of the SPINE of PebA and PebB via Western Blot analysis.

(A) Analysis of the purification fractions of Strep-tagged PebA after addition of different concentrations of the crosslinking reagent formaldehyde. After induction with 200 ng/µl anhydrotetracycline the cells were grown under shaking conditions at 30 °C for 2.5 h and subsequently formaldehyde was added to the cells. Each flask was then incubated for another 30 min at 30 °C before harvesting and purification on Streptactin agarose. Samples of the purification steps were taken for SDS-PAGE and Western Blot analysis. **(B)** Western Blot analysis with Streptactin-AP conjugate antibody to verify PebA production and also crosslinking events with PebA. **(C)** Western Blot analysis with anti-His_6 antibody to detect crosslinked PebB which is also purified together with PebA on Streptactin agarose. (MW = protein ladder (PageRuler™ Prestained, Thermo Scientific); F = flow fraction; W = washing fraction; E = elution fraction; α = antibody specific for the used Tag).

3.7 Integration of genes for phycobilin biosynthesis into *E. coli* BL21 (DE3)

As a side project of this work the construction of an *E. coli* strain with incorporated genes for phycobilin biosynthesis was planned and conducted. To integrate the phycobilin biosynthesis genes into *E. coli*, the gene for an appropriate heme oxygenase had to be cloned into the host's genome first. For this, the heme oxygenase gene *ho1* from *Synechocystis sp.* PCC6803 was linked with the selective marker for kanamycin selection and integrated into the *lacZ* locus of *E. coli* BL21 (DE3) without destroying the native *lac*-promotor. Transformants were then grown under selection for kanamycin and β-galactosidase activity. White colonies were screened via PCR with internal *lacZYA* primers and positive insertions were subsequently sequenced.

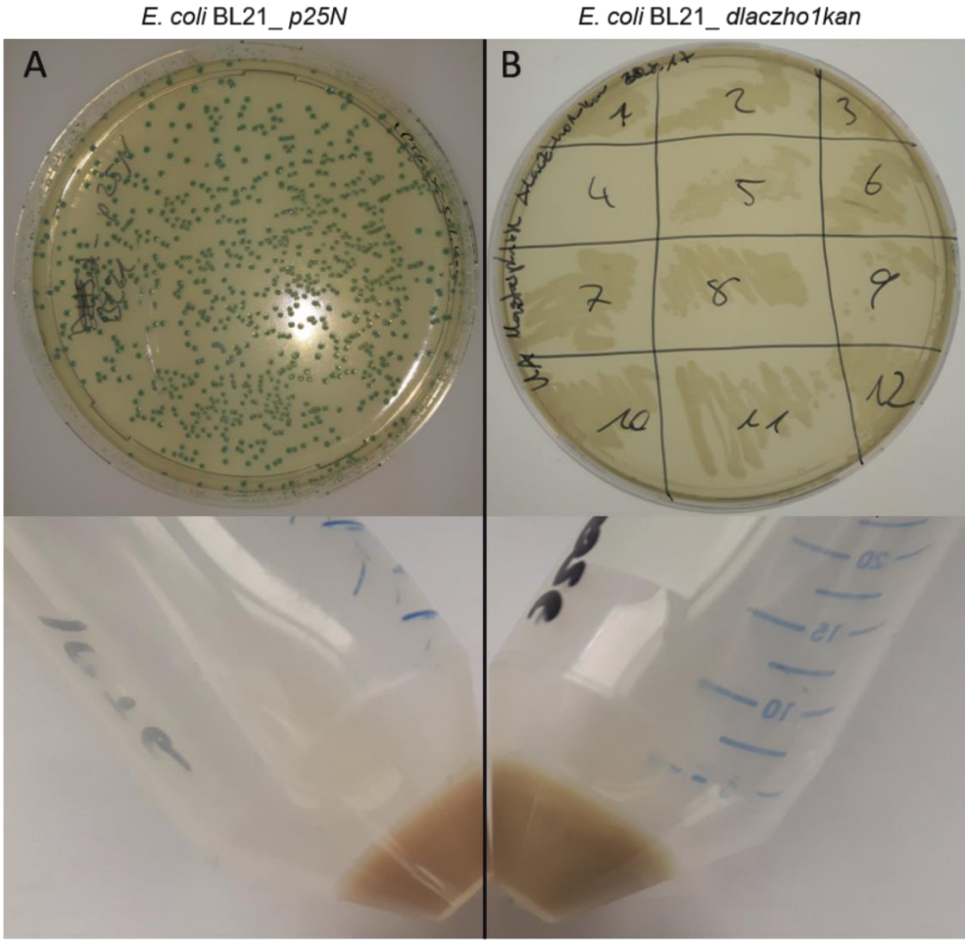

Figure 3.16: Comparison of *E. coli* Bl21 WT and the mutant after chromosomal integration of *ho1*.

(A) *E coli* BL21 (DE3) WT was transformed with the p25N plasmid only to integrate a kanamycin resistance and plated on LB agar containing Kanamycin and 50 µg/ml X-Gal. The β-galactosidase activity was observed by the appearance of blue colonies since this WT strain still possess a functional *lacZ* gene. Furthermore, growing the cells to an OD_{578} = 0.5 an induction with 10% lactose led to normal brownish colored cells after harvesting after 3 h of incubation. **(B)** Several *E. coli* BL21_*dlacZho1kan* mutants showed a defect in β-galactosidase activity on X-Gal plates. All colonies appeared in white color. An induction of the *ho1* expression by the addition of 10% lactose led to slightly green colored cells.

The first screening of the newly generated *E. coli* mutants revealed a defect in the *lacZ* gene. All transformed colonies appeared white in color compared to the WT strain with no mutations inside the *lac*-operon (Fig. 3.16 A). Interestingly, the mutants could be grown normally in liquid culture using non-selective growing conditions similar to the WT strain (see section 2.2.3). The induction of *ho1* expression with 10% lactose led to the formation of slightly green colored cells, indicating a functional heme oxygenase activity. Only the verification of the mutant strains failed so far. The PCR reactions from purified DNA of the mutants mostly showed fragments of non-correct sizes (2.1 kb for the deletion mutant compared to 3.1 kb for the WT gene). Due to time reasons this project was not finished during this work but the idea of tetrapyrrole biosynthesis in *E. coli* should be continued in following projects.

4 Discussion

The main objective of this work was to get a closer look into the interaction of PebA and PebB during phycoerythrobilin biosynthesis. Both enzymes are involved in PEB formation and during the biosynthesis an intermediate molecule is formed and transferred from one enzyme to the subsequent following enzyme. The intermediate molecule 15,16-dihydrobiliverdin is made by PebA and further reduced to phycoerythrobilin by PebB. In earlier studies several hints for protein-protein interaction were found as well as some indications for a substrate channeling process. The genomic localization of *pebA* and *pebB* points to an interaction or a cooperation during the pigment biosynthesis. Also, the fact that the intermediate 15,16-DHBV needs to be rapidly processed because of the high instability of this molecule is a hint for a substrate channeling. Moreover, the PEB formation occurs in yet two known pathways mediated by either the PebAB interaction or by single enzyme systems like the phage originated FDBRs PebS/PcyX. Since these stand-alone enzymes from phages can catalyze the identical reaction as the cyanobacterial system the question why these FDBRs are still not incorporated into the cyanobacterial genome was raised. PebA and PebS for example share a high structural homology but PebA stops the reaction process right after the DHBV formation whereas PebS proceeds further with the PEB formation (Busch *et al.*, 2011a; Dammeyer and Frankenberg-Dinkel, 2006). During this project, several hints for a directional channeling process were gathered by the determination of new binding constants (see section 4.1), by the newly developed “on-column” assay (see section 4.2), by biochemical analysis (see section 4.3) and by cross-linking and BacTH experiments (see section 4.4).

4.1 High affinity to DHBV is the key step in PEB formation

The proteins PebA and PebB used during this study are originated from *Synechococcus sp.* WH 8020, a CCA capable marine cyanobacterium. Photosynthetic marine organisms encounter several light conditions during their life cycles. In order to adapt to changes in the availability of light, cyanobacteria are able to change their composition of their phycobiliproteins in the phycobilisomes. Interestingly, red algae and cryptophytes do not undergo this process (Gutu and Kehoe, 2012). Along with the reorganization of the phycobiliprotein content the appropriate chromophores need to be newly synthesized by FDBRs and then attached to the PBP by lyases (Scheer and Zhao, 2008). During exposure to green light conditions, which occur in moderate depth of water, the genes *pebAB* were highly expressed (Alvey *et al.*, 2003). The phycobilisomes were recomposed and more PE is incorporated into the PBS antennae structures. In CCA capable cyanobacteria the FDBRs PebA and PebB are responsible for the PEB biosynthesis. The recombinant production of PebA and PebB was successful in view of protein yields. Along with the co-produced chaperones GroEL and GroES, the yield was even higher.

The co-translational folding mediated by the additional chaperones played an important role in protein stability (Wruck *et al.*, 2017). Therefore, PebA and PebB showed a very high stability after purification indicated by a high enzyme activity even after storage for several weeks. Since DHBV is a labile molecule, which is known from previous projects, a secured transfer of the intermediate to PebB is mandatory. A metabolic channeling ensures a direct transfer of DHBV from PebA to PebB without releasing the molecule into the cytosol. The presence of this molecule plays an important role during the postulated interaction and it its suggested to enhance the transfer process. Both purified FDBRs were analyzed for their binding affinity to their product and/or substrate 15,16-DHBV. Via fluorescence titration, a reevaluation of the binding affinities to DHBV was made with the help of the intrinsic fluorescence of the FDBR:DHBV complex (Dammeyer and Frankenberg-Dinkel, 2006). Here, the previously calculated K_d-value for the affinity of DHBV to PebA was confirmed in a similar range (PebA:DHBV = 1.70 µM). This high affinity to the product means that DHBV will stay in the binding pocket of PebA after the reaction. The relatively rigid binding of DHBV in the active site of PebA also confirms the suggestion of a channeling mechanism which was also indicated in the earlier study with a similar method (Dammeyer and Frankenberg-Dinkel, 2006). On the other hand, the affinity of PebB to DHBV was shown to be 7x higher than calculated as in our previous work. The high affinity was indicated by a K_d-value in a nanomolar range (PebB:DHBV = 0,27 µM). The higher affinity of PebB to DHBV than PebA is the key step for the channeling process which ensures the transfer of DHBV out of PebAs binding pocket. On the other hand, the binding affinity to the product of PebB PEB was no reevaluated but its rather low compared to the intermediate DHBV (PebB:PEB = 5.8 µM, Dammeyer *et. al.*, 2006). This means, after PEB formation the binding pocket is available again for a new molecule of DHBV based on the higher affinity to its substrate. This already high affinity of PebB to DHBV is increased even more when the intermediate DHBV forms a complex with the prior enzyme PebA (K_d = 0.18 µM). The initial hypothesis of the importance of DHBV to enable the channeling process is confirmed. Without bound DHBV the affinity of PebB to PebA is in a low micromolar range (1.26 µM), but this result has to be repeated since only one approach led to a result. Several approaches were not measurable afterwards. This data fit perfectly with the suggestion of a channeling process. PebA holds DHBV until this molecule is picked up by PebB based on the high affinity. When PEB is formed it will be picked by a PEB-specific lyase so the affinity for the product has to be lower than for the substrate. The driving force behind the PEB biosynthesis is PebB since the high affinity to the PebA:DHBV complex leads to a rapid transfer without releasing the already formed DHBV to the cytosol. With the release of DHBV from PebA this FDBR is capable to acquire a new substrate molecule BV and can start a new turnover to DHBV. These results point to a further question whether the whole pathway of PEB biosynthesis proceeds via the channeling of all involved molecules: heme, BV and DHBV.

Examples for this kind of channels are also known from other tetrapyrrole biosynthesis pathways. During ALA biosynthesis the enzymes GluTR and GSAT form a direct channel to convert the substrates glycine and succinyl-CoA to ALA (Beale, 1999). Also, during vitamin B12 formation an example of a substrate channel is known for HBA. The enzyme CobH has a high affinity to hold HBA in its binding pocket until the subsequent enzyme CobNST picks it up (Deery *et al.*, 2012). This kind of transfer seems quite similar to the PebA and PebB interaction. A closer look into several tetrapyrrole biosynthesis pathways (heme, chlorophyll or cobalamins) reveals that there are several steps where labile intermediates have to be transferred to the subsequent following enzyme. It is known for several multi-cascaded reactions that the involved enzymes are not free-floating through the cytosol but the reactions are catalyzed by forming multienzyme complexes (so called metabolons or metabolic channels).The related enzymes in one metabolic pathway can form efficient enzyme-to-enzyme channels where the substrates can pass through which leads to an increase in the catalytic performance of all involved enzymes (Figure 4.1) (Lee *et al.*, 2012; Proschel *et al.*, 2015). The increased efficiency is based on the close proximity of the active sites of the enzymes allowing a direct transfer to maintain the flux of the substrate.

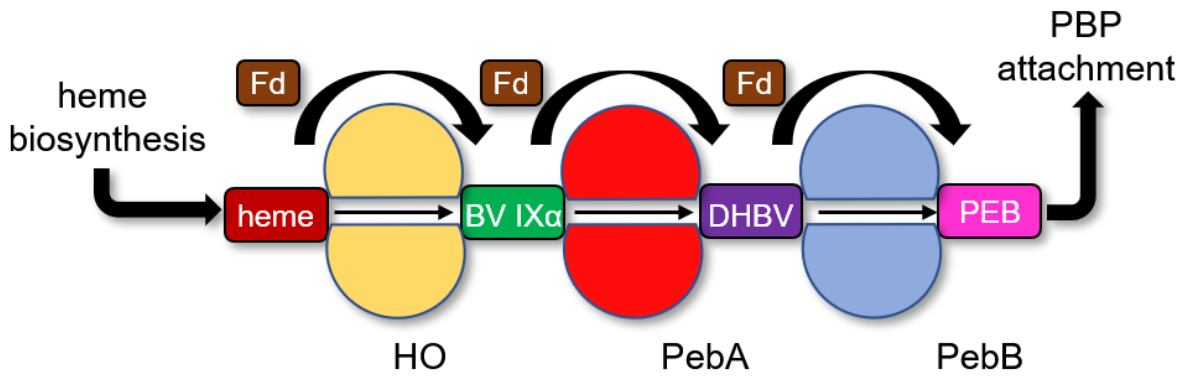

Figure 4.1: Model of the substrate channeling process during PEB formation.

Heme is taken from the heme biosynthesis pathway by the heme oxygenase to produce BV IXα, the first linear tetrapyrrole in chromophore biosynthesis, and this marks the start of the channeling process for pigment synthesis. A rapid PEB formation is ensured when all products are channeled in a fast manner between the involved enzymes. HO = heme oxygenase, Fd = ferredoxin, BV IXα = biliverdin IXα, DHBV = 15,16-dihydrobiliverdin, PEB = phycoerythrobilin, PBP = phycobiliprotein. (Adapted after Proschel *et al.*, 2015)

By forming those enzyme complexes the local concentration of the intermediates is higher around this complex which then favors the kinetics of the reactions. Also, the formed “pipeline” favors the correct synthesis of the final product and lowers the chance of side reactions or diffusion (Sweetlove and Fernie, 2013). Therefore, an interaction of PebA to the corresponding heme oxygenase as well as the involved ferredoxins is very likely as it was already shown during PCB biosynthesis (Okada, 2009).

In mammals the biliverdin reductase also showed an interaction with the heme oxygenase-2 and the corresponding electron donor cytochrome P450 reductase (Spencer *et al.*, 2014). In future experiments the interaction of PebA to a cyanobacterial HO should be tested as well as the determination of binding affinities to BV. For an optimal channeling process the K_d-value for PebA:BV has to be lower than to the product DHBV. Another interesting point is the way how the intermediate DHBV is transferred between both enzymes. In PebA the substrate BV IXα faces into the active site with the A- & D-ring pointing into the binding pocket, whereas the propionate side chains are directed to the outside of the enzyme. After the reduction of the C15 – C16 double bond it is suggested that the product DHBV remains in this position. After discussion with our long-term cooperation partner for FDRB crystallography at the Ruhr-University in Bochum, new insights came up regarding the orientation of DHBV in the binding pocket of PebB. During crystallographic experiments with PebB from the cryptophyte *Guillardia theta*, they were able to see how DHBV is bound in the enzyme's binding pocket. Interestingly, also DHBV is bound with the A- & D-ring facing into the enzymes active site but the orientation of the tetrapyrrole molecule is inverted. This means that somehow the DHBV is turned around during the transfer between both protein (unpublished Data from Johannes Sommerkamp, Protein Crystallography Group, Ruhr-University Bochum). There are not many options how this inversion can happen, but it will depend on the kind of interaction. During a proximity channel, DHBV can perform a turnaround in the split second where it is situated right between both interaction partners before it enters the active site of PebB. This may happen when the active sites of both enzymes are facing each other and when there is no direct contact. If the enzymes are located side by side so that the intermediate molecule can just "slide" from one the other then PebB has to be turned "face down" to explain the orientation of DHBV. Here, either proximity or direct channel are valid explanations for the turnaround situation of DHBV.

4.2 Immobilized FDBRs are still active and "on-column" assay confirmed the substrate channeling

The development of the "on-column" assays was considered as a success since all of the used FDBRs retained their activity on the column material. This is the first description of an activity assay with immobilized FDBRs. Surprisingly, the addition of an OSS is still crucial for the enzymatic activity because the assays were performed under aerobic conditions anyway. But the uprising radicals during this assay might inhibit the FDBR activity. With this method the tight binding ability of PebA to DHBV was also confirmed which was determined by fluorescent titration in the past and again during this work (Dammeyer and Frankenberg-Dinkel, 2006). Realizing the fact that DHBV remains bound to PebA after the assay on the column, we extended the "on-column" experiment with an additional washing step including PebB in the washing buffer before the elution. In this case PebB was not able to bind to the column material due to a different tag but was able to pull out DHBV from PebA (Figure 4.2).

DHBV not only co-eluted with PebB but also formed the typical FDBR:bilin complex with the enzyme indicated by the following UV-Vis spectroscopy after migration through the column. As it was shown that DHBV is being transferred on the column, a coupled enzyme assay was tested on the column, with both PebA and PebB immobilized on the column. Conducting a coupled FDBR assay on the column was also newly developed but the results were also satisfactory in view of enzyme activity. After HPLC analysis the products of both FDBRs (DHBV and PEB) were detectable. This observation suggests that PEB is released after the reaction since the proteins remained on the column. In earlier studies it was shown that PebB shows a much lower affinity to PEB (K_d = 5.8 µM) than to DHBV suggesting in presence of the intermediate PEB will be replaced by DHBV (Dammeyer and Frankenberg-Dinkel, 2006). *In vivo*, PEB is then picked up by phycobiliprotein lyases and afterwards attached to the phycoerythrin via the conserved cysteine site, so a release of the product makes absolutely sense to maintain the process of re-chromophorylation (Scheer and Zhao, 2008; Zhao *et al.*, 2007a; Zhao *et al.*, 2007b). DHBV was also found in similar amounts next to the elution of PEB. It is possible, that DHBV was pulled out by PebB due to the high affinity but not further processed.

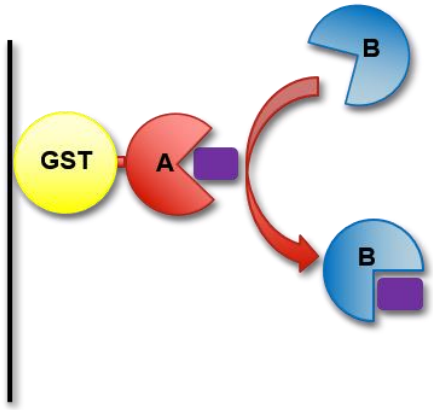

Figure 4.2: Pictogram of the DHBV transfer on the column.

GST-tagged PebA is bound to GST-sepharose and DHBV is still bound after the reaction. The washing step including PebB in the buffer showed the uptake of DHBV by PebB.

Maybe PebB was not able to pick it entirely up since the enzymes were both immobilized on the columns and the “natural” dynamics of the interaction was interrupted. Or, the PebB activity as lowered due to the immobilization and the velocity of PEB formation was downregulated. In either case DHBV was washed from of the column before its further reduction. This might be a hint that both PebA and PebB do not necessarily need a physical interaction for the transfer of DHBV, a close distance might be adequate for the transfer. This effect is called proximity channeling and is described as a phenomenon where the active sites of the involved enzymes are close to each other so the intermediate can be further processed before it can escape by diffusion (Bauler *et al.*, 2010).

Whether or not this is a “real” channel or just an enhanced transfer needs to be further investigated. But the high affinities of the investigated FDBRs to DHBV speaks for a real channel process where PebA enables the channeling to PebB. The interaction of PebA and PebB is supposed to be transient so the affinity to the intermediate DHBV has to be as high as possible to ensure a rapid transfer.

4.3 The fusion protein PebAgB shows PebS-like activity

With the construction of a fusion protein of PebA and PebB more insight into the required proximity of both enzymes or of the structural properties that results into the supposed interaction was expected. On the genome of *Synechococcus sp.* WH8020 the genes for *pebA* and *pebB* are overlapping by sharing a stop-start codon. Luckily, just an insertion of a guanine base was enough to create a translational fusion of both expressed proteins by shifting *pebB* into the same transcriptional frame of *pebA*. As a result of the fusion a Valine was created as a diminutive linker amino acid between both enzymes making the fusion rigid in conformation. Sadly, all approaches of structural studies failed due to the low yield after production. During production and purification of the fusion protein some issues occurred.

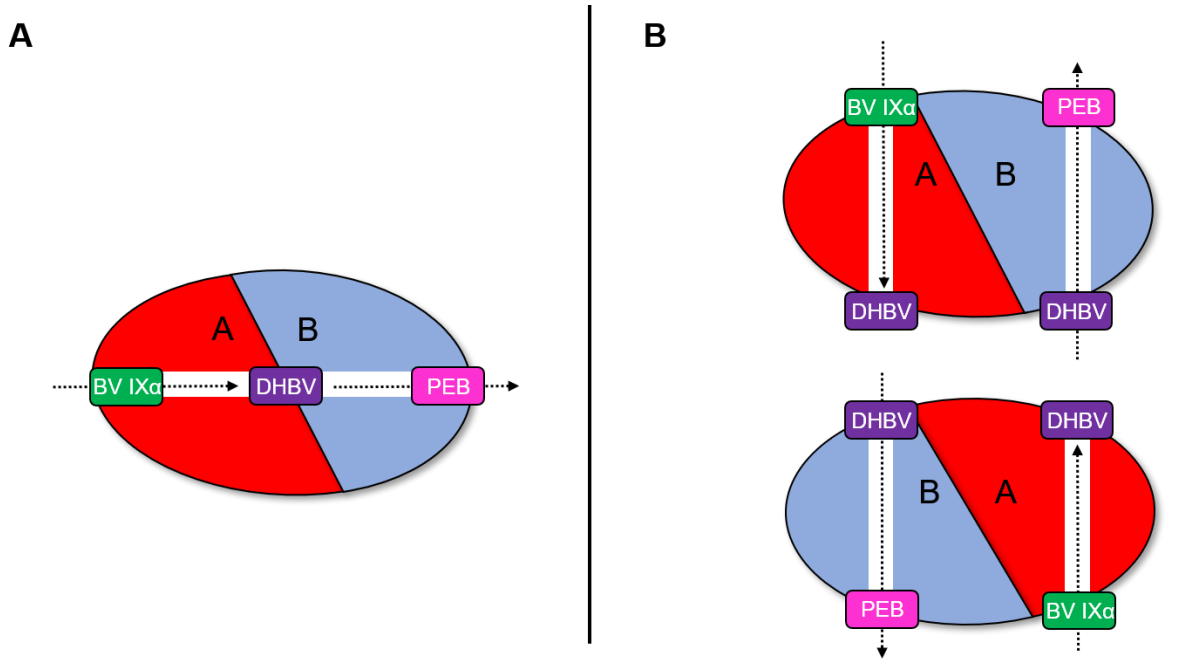

Figure 4.3: Model of the different transfer processes of DHBV within the fusion protein PebAgB

The translational fusion of PebA and PebB leads to the hypothesis that the PEB formation can occur in two ways in dependence of the location of each active site. **(A)** With the linkage between PebA and PebB each active site is facing its interaction partner. Therefore, the conversion of BV IXα to DHBV is mediated in the PebA part of the fusion before the intermediate will be transferred rapidly to the PebB part to get further converted to PEB: This way corresponds to the PebS reaction mechanisms where all steps are performed in one single protein but only in two different reaction centres. **(B)** With the fusion of PebA and PebB the active sites of each enzyme are turned away from the fused interaction partner. Then, it is also possible that two molecules of the enzymes are performing an interaction by proximity channel to produce PEB out of DHBV. (BV = biliverdin; DHBV = dihydrobiliverdin; PEB = phycoerythrobilin; A = PebA part of the fusion protein; B= PebB part of the fusion protein)

The yield was quite low compared to single FDBR production like PebA or PebS and it was just enough protein for activity measurements only. The main focus of characterizing the fusion enzyme was on biochemistry data. For this, also the biochemical activity of PebAgB was compared with the phage originated PebS in view of reaction mechanism and we were able to show the identical product and intermediate formation as the phage enzyme. The PEB formation within the fusion enzymes reaction is believed to happen in two different ways. It is possible that with the fusion of both enzymes an artificial tunnel is formed where the intermediate DHBV can be channeled between both partners within the fusion. Another option, when no tunnel is formed, the formation of a “guiding rail” where the intermediate DHBV can slide from one protein to the other one (Fig. 4.3 A). But it is also possible that two molecules of the fusion protein come together in an inverted direction and a double interaction occurs with each part of the fusion protein. Here, the newly produced DHBV may be transferred from one fusion molecule to the other one before it will be further processed to PEB. This may occur if the active sites of the fusion protein are turned away from each other (Fig. 4.3 B). The argument that speaks for variant A is that the PEB formation is based on the high affinity of DHBV to PebB. As shown above the high affinity of PebB to DHBV results in a drag-out of the intermediate DHBV from PebA. The fusion of both enzymes enhances the affinity of PebB to DHBV by putting both enzymes in a contiguous distance so DHBV can pass rapidly to the subsequently FDBR to get further reduced to PEB. But there is more sufficient information about the structural properties of the fusion protein needed to solve this question. Time-coursed FDBR assays revealed a more PebS-like PEB formation which can be explained by the proximity of each active site. Both PebAgB and PebS showed a fast DHBV formation and a delayed PEB formation indicated by the later time-points where an increase of this product was detected. On the other side the PebAB dual enzyme system showed a PEB formation in earlier stages almost simultaneously together with the DHBV formation. All in all, the dual enzyme system seems to be a bit slower in terms of PEB formation than PebAgB and/or PebS. In *Prochlorococcus marinus* MED4 PebS is supposed to enhance the energy conservation of the host cell (Dammeyer *et al.*, 2008a). Bringing only one enzyme for PEB formation is a more efficient way for the phage than the incorporation of genes for two enzymes as it is already present in cyanobacterial genomes and phages tend to compress their genomes. With our data we can only speculate why cyanobacteria conserved the dual enzyme system because until today no cyanobacterial species is known having *pebS* incorporated into their genome. The fine-tuning of the PEB formation performed by two enzymes during chromatic adaptation is maybe an advantage for the bacteria due to the slower reaction velocity. The adaption to a different light condition with all involved processes of phycobilisome restructuring is a cost-intensive procedure. Chromophore biosynthesis is maybe the step of this procedure where the bacteria can “take a breath” during this event.

4.4 Alternative interaction studies confirmed a transient interaction

In addition to the biochemical interaction studies, the interaction of PebA and PebB was also examined with *in vivo* methods. On the one hand, both proteins were expressed as fusions together with fragments of the adenylate cyclase (AC) from *Bordetella pertussis* during Bacterial Two-Hybrid experiments. This method turned out to be unsuitable for the investigation of this interaction. PebA and PebB showed and interaction as expected and the intensity of the red or blue coloration of the bacterial cells depended on the direction of the fusion with the AC-fragments. The strongest interaction was detected with the N-terminal T18 fusion to PebA together with the C-terminal T25 fusion with PebB. This interaction showed a similar intensity to the positive control which is a quit good indicator for intense interaction. The fusion of a fragment C-terminally to PebA and PebB, respectively, revealed a loss in interaction observed by a weak coloration of the cells. But the other way around when the N-terminus of PebB is fused to the T18 fragment and the N-terminus of PebA is fused to T25 fragment the intensity of the interaction is as strong as the positive control. Taken together, the C-terminus of PebA might be involved in the interaction. The control experiment with PcyA together with PebA or PebB also revealed some strong and weak interactions depending of the orientation of the fragments. As long as the C-terminus of PebA is not “blocked” by a fusion with the AC-fragments the interaction occurred. This is not true for PebB. This enzyme also showed an interaction with PcyA regardless of the orientation of the fused AC-fragments. Quite surprising was the result of the control experiment of PebA or PebB together with the regulator protein MsrF from *M. acetivorans*. MsrF controls the expression of the methyltransferase *mtsD* and an interaction was not expected. Unfortunately, it turned out that even with this protein an interaction was observed and the intensity in all combinations was identical with the positive control. Here, the suggestion of some issues with this method was obvious. To improve this method in view of PebA and PebB interaction this experiment needs to be repeated. That both proteins interact was more than expectable since there were several data collected ahead of this experiment (Dammeyer and Frankenberg-Dinkel, 2006). The interesting question would be, if there is an increased interaction when PebA carries the substrate DHBV for PebB. For this, also a heme oxygenase has to be provided for the *E. coli* cells. This can be achieved by integrating a *ho1* gene (preferably a cyanobacterial origin like the *ho1* from *Synchecocystis sp.* PCC6803) into the chromosome of the used *E. coli* strain using one of the several genome-editing methods (see section 4.5). The enhancement effect of DHBV on the interaction was shown by the previous experiments in this work and an *E. coli* strain capable of synthesizing BV IXα would be helpful for this experiment. To investigate the physical requirements for the postulated interaction cross-linking experiments were performed. The idea was to determine the amino acids on each enzyme’s surface who are involved in the interaction. The cross-linking of proteins is a well-established method to investigate protein-protein interactions.

The amino acids responsible for the interaction of PebA and PebB should be identified via mass spectrometry. In this work, cross-linking via the SPINE method was used as a simple and fast detection for cross-linked proteins. The original experiment was performed in the Gram-positive model bacteria *Bacillus subtilis* but the adaptation to *E. coli* turned out to be functional as well. This method combines the highly specific purification with a reversible cross-linking to get an insight into the expected interaction. To use the SPINE method both interaction partner has to be recombinantly produced in *E. coli* BL21 and one protein carries a Strep-tag (Herzberg *et al.*, 2007). Formaldehyde is a small molecule which is able to overcome the restrictive cell membrane of the cells but in higher concentrations it is also toxic for the bacteria. In order to find the best conditions, some optimization had to be made before the actual experiments were performed. The cross-linking ability of formaldehyde is mainly the condensation of primary amines of the protein surfaces which occur for example in lysine and a methylene bridge is formed. The distance of such a cross-linking event is ~ 2 Å, so only when a close proximity of the investigated proteins is given they get linked together (Solomon and Varshavsky, 1985). It turned out that low concentrations of formaldehyde of 0.2 – 0.6 % were enough to detect cross-linked proteins. Higher concentrations were also tested but led to insoluble or degraded proteins. Even with 0.6 % of formaldehyde a slight diffuse look of the SDS – gel or Western Blot membrane was observed, so no higher concentrations were used. It has to be mentioned that the cross-linking worked in general. Each produced protein could be detected after the purification and also signals were detectable in the elution fractions corresponding to the molecular weight of two FDBRs. The final evidence for cross-linked proteins showed the detection via the anti-His-antibody since a signal can only occur when PebB is co-purified with PebA after affinity chromatography via Streptactin agarose. But not every molecule of PebB was cross-linked because it was also found in the flow fractions. In order to find out if the PebA and PebB interaction is affected in the presence of DHBV a coproduction together with the Ho1 of *Synechocystis sp.* PCC 6803 was performed. During the MST experiments it was observed that the PebA:DHBV has much higher affinity to PebB than the FDBR without the bound ligand. The expectation was to observe a higher yield of cross-linked proteins (and hopefully also the heme oxygenase linked to PebA), but somehow the coproduction did not work as intended. Either the Ho1 was not produced or one of the FDBRs were not detectable via Western Blot analysis. This part of the project showed that both PebA and PebB have a high affinity to each other and they come into a very short distance in order to get cross-linked and this is a requirement for a channeling process. For the future, cross-linking experiments together with a following MS-spectroscopy have to be performed with purified proteins *in vitro*, since PebA and PebB possess an already high affinity to each other. The advantage of conducting *in vitro* cross-linking opens the possibility to use alternative cross-linking reagents like glutaraldehyde or disuccinimidyl suberate (DSS).

Those reagents are provided with more than one reactive group which can interact with protein surfaces in order to cross-link them. Also, these cross-linkers are not able to diffuse through bacterial membranes which make them well suited for *in vitro* approaches.

In summary, PebA and PebB seem to interact in a short manner during their involvement in pigment biosynthesis. Both alternative protein-protein interaction methods (BacTH & SPINE) revealed a transient cooperation since there was no clear evidence of a physical interaction. Especially the BacTH system turned out to be not as informative as expected. Some interactions occurred but it is clearly not an evidence for a specific interaction. In contrast, the SPINE experiment turned out to be as a more reliable method which can be followed up in future experiments. But the fact that just a tiny cross-linking reagent like formaldehyde is enough to cross-link both PebA and PebB can support the hypothesis of a proximity channel as well as the direct channeling mechanism.

4.5 The colored future – the vision of pigment biosynthesis in *E. coli*

The research on enzymes which uses biliverdin IXα as their substrate causes some troubles when those proteins were recombinantly produced in *E. coli* or other hosts who do not possess a *ho* gene in their genome. In that case, an additional plasmid has to be introduced into the *E. coli* cells which provides a gene for the right heme oxygenase to provide BV IXα to the appropriate FDBR. But then also more issues can occur by using additional selection markers. *E. coli* cells can be exposed to a higher stress level and that may have an influence on the protein production. Having an *E. coli* strain that is capable of synthesizing a heme oxygenase from its genome by using the intracellular heme to provide biliverdin IXα for the produced FDBRs would be advantageous for research purposes. The interaction studies of PebA and PebB could be extended by observing the role of produced DHBV during the cross-linking experiments, for example. Here, the influence of DHBV for the postulated interaction may be examined more precisely. The co-production of the heme oxygenase failed several times for unknown reason. A genome encoded heme oxygenase would have had an advantage. Pigment biosynthesis in *E. coli* is already described but it only relies on the corresponding plasmids. For example, the scalable production of biliverdin IXα in *E. coli* has been described and the green tetrapyrrole can be purified and used for clinical applications (D. Chen *et al.*, 2012). Furthermore, also the pink pigment phycoerythrobilin can be produced in a large scale in bioreactors via the introduction of the expression plasmids pTD*ho1_pebS* (Dammeyer *et al.*, 2008b; Stiefelmaier *et al.*, 2018). The produced PEB can be used for either its antioxidant properties (Yabuta *et al.*, 2010) or as holo-PE to serve as a non-toxic food additive to colorize food products (Eriksen, 2008). Nevertheless, non-plasmid-based pigment biosynthesis is not described yet and the advantages of having such a system are self-explaining.

No additional selective marker has to be used when investigating FDBRs which causes less stress for the cells. Furthermore, a genome-based heme oxygenase in *E. coli* can be controlled by constructing an inducible promotor upstream of the gene. During this work, the phage lambda mediated chromosomal integration of heterologous genes was chosen to introduce new genes into *E. coli* BL21 (DE3), called the λ-Red recombineering, (Datsenko and Wanner, 2000). In theory, this recombineering technique allows the insertion of genes at any positions on the chromosome based on the *recET* recombinase system of the *E. coli* specific phage λ (Zhang and Young, 1999). The decision to integrate the generated cassette into the sugar metabolism operon *lacZYA* was based on an earlier publication where genes for carotenoids productions were integrated into *E. coli*. The advantage of deleting the *lacZ* gene is that the knockout can be easily checked by measuring the activity of the β-galactosidase and the gene disruption is not lethal. The generated insertion cassette *frt-ho1-kan-frt* was successfully constructed. This cassette contained not only the *ho1* gene of interest but also a selection marker for kanamycin as well as a mini multiple cloning site to integrate FDBR genes downstream to the *ho1*. Additional *frt* sites were included for marker removal. The integration of the cassette into the host worked in general. As a control, the transformed cells were plated on X-Gal agar plates to verify the absence of the β-galactosidase in the transformants and to compare them with the *E. coli* BL21 (DE3) origin strain. White colonies verified the deletion of the *lacZ* gene and the cassette integration was successful in first place. Also, the slight greenish color of the cells after growing them in liquid culture showed the activity of the incorporated heme oxygenase. Compared to heme oxygenase overproduction where the green color dominates the appearance (Cornejo *et al.*, 1998) the newly generated Strain *E. coli* BL21_*frt_ho1_kan* possess only one copy of the gene and so the green color is weaker. The genomic verification of the new strain failed several times for unknown reason. In order to verify the correct integration of the cassette into the chromosome PCR was performed. The obtained amplicons were not congruent to the expected fragment sizes or in some cases no fragments were detectable. The verification of correct generated strains has to be made in the future. Theoretically, the data point to an insertion but the chromosomal position of the cassette was not clear. Another approach could be the insertion into a different *E. coli* strain because the here used *E. coli* BL21 (DE3) possesses a region with a similar DNA sequence as the *lac*-operon. This region contains the gene for the T7-RNA polymerase and may prevent a correct insertion. But the deficiency in β-galactosidase activity in the mutants speaks against an insertion into this alternative gene locus. Hypothesized, the verification of the strain would have been successful more strains should be constructed. Those strains will not only carry the gene for BV synthesis but also genes for pigment biosynthesis (PCB & PEB). For this the FDBR genes *pebS* and *pcyA* would have been cloned into the mini multiple cloning sites of the integration cassette and new *E coli* strains capable of pigment formation could be generated.

With this system, any other FDBR (except PebB) could have been employed into the *E. coli* chromosome to construct a whole set of pigment making bacteria for our future research.

Conclusion and outlook

With this study we tried to get profound knowledge of the PEB biosynthesis in cyanobacteria based on the CCA capable strain *Synechococcus sp.* WH8020 and how PebA and PebB are cooperating during chromophore production. Our results lead to the conclusion that PebA has two tasks to fulfill. On the one hand it catalyzes the reduction step from BV to DHBV, on the other hand PebA enhances the affinity of the intermediate to the subsequent FDBR PebB. PebB acts as the driving force in PEB formation due to the rapid pull-out of DHBV from PebA, so this FDBR is able to acquire a new substrate molecule. With the obtained data, this work was able to show that a physical interaction is not mandatory due to the high affinity of both proteins to DHBV. Based on the transient interaction of PebA and PebB a metabolic channeling by proximity is the most likely kind of transfer.

For future work, the cross-linking experiments should be repeated along with mass spectrometry analysis to reveal the amino acids which are responsible for the interaction. Ideally, the cross-links shall be performed not only with the FDBRs but also with the corresponding heme oxygenase and/or the appropriate ferredoxin. Also, the MST measurements will be repeated to get more precise K_d-values for the interaction of PebA and PebB when bound to the ligand DHBV. Additionally, affinity constants can be determined for PebA to BV IXα as well as for the heme oxygenase to get more insights into the whole substrate channeling pathway until the final pigment PEB is synthesized.

5 Summary

The transfer of substrates between to enzymes within a biosynthesis pathway is an effective way to synthesize the specific product and a good way to avoid metabolic interference. This process is called metabolic channeling and it describes the (in-)direct transfer of an intermediate molecule between the active sites of two enzymes. By forming multi-enzyme cascades the efficiency of product formation and the flux is elevated and intermediate products are transferred and converted in a correct manner by the enzymes.

During tetrapyrrole biosynthesis several substrate transfer events occur and are prerequisite for an optimal pigment synthesis. In this project the metabolic channeling process during the pink pigment phycoerythrobilin (PEB) was investigated. The responsible ferredoxin-dependent bilin reductases (FDBR) for PEB formation are PebA and PebB. During the pigment synthesis the intermediate molecule 15,16-dihydrobiliverdin (DHBV) is formed and transferred from PebA to PebB. While in earlier studies a metabolic channeling of DHBV was postulated, this work revealed new insights into the requirements of this protein-protein interaction. It became clear, that the most important requirement for the PebA/PebB interaction is based on the affinity to their substrate/product DHBV. The already high affinity of both enzymes to each other is enhanced in the presence of DHBV in the binding pocket of PebA which leads to a rapid transfer to the subsequent enzyme PebB. DHBV is a labile molecule and needs to be rapidly channeled in order to get correctly further reduced to PEB. Fluorescence titration experiments and transfer assays confirmed the enhancement effect of DHBV for its own transfer.

More insights became clear by creating an active fusion protein of PebA and PebB and comparing its reaction mechanism with standard FDBRs. This fusion protein was able to convert biliverdin IXα (BV IXα) to PEB similar to the PebS activity, which also can convert BV IXα via DHBV to PEB as a single enzyme. The product and intermediate of the reaction were identified via HPLC and UV-Vis spectroscopy.

The results of this work revealed that PebA and PebB interact via a proximity channeling process where the intermediate DHBV plays an important role for the interaction. It also highlights the importance of substrate channeling in the synthesis of PEB to optimize the flux of intermediates through this metabolic pathway.

6 Zusammenfassung

Der Transfer von Substraten zwischen Enzymen innerhalb eines Biosyntheseweges ist ein effektiver Weg, das spezifische Produkt zu synthetisieren und eine gute Möglichkeit, Stoffwechselstörungen zu vermeiden. Dieser Prozess wird als *metabolic channeling* bezeichnet und beschreibt den (in-)direkten Transfer eines Intermediats zwischen den aktiven Zentren zweier beteiligter katalytischer Enzyme. Durch die Bildung von Multi-Enzym-Kaskaden werden die Effizienz der Produktbildung als auch der Flux erhöht und die Intermediate werden von den Enzymen korrekt übertragen und umgesetzt.

Bei der Tetrapyrrolbiosynthese treten viele Substrattransferereignisse auf und sie sind Voraussetzung für eine optimale Pigmentsynthese. In diesem Projekt wurde der *metabolic channeling*-Prozess beim pinken Pigment Phycoerythrobilin (PEB) untersucht. Die für die PEB-Bildung verantwortlichen Ferredoxinabhängigen Bilinreduktasen (FDBR) sind PebA und PebB. Bei der Pigmentsynthese wird das Intermediat 15,16-Dihydrobiliverdin (DHBV) gebildet und von PebA auf PebB übertragen. Während in früheren Studien ein *metabolic channeling* des DHBV postuliert wurde, zeigt diese Arbeit neue Erkenntnisse über die Vorrausetzungen dieser Protein-Protein-Interaktion. Es wurde deutlich, dass die wichtigste Anforderung für die PebA/PebB-Interaktion die Affinität zu ihrem Substrat/Produkt DHBV ist. Die bereits hohe Affinität beider Enzyme zueinander wird in Gegenwart von DHBV in der Bindungstasche von PebA verstärkt, was zu einer schnelleren Übertragung auf das nachfolgende Enzym PebB führt. DHBV ist ein instabiles Molekül und muss schnell übertragen werden um korrekt weiter zu PEB reduziert zu werden. Fluoreszenztitrationsexperimente und Transferassays bestätigen den Verstärkungseffekt von DHBV für den eigenen Transfer.

Weitere Erkenntnisse der Substratübertragung wurden durch die Erstellung eines aktiven Fusionsproteins aus PebA und PebB und den Vergleich seines Reaktionsmechanismus mit Standard-FDBRs deutlich. Dieses Fusionsprotein PebAgB setzt Biliverdin IXα (BV IXα) zu PEB um, welche damit eine starke Ähnlichkeit zu der PebS-Aktivität besitzt, die auch BV IXα über DHBV in PEB als einzelnes Enzym umwandeln kann. Das Produkt und das Intermediate dieser Reaktionen wurden mittels HPLC und UV-Vis-Spektroskopie identifiziert.

Die Ergebnisse dieser Arbeit zeigen, dass PebA und PebB über einen *proximity-channeling*-Prozess interagieren, bei dem DHBV eine wichtige Rolle für die Interaktion spielt. Weiterhin wird die Bedeutung der Substratkanalisierung bei der Synthese von PEB unterstrichen, welche verantwortlich ist, den Flux der Intermediate während diesem Stoffwechselweg zu optimieren.

Appendix

- DNA sequence of *pebAgB* after base insertion (the inserted guanin is marked red):

>*pebAgB* (base exchange mutagenesis in *pebAB* operon of *Synechococcus sp.* WH8020)
ATGTTTGATTCATTTCTCAATGAGCTTCATTCAGATATCACCAAGAGAGGTGGATCTCCC
CTTCCTTTACCGGAAGGTCTAGAAGAATGCAGATCTTCAAAATCATCCAGTGTCATTCAG
AGCTGGCTTTGGGATGTTCCTGGCTTTCGGCGCTGGAGGGTCACTCGACTTGATGCAG
GCGACAGCCTGCAAGTTTTCAATTCTGTTGCATATCCTGATTACAACTATGATCACCCCT
TAATGGGAGTTGATCTCCTCTGGTTCGGGGCCCGTCAGAAGCTTGTTGCCGTACTCGAT
TTCCAGCCCTTGGTCCAAGACAAAGACTATCTTGATCGCTATTTTTCTGGTCTCAAGGAA
CTGAATCAACGATTTCCAGATCTCAATGGTGAGGAAACGATGCGTTCATTTGATCCAAAT
CAGTATTTTTCTTCATGGTTACTGTTCTGTCGCGGAGGTGCGGAACAAGCTGATTTATCC
CTACCAAAGGCTTTTAGTGCATTCTTAAAAGCATACTGGGATTTACATGACAATGCCAAA
AGCATTCCCTCAACTATTCCTCCAGAAGAAGTTAAGAACCTGCAGGACAAATACGATATT
TACAGCGCCGAACGGGATCCAGCACACGGACTCTTTACAAGCCATTTCGGGAAAGACT
GGTCAAATCGGTTCCTCCATGAGTTTTTATTCCCCGCCTCCTCCTCTCACAAA**G**TGACAA
ATCAAAGATTCAAAAGCACAGACCCTGTCAACATCGAAGGATGGTCATGGCAACCCTTT
CTTGAAGATGCCATCAAGCGCCTAGAAGGCTTAAATGTTGAACCATACCCAGTTCCCGA
TCGTTTTTTACAACGCGAAGATCAAACTGGATCAAAATCAAAATCAATTCCTGTCACGAC
AGCAACCTGGGCTTGCAAAACAGAGAAATTCAGACAAGTCAGAGCTGCCTGCGTCAGT
GCTGGATCAGCAGCATCTGTTTTGAATTTTGTGATCAATCCAAAGTCCACCTATGACTTA
CCTTTTTTTGGCGGTGATTTGGTAACGCTCCCCGCAGGACATTTGCTTGCACTAGACCT
TCAACCCGCCATCAAAACAGACGAGGTCCACACCACTCATGTTTGGGATCGACTCATTC
CCATTTTTGAGCGTTGGCGAGATCAACTGCCTTATGGAGGGCCAATTCCAGAGGAGGC
GCAGCCCTTTTTCTCCCCTGGATTCCTGTGGACTCGACTGCCCCTTGGAGAGGAAGGC
GACGAGTTGATTCAATCCATCGTCCGACCTGCGTTCAATGATTATTTAGACCTCTACCTC
GAACTAGCTGCCTCAGCCGAGCGCGTGACCGATGAGCGCAGCGAGGTCCTTCTACAAG
GGCAAAGAAAATACACAGATTATCGAGCCGAAAAAGACCCTGCGCGCGGAATGTTGACT
CGCTTTCATGGCAGCGAATGGACCGAGGCATACATCCACACTGTGCTTTTTGATCTA

- Gene disruption of *lacZ* of *E. coli* BL21 (DE3) via λ – Red recombineering:

Integration DNA sequence (2148 bp of linear DNA)

>*lacZ_ho1_kan_frt* (homologues flanking sequence to *lacZ*; *ho1* from *Synechocystis sp.* PCC6803; kanamycin resistance marker; *frt*-sites; restriction sites for *Bam*HI and *Eco*RI)
GCTCGTATGTTGTGTGAAATTGTGAGCGGATAACAATTTCACACAGGAAACAGCTATGA
GTGTCAACTTAGCTTCCCAGTTGCGGGAAGGGACGAAAAAATCCCACTCCATGGCGGA
GAACGTCGGCTTTGTCAAATGCTTCCTCAAGGGCGTTGTCGAGAAAAATTCCTACCGTA
AGCTGGTTGGCAATCTCTACTTTGTCTACAGTGCCATGGAAGAGGAAATGGCAAAATTT
AAGGACCATCCCATCCTCAGCCACATTTACTTCCCCGAACTCAACCGCAAACAAAGCCT
AGAGCAAGACCTGCAATTCTATTACGGCTCCAACTGGCGGCAAGAAGTGAAAATTTCTG
CCGCTGGCCAAGCCTATGTGGACCGAGTCCGGCAAGTGGCCGCTACGGCCCCTGAATT
GTTGGTGGCCCATTCCTACACCCGTTACCTGGGGGATCTTTCCGGCGGTCAAATTCTCA
AGAAAATTGCCCAAAATGCCATGAATCTCCACGATGGTGGCACAGCTTTCTATGAATTTG
CCGACATTGATGACGAAAAGGCTTTTAAAAATACCTACCGTCAAGCTATGAATGATCTGC
CCATTGACCAAGCCACCGCCGAACGGATTGTGGATGAAGCCAATGACGCCTTTGCCAT
GAACATGAAAATGTTCAACGAACTTGAAGGCAACCTGATCAAGGCGATCGGCATTATGG
TGTTCAACAGCCTCACCCGTCGCCGCAGTCAAGGCAGCACCGAAGTTGGCCTCGCCAC
CTCCGAAGGCTAGTTAAAGAGGAATGGATCCGAATTCCTGCAGTTCGAAGTTCCTATTC
TCTAGAAAGTATAGGAACTTCAGAGCGCTTTTGAAGCTCACGCTGCCGCAAGCACTCAG
GGCGCAAGGGCTGCTAAAGGAAGCGGAACACGTAGAAAGCCAGTCCGCAGAAACGGT
GCTGACCCCGGATGAATGTCAGCTACTGGGCTATCTGGACAAGGGAAAACGCAAGCGC
AAAGAGAAAGCAGGTAGCTTGCAGTGGGCTTACATGGCGATAGCTAGACTGGGCGGTT
TTATGGACAGCAAGCGAACCGGAATTGCCAGCTGGGGCGCCCTCTGGTAAGGTTGGGA
AGCCCTGCAAAGTAAACTGGATGGCTTTCTTGCCGCCAAGGATCTGATGGCGCAGGGG
ATCAAGATCTGATCAAGAGACAGGATGAGGATCGTTTCGCATGATTGAACAAGATGGAT
TGCACGCAGGTTCTCCGGCCGCTTGGGTGGAGAGGCTATTCGGCTATGACTGGGCACA
ACAGACAATCGGCTGCTCTGATGCCGCCGTGTTCCGGCTGTCAGCGCAGGGGCGCCC
GGTTCTTTTTGTCAAGACCGACCTGTCCGGTGCCCTGAATGAACTGCAGGACGAGGCA
GCGCGGCTATCGTGGCTGGCCACGACGGGCGTTCCTTGCGCAGCTGTGCTCGACGTT
GTCACTGAAGCGGGAAGGGACTGGCTGCTATTGGGCGAAGTGCCGGGGCAGGATCTC
CTGTCATCTCACCTTGCTCCTGCCGAGAAAGTATCCATCATGGCTGATGCAATGCGGCG
GCTGCATACGCTTGATCCGGCTACCTGCCCATTCGACCACCAAGCGAAACATCGCATC
GAGCGAGCACGTACTCGGATGGAAGCCGGTCTTGTCGATCAGGATGATCTGGACGAAG
AGCATCAGGGGCTCGCGCCAGCCGAACTGTTCGCCAGGCTCAAGGCGCGCATGCCCG
ACGGCGAGGATCTCGTCGTGACCCATGGCGATGCCTGCTTGCCGAATATCATGGTGGA
AAATGGCCGCTTTTCTGGATTCATCGACTGTGGCCGGCTGGGTGTGGCGGACCGCTAT
CAGGACATAGCGTTGGCTACCCGTGATATTGCTGAAGAGCTTGGCGGCGAATGGGCTG
ACCGCTTCCTCGTGCTTTACGGTATCGCCGCTCCCGATTCGCAGCGCATCGCCTTCTAT
CGCCTTCTTGACGAGTTCTTCTAATAAGGGGATCTTGAAGTTCCTATTCCGAAGTTCCTA
TTCTCTAGAAAGTATAGGAACTTCGAAGCAGCTCCAGCCTACACAATCGCCGCCGGTCG
CTACCATTACCAGTTGGTCTGGTGTCAAAAATAATAATAACCGGGC

- Cloning plasmid pUC *ho1_kan* for integration DNA for λ – Red recombineering:

  The integration cassette *lacZ_ho1_kan_frt* (homologues flanking sequences to *lacZ*; *ho1* from *Synechocystis sp.* PCC6803; kanamycin resistance marker; *frt*-sites; restriction sites for *Bam*HI and *Eco*RI) was cloned onto pYPRUB168 vector containing an ampicillin resistance marker and *Sma*I restriction site to integrate linear DNA.

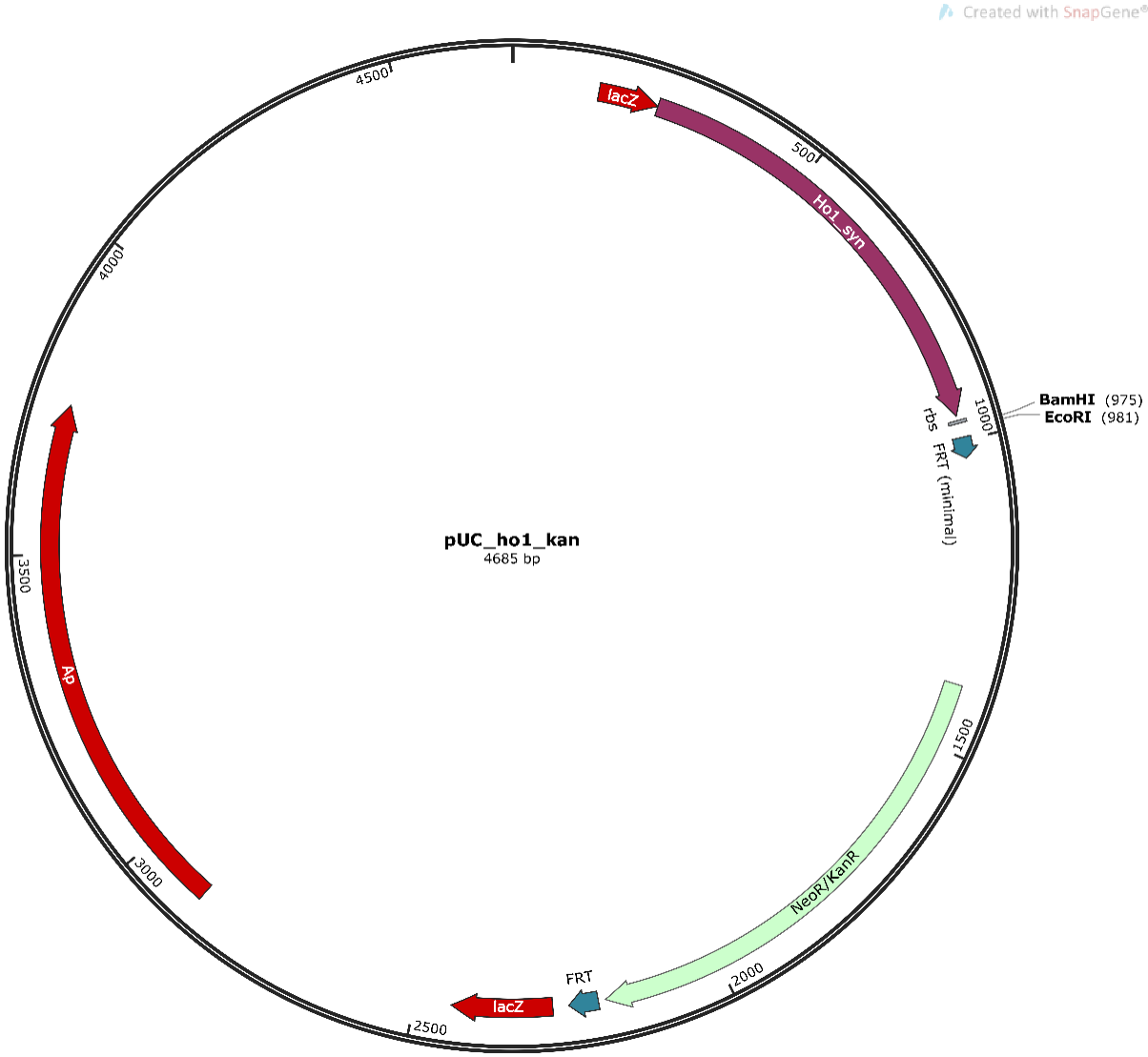

- Raw MST-Tracee of interaction between PebB* and the PebA:DHBV complex:

  The MST measurement were conducted with two different MST power settings (green lines = 20% MST power & red lines = 40% MST power) and then the change in fluorescence was plotted against the time.

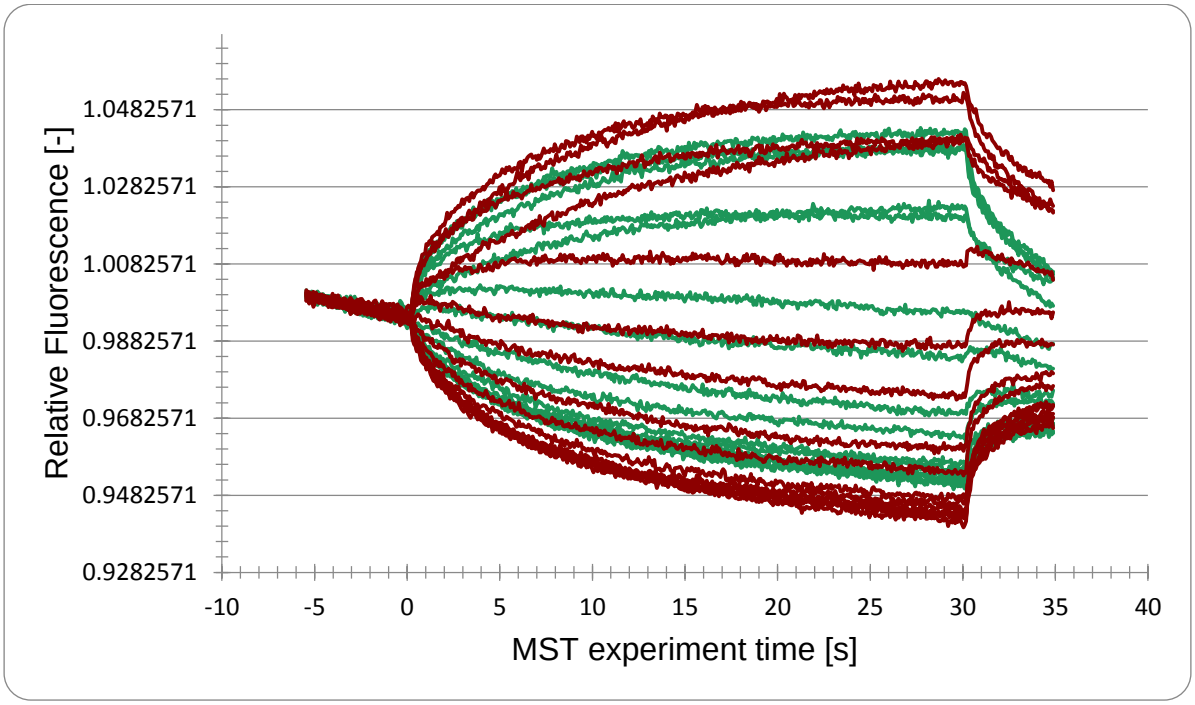

References

Aaij, C., & Borst, P. (1972). The gel electrophoresis of DNA. *Biochimica et Biophysica Acta, 269*(2), 192-200.

Abraham, N. G., Drummond, G. S., Lutton, J. D., & Kappas, A. (1996). The biological significance and physiological role of heme oxygenase. *Cellular Physiology and Biochemistry, 6*(3), 129-168.

Albermann, C., Trachtmann, N., & Sprenger, G. A. (2010). A simple and reliable method to conduct and monitor expression cassette integration into the Escherichia coli chromosome. *Biotechnology Journal, 5*(1), 32-38.

Alvey, R. M., Karty, J. A., Roos, E., Reilly, J. P., & Kehoe, D. M. (2003). Lesions in phycoerythrin chromophore biosynthesis in Fremyella diplosiphon reveal coordinated light regulation of apoprotein and pigment biosynthetic enzyme gene expression. *Plant Cell, 15*(10), 2448-2463.

Bauler, P., Huber, G., Leyh, T., & McCammon, J. A. (2010). Channeling by Proximity: The Catalytic Advantages of Active Site Colocalization Using Brownian Dynamics. *Journal of Physical Chemistry Letters, 1*(9), 1332-1335.

Beale, S. I. (1999). Enzymes of chlorophyll biosynthesis. *Photosynthesis Research, 60*(1), 43-73.

Beale, S. I., & Cornejo, J. (1984a). Enzymatic heme oxygenase activity in soluble extracts of the unicellular red alga, Cyanidium caldarium. *Archives of Biochemistry and Biophysics, 235*(2), 371-384.

Beale, S. I., & Cornejo, J. (1984b). Enzymic Transformation of Biliverdin to Phycocyanobilin by Extracts of the Unicellular Red Alga Cyanidium caldarium. *Plant Physiology, 76*(1), 7-15.

Beale, S. I., & Cornejo, J. (1991). Biosynthesis of phycobilins. 3(Z)-phycoerythrobilin and 3(Z)-phycocyanobilin are intermediates in the formation of 3(E)-phycocyanobilin from biliverdin IX alpha. *Journal of Biological Chemistry, 266*(33), 22333-22340.

Bibby, T. S., Mary, I., Nield, J., Partensky, F., & Barber, J. (2003). Low-light-adapted Prochlorococcus species possess specific antennae for each photosystem. *Nature, 424*(6952), 1051-1054.

Blot, N., Wu, X. J., Thomas, J. C., Zhang, J., Garczarek, L., Bohm, S., Tu, J. M., Zhou, M., Ploscher, M., Eichacker, L., Partensky, F., Scheer, H., & Zhao, K. H. (2009). Phycourobilin in trichromatic phycocyanin from oceanic cyanobacteria is formed post-translationally by a phycoerythrobilin lyase-isomerase. *Journal of Biological Chemistry, 284*(14), 9290-9298.

Bose, A., Kulkarni, G., & Metcalf, W. W. (2009). Regulation of putative methyl-sulphide methyltransferases in Methanosarcina acetivorans C2A. *Molecular Microbiology, 74*(1), 227-238.

Bryant, D. A., Stirewalt, V. L., Glauser, M., Frank, G., Sidler, W., & Zuber, H. (1991). A small multigene family encodes the rod-core linker polypeptides of Anabaena sp. PCC7120 phycobilisomes. *Gene, 107*(1), 91-99.

Busch, A. W., Reijerse, E. J., Lubitz, W., Frankenberg-Dinkel, N., & Hofmann, E. (2011a). Structural and mechanistic insight into the ferredoxin-mediated two-electron reduction of bilins. *Biochemical Journal, 439*(2), 257-264.

Busch, A. W., Reijerse, E. J., Lubitz, W., Hofmann, E., & Frankenberg-Dinkel, N. (2011b). Radical mechanism of cyanophage phycoerythrobilin synthase (PebS). *Biochemical Journal, 433*(3), 469-476.

Castellana, M., Wilson, M. Z., Xu, Y., Joshi, P., Cristea, I. M., Rabinowitz, J. D., Gitai, Z., & Wingreen, N. S. (2014). Enzyme clustering accelerates processing of intermediates through metabolic channeling. *Nature Biotechnology, 32*(10), 1011-1018.

Chen, D., Brown, J. D., Kawasaki, Y., Bommer, J., & Takemoto, J. Y. (2012). Scalable production of biliverdin IXalpha by Escherichia coli. *BMC Biotechnology, 12*, 89.

Chen, Y. R., Su, Y. S., & Tu, S. L. (2012). Distinct phytochrome actions in nonvascular plants revealed by targeted inactivation of phytobilin biosynthesis. *Proceedings of the National Academy of Sciences of the United States of America, 109*(21), 8310-8315.

Chisholm, S. W. (1992). Phytoplankton Size. In P. G. Falkowski, A. D. Woodhead, & K. Vivirito (Eds.), *Primary Productivity and Biogeochemical Cycles in the Sea* (pp. 213-237). Boston, MA: Springer US.

Christina, H., Flórez, W. L. A., Bastian, D., Sebastian, H., Jörg, S., & M., C. F. (2007). SPINE: A method for the rapid detection and analysis of protein–protein interactions in vivo. *PROTEOMICS, 7*(22), 4032-4035.

Cole, W., Chapman, D. J., & Siegelman, H. W. (1967). Structure of phycocyanobilin. *Journal of the American Chemical Society, 89*(14), 3643-3645.

Cornejo, J., & Beale, S. I. (1988). Algal heme oxygenase from Cyanidium caldarium. Partial purification and fractionation into three required protein components. *Journal of Biological Chemistry, 263*(24), 11915-11921.

Cornejo, J., Willows, R. D., & Beale, S. I. (1998). Phytobilin biosynthesis: cloning and expression of a gene encoding soluble ferredoxin-dependent heme oxygenase from Synechocystis sp. PCC 6803. *Plant Journal, 15*(1), 99-107.

Dammeyer, T., Bagby, S. C., Sullivan, M. B., Chisholm, S. W., & Frankenberg-Dinkel, N. (2008a). Efficient phage-mediated pigment biosynthesis in oceanic cyanobacteria. *Curr Biol, 18*(6), 442-448.

Dammeyer, T., & Frankenberg-Dinkel, N. (2006). Insights into phycoerythrobilin biosynthesis point toward metabolic channeling. *Journal of Biological Chemistry, 281*(37), 27081-27089.

Dammeyer, T., Hofmann, E., & Frankenberg-Dinkel, N. (2008b). Phycoerythrobilin synthase (PebS) of a marine virus. Crystal structures of the biliverdin complex and the substrate-free form. *Journal of Biological Chemistry, 283*(41), 27547-27554.

Datsenko, K. A., & Wanner, B. L. (2000). One-step inactivation of chromosomal genes in Escherichia coli K-12 using PCR products. *Proceedings of the National Academy of Sciences of the United States of America, 97*(12), 6640-6645.

de Marsac, N. T., & Cohen-bazire, G. (1977). Molecular composition of cyanobacterial phycobilisomes. *Proceedings of the National Academy of Sciences of the United States of America, 74*(4), 1635-1639.

Deery, E., Schroeder, S., Lawrence, A. D., Taylor, S. L., Seyedarabi, A., Waterman, J., Wilson, K. S., Brown, D., Geeves, M. A., Howard, M. J., Pickersgill, R. W., & Warren, M. J. (2012). An enzyme-trap approach allows isolation of intermediates in cobalamin biosynthesis. *Nature Chemical Biology, 8*(11), 933-940.

Dueber, J. E., Wu, G. C., Malmirchegini, G. R., Moon, T. S., Petzold, C. J., Ullal, A. V., Prather, K. L., & Keasling, J. D. (2009). Synthetic protein scaffolds provide modular control over metabolic flux. *Nature Biotechnology, 27*(8), 753-759.

Eriksen, N. T. (2008). Production of phycocyanin - a pigment with applications in biology, biotechnology, foods and medicine. *Applied Microbiology and Biotechnology, 80*(1), 1-14.

Fairchild, C. D., & Glazer, A. N. (1994). Nonenzymatic bilin addition to the alpha subunit of an apophycoerythrin. *Journal of Biological Chemistry, 269*(46), 28988-28996.

Flombaum, P., Gallegos, J. L., Gordillo, R. A., Rincon, J., Zabala, L. L., Jiao, N., Karl, D. M., Li, W. K., Lomas, M. W., Veneziano, D., Vera, C. S., Vrugt, J. A., & Martiny, A. C. (2013). Present and future global distributions of the marine Cyanobacteria Prochlorococcus and Synechococcus. *Proceedings of the National Academy of Sciences of the United States of America, 110*(24), 9824-9829.

Frankenberg-Dinkel, N. (2004). Bacterial heme oxygenases. *Antioxidants & Redox Signaling, 6*(5), 825-834.

Frankenberg, N., & Lagarias, J. C. (2003). Phycocyanobilin:ferredoxin oxidoreductase of Anabaena sp. PCC 7120. Biochemical and spectroscopic. *Journal of Biological Chemistry, 278*(11), 9219-9226.

Frankenberg, N., Mukougawa, K., Kohchi, T., & Lagarias, J. C. (2001). Functional genomic analysis of the HY2 family of ferredoxin-dependent bilin reductases from oxygenic photosynthetic organisms. *Plant Cell, 13*(4), 965-978.

Fromme, R., Ishchenko, A., Metz, M., Chowdhury, S. R., Basu, S., Boutet, S., Fromme, P., White, T. A., Barty, A., Spence, J. C., Weierstall, U., Liu, W., & Cherezov, V. (2015). Serial femtosecond crystallography of soluble proteins in lipidic cubic phase. *IUCrJ, 2*(Pt 5), 545-551.

Gibson, D. G., Young, L., Chuang, R. Y., Venter, J. C., Hutchison, C. A., & Smith, H. O. (2009). Enzymatic assembly of DNA molecules up to several hundred kilobases. *Nature Methods, 6*(5), 343-U341.

Gill, S. C., & von Hippel, P. H. (1989). Calculation of protein extinction coefficients from amino acid sequence data. *Analytical Biochemistry, 182*(2), 319-326.

Gisk, B., Wiethaus, J., Aras, M., & Frankenberg-Dinkel, N. (2012). Variable composition of heme oxygenases with different regiospecificities in Pseudomonas species. *Archives of Microbiology, 194*(7), 597-606.

Glazer, A. N. (1977). Structure and molecular organization of the photosynthetic accessory pigments of cyanobacteria and red algae. *Molecular and Cellular Biochemistry, 18*(2-3), 125-140.

Glazer, A. N. (1985). Light harvesting by phycobilisomes. *Annual Review of Biophysics and Biophysical Chemistry, 14*, 47-77.

Glazer, A. N., Chan, C., Williams, R. C., Yeh, S. W., & Clark, J. H. (1985). Kinetics of energy flow in the phycobilisome core. *Science, 230*(4729), 1051-1053.

Goericke, R., & Repeta, D. J. (1992). The Pigments of Prochlorococcus-Marinus - the Presence of Divinyl Chlorophyll-a and Chlorophyll-B in a Marine Prokaryote. *Limnology and Oceanography, 37*(2), 425-433.

Goericke, R., & Welschmeyer, N. A. (1993). The marine prochlorophyte Prochlorococcus contributes significantly to phytoplankton biomass and primary production in the Sargasso Sea. *Deep Sea Research Part I: Oceanographic Research Papers, 40*(11), 2283-2294.

Gossauer, A., & Klahr, E. (1979). Synthesen von Gallenfarbstoffen, VIII. Totalsynthese des racem. Phycoerythrobilin-dimethylesters. *Chemische Berichte, 112*(6), 2243-2255.

Grossman, A. R., Schaefer, M. R., Chiang, G. G., & Collier, J. L. (1993). The phycobilisome, a light-harvesting complex responsive to environmental conditions. *Microbiology and Molecular Biology Reviews, 57*(3), 725-749.

Gutu, A., & Kehoe, D. M. (2012). Emerging Perspectives on the Mechanisms, Regulation, and Distribution of Light Color Acclimation in Cyanobacteria. *Molecular Plant, 5*(1), 1-13.

Hagiwara, Y., Sugishima, M., Takahashi, Y., & Fukuyama, K. (2006). Crystal structure of phycocyanobilin:ferredoxin oxidoreductase in complex with biliverdin IXalpha, a key enzyme in the biosynthesis of phycocyanobilin. *Proceedings of the National Academy of Sciences of the United States of America, 103*(1), 27-32.

Heirwegh, K. P., Blanckaert, N., & Van Hees, G. (1991). Synthesis, chromatographic purification, and analysis of isomers of biliverdin IX and bilirubin IX. *Analytical Biochemistry, 195*(2), 273-278.

Herzberg, C., Weidinger, L. A. F., Dörrbecker, B., Hübner, S., Stülke, J., & Commichau, F. M. (2007). SPINE: A method for the rapid detection and analysis of protein–protein interactions in vivo. *PROTEOMICS, 7*(22), 4032-4035.

Hess, W. R., Partensky, F., van der Staay, G. W., Garcia-Fernandez, J. M., Borner, T., & Vaulot, D. (1996). Coexistence of phycoerythrin and a chlorophyll a/b antenna in a marine prokaryote. *Proceedings of the National Academy of Sciences of the United States of America, 93*(20), 11126-11130.

Hess, W. R., Schendel, R., Rudiger, W., Fieder, B., & Borner, T. (1992). Components of chlorophyll biosynthesis in a barley albina mutant unable to synthesize delta-aminolevulinic acid by utilizing the transfer RNA for glutamic acid. *Planta, 188*(1), 19-27.

Ho, M. Y., Soulier, N. T., Canniffe, D. P., Shen, G., & Bryant, D. A. (2017). Light regulation of pigment and photosystem biosynthesis in cyanobacteria. *Current Opinion in Plant Biology, 37*, 24-33.

Hyde, C. C., Ahmed, S. A., Padlan, E. A., Miles, E. W., & Davies, D. R. (1988). Three-dimensional structure of the tryptophan synthase alpha 2 beta 2 multienzyme complex from Salmonella typhimurium. *Journal of Biological Chemistry, 263*(33), 17857-17871.

Joshua, S., & Mullineaux, C. W. (2004). Phycobilisome diffusion is required for light-state transitions in cyanobacterial. *Plant Physiology, 135*(4), 2112-2119.

Kahn, K., Mazel, D., Houmard, J., Tandeau de Marsac, N., & Schaefer, M. R. (1997). A role for cpeYZ in cyanobacterial phycoerythrin biosynthesis. *Journal of Bacteriology, 179*(4), 998-1006.

Karimova, G., Pidoux, J., Ullmann, A., & Ladant, D. (1998). A bacterial two-hybrid system based on a reconstituted signal transduction pathway. *Proceedings of the National Academy of Sciences of the United States of America, 95*(10), 5752-5756.

Kehoe, D. M. (2010). Chromatic adaptation and the evolution of light color sensing in cyanobacteria. *Proceedings of the National Academy of Sciences of the United States of America, 107*(20), 9029-9030.

Kohchi, T., Mukougawa, K., Frankenberg, N., Masuda, M., Yokota, A., & Lagarias, J. C. (2001). The Arabidopsis HY2 gene encodes phytochromobilin synthase, a ferredoxin-dependent biliverdin reductase. *Plant Cell, 13*(2), 425-436.

Lagarias, J. C., & Rapoport, H. (1980). Chromopeptides from phytochrome. The structure and linkage of the PR form of the phytochrome chromophore. *Journal of the American Chemical Society, 102*(14), 4821-4828.

Ledermann, B., Aras, M., & Frankenberg-Dinkel, N. (2017). Biosynthesis of Cyanobacterial Light-Harvesting Pigments and Their Assembly into Phycobiliproteins. In P. C. Hallenbeck (Ed.), *Modern Topics in the Phototrophic Prokaryotes: Metabolism, Bioenergetics, and Omics* (pp. 305-340). Cham: Springer International Publishing.

Ledermann, B., Beja, O., & Frankenberg-Dinkel, N. (2016). New biosynthetic pathway for pink pigments from uncultured oceanic viruses. *Environmental Microbiology, 18*(12), 4337-4347.

Lee, H., DeLoache, W. C., & Dueber, J. E. (2012). Spatial organization of enzymes for metabolic engineering. *Metabolic Engineering, 14*(3), 242-251.

Liberton, M., Page, L. E., O'Dell, W. B., O'Neill, H., Mamontov, E., Urban, V. S., & Pakrasi, H. B. (2013). Organization and flexibility of cyanobacterial thylakoid membranes examined by neutron scattering. *Journal of Biological Chemistry, 288*(5), 3632-3640.

Liu, L. N. (2016). Distribution and dynamics of electron transport complexes in cyanobacterial thylakoid membranes. *Biochimica et Biophysica Acta, 1857*(3), 256-265.

Liu, Y., & Ortiz de Montellano, P. R. (2000). Reaction intermediates and single turnover rate constants for the oxidation of heme by human heme oxygenase-1. *Journal of Biological Chemistry, 275*(8), 5297-5307.

MacColl, R. (1998). Cyanobacterial phycobilisomes. *Journal of Structural Biology, 124*(2-3), 311-334.

Margulis, L. (1970). *Origin of Eukaryotic Cells: Evidence and Research Implications for a Theory of the Origin and Evolution of Microbial, Plant, and Animal Cells on the Precambrian Earth*: Yale University Press.

Marx, A., & Adir, N. (2013). Allophycocyanin and phycocyanin crystal structures reveal facets of phycobilisome assembly. *Biochimica et Biophysica Acta, 1827*(3), 311-318.

McDowell, M. T., & Lagarias, J. C. (2001). Purification and biochemical properties of phytochromobilin synthase from etiolated oat seedlings. *Plant Physiology, 126*(4), 1546-1554.

Montellano, P. R. (2000). The mechanism of heme oxygenase. *Current Opinion in Chemical Biology, 4*(2), 221-227.

Moore, L. R., & Chisholm, S. W. (1999). Photophysiology of the marine cyanobacterium Prochlorococcus: Ecotypic differences among cultured isolates. *Limnology and Oceanography, 44*(3), 628-638.

Moore, L. R., Rocap, G., & Chisholm, S. W. (1998). Physiology and molecular phylogeny of coexisting Prochlorococcus ecotypes. *Nature, 393*(6684), 464-467.

Mullineaux, C. W. (2014). Co-existence of photosynthetic and respiratory activities in cyanobacterial thylakoid membranes. *Biochimica et Biophysica Acta, 1837*(4), 503-511.

Mullineaux, C. W., Tobin, M. J., & Jones, G. R. (1997). Mobility of photosynthetic complexes in thylakoid membranes. *Nature, 390*(6658), 421-424.

Mullis, K. B., & Faloona, F. A. (1987). Specific synthesis of DNA in vitro via a polymerase-catalyzed chain reaction. *Methods in Enzymology, 155*, 335-350.

Muramoto, T., Kohchi, T., Yokota, A., Hwang, I. H., & Goodman, H. M. (1999). The Arabidopsis photomorphogenic mutant hy1 is deficient in phytochrome chromophore biosynthesis as a result of a mutation in a plastid heme oxygenase. *Plant Cell, 11*(3), 335-347.

Narayanaswamy, R., Levy, M., Tsechansky, M., Stovall, G. M., O'Connell, J. D., Mirrielees, J., Ellington, A. D., & Marcotte, E. M. (2009). Widespread reorganization of metabolic enzymes into reversible assemblies upon nutrient starvation. *Proceedings of the National Academy of Sciences of the United States of America, 106*(25), 10147-10152.

Nisbet, E. G., & Nisbet, R. E. R. (2008). Methane, oxygen, photosynthesis, rubisco and the regulation of the air through time. *Philosophical Transactions of the Royal Society of London. Series B, Biological Sciences, 363*(1504), 2745-2754.

Nürnberg, D. J., Morton, J., Santabarbara, S., Telfer, A., Joliot, P., Antonaru, L. A., Ruban, A. V., Cardona, T., Krausz, E., Boussac, A., Fantuzzi, A., & Rutherford, A. W. (2018). Photochemistry beyond the red limit in chlorophyll f–containing photosystems. *Science, 360*(6394), 1210-1213.

Okada, K. (2009). The novel heme oxygenase-like protein from Plasmodiumfalciparum converts heme to bilirubin IXalpha in the apicoplast. *FEBS Letters, 583*(2), 313-319.

Ovadi, J. (1991). Physiological significance of metabolic channelling. *Journal of Theoretical Biology, 152*(1), 1-22.

Paiva-Silva, G. O., Cruz-Oliveira, C., Nakayasu, E. S., Maya-Monteiro, C. M., Dunkov, B. C., Masuda, H., Almeida, I. C., & Oliveira, P. L. (2006). A heme-degradation pathway in a blood-sucking insect. *Proceedings of the National Academy of Sciences of the United States of America, 103*(21), 8030-8035.

Proschel, M., Detsch, R., Boccaccini, A. R., & Sonnewald, U. (2015). Engineering of Metabolic Pathways by Artificial Enzyme Channels. *Frontiers in Bioengineering and Biotechnology, 3*, 168.

Ratliff, M., Zhu, W., Deshmukh, R., Wilks, A., & Stojiljkovic, I. (2001). Homologues of neisserial heme oxygenase in gram-negative bacteria: degradation of heme by the product of the pigA gene of Pseudomonas aeruginosa. *Journal of Bacteriology, 183*(21), 6394-6403.

Redlinger, T., & Gantt, E. (1981). Phycobilisome Structure of Porphyridium cruentum: POLYPEPTIDE COMPOSITION. *Plant Physiology, 68*(6), 1375-1379.

Reniere, M. L., Ukpabi, G. N., Harry, S. R., Stec, D. F., Krull, R., Wright, D. W., Bachmann, B. O., Murphy, M. E., & Skaar, E. P. (2010). The IsdG-family of haem oxygenases degrades haem to a novel chromophore. *Molecular Microbiology, 75*(6), 1529-1538.

Rhee, S., Miles, E. W., & Davies, D. R. (1998). Cryo-crystallography of a true substrate, indole-3-glycerol phosphate, bound to a mutant (alphaD60N) tryptophan synthase alpha2beta2 complex reveals the correct orientation of active site alphaGlu49. *Journal of Biological Chemistry, 273*(15), 8553-8555.

Rhie, G., & Beale, S. I. (1992). Biosynthesis of phycobilins. Ferredoxin-supported nadph-independent heme oxygenase and phycobilin-forming activities from Cyanidium caldarium. *Journal of Biological Chemistry, 267*(23), 16088-16093.

Richaud, C., & Zabulon, G. (1997). The heme oxygenase gene (pbsA) in the red alga Rhodella violacea is discontinuous and transcriptionally activated during iron limitation. *Proceedings of the National Academy of Sciences of the United States of America, 94*(21), 11736-11741.

Richter, A. S., & Grimm, B. (2013). Thiol-based redox control of enzymes involved in the tetrapyrrole biosynthesis pathway in plants. *Frontiers in Plant Science, 4*, 371.

Roth, J. R., Lawrence, J. G., Rubenfield, M., Kieffer-Higgins, S., & Church, G. M. (1993). Characterization of the cobalamin (vitamin B12) biosynthetic genes of Salmonella typhimurium. *Journal of Bacteriology, 175*(11), 3303-3316.

Rudolf, L. (1928). Die Chromoproteide der Rotalgen. I. *Justus Liebigs Annalen der Chemie, 461*(1), 46-89.

Sambrook, J. (2001). *Molecular cloning : a laboratory manual*: Third edition. Cold Spring Harbor, N.Y. : Cold Spring Harbor Laboratory Press, [2001] ©2001.

Sambrook, J., Fritsch, E. F., & Maniatis, T. (1989). *Molecular cloning : a laboratory manual*. Cold Spring Harbor, N.Y.: Cold Spring Harbor Laboratory.

Schacter, B. A., Nelson, E. B., Marver, H. S., & Masters, B. S. (1972). Immunochemical evidence for an association of heme oxygenase with the microsomal electron transport system. *Journal of Biological Chemistry, 247*(11), 3601-3607.

Scheer, H., & Zhao, K. H. (2008). Biliprotein maturation: the chromophore attachment. *Molecular Microbiology, 68*(2), 263-276.

Schmitt, M. P. (1997). Utilization of host iron sources by Corynebacterium diphtheriae: Identification of a gene whose product is homologous to eukaryotic heme oxygenases and is required for acquisition of iron from heme and hemoglobin. *Journal of Bacteriology, 179*(3), 838-845.

Schonknecht, G., Chen, W. H., Ternes, C. M., Barbier, G. G., Shrestha, R. P., Stanke, M., Brautigam, A., Baker, B. J., Banfield, J. F., Garavito, R. M., Carr, K., Wilkerson, C., Rensing, S. A., Gagneul, D., Dickenson, N. E., Oesterhelt, C., Lercher, M. J., & Weber, A. P. (2013). Gene transfer from bacteria and archaea facilitated evolution of an extremophilic eukaryote. *Science, 339*(6124), 1207-1210.

Shively, J. M., Ball, F., Brown, D. H., & Saunders, R. E. (1973). Functional organelles in prokaryotes: polyhedral inclusions (carboxysomes) of Thiobacillus neapolitanus. *Science, 182*(4112), 584-586.

Siegel, D. A., & Franz, B. A. (2010). Oceanography: Century of phytoplankton change. *Nature, 466*(7306), 569, 571.

Six, C., Thomas, J. C., Garczarek, L., Ostrowski, M., Dufresne, A., Blot, N., Scanlan, D. J., & Partensky, F. (2007). Diversity and evolution of phycobilisomes in marine Synechococcus spp.: a comparative genomics study. *Genome Biology, 8*(12), R259.

Solomon, M. J., & Varshavsky, A. (1985). Formaldehyde-mediated DNA-protein crosslinking: a probe for in vivo chromatin structures. *Proceedings of the National Academy of Sciences of the United States of America, 82*(19), 6470-6474.

Spencer, A. L., Bagai, I., Becker, D. F., Zuiderweg, E. R., & Ragsdale, S. W. (2014). Protein/protein interactions in the mammalian heme degradation pathway: heme oxygenase-2, cytochrome P450 reductase, and biliverdin reductase. *Journal of Biological Chemistry, 289*(43), 29836-29858.

Steglich, C., Frankenberg-Dinkel, N., Penno, S., & Hess, W. R. (2005). A green light-absorbing phycoerythrin is present in the high-light-adapted marine cyanobacterium Prochlorococcus sp. MED4. *Environmental Microbiology, 7*(10), 1611-1618.

Stiefelmaier, J., Ledermann, B., Sorg, M., Banek, A., Geib, D., Ulber, R., & Frankenberg-Dinkel, N. (2018). Pink bacteria-Production of the pink chromophore phycoerythrobilin with Escherichia coli. *Journal of Biotechnology, 274*, 47-53.

Stoebe, B., & Maier, U. G. (2002). One, two, three: nature's tool box for building plastids. *Protoplasma, 219*(3-4), 123-130.

Studier, F. W., & Moffatt, B. A. (1986). Use of Bacteriophage-T7 Rna-Polymerase to Direct Selective High-Level Expression of Cloned Genes. *Journal of Molecular Biology, 189*(1), 113-130.

Sweetlove, L. J., & Fernie, A. R. (2013). The spatial organization of metabolism within the plant cell. *Annual Review of Plant Biology, 64*, 723-746.

Tandeau de Marsac, N. (1977). Occurrence and nature of chromatic adaptation in cyanobacteria. *Journal of Bacteriology, 130*(1), 82-91.

Terry, M. J., Mcdowell, M. T., & Lagarias, J. C. (1995). (3z)-Phytochromobilin and (3e)-Phytochromobilin Are Intermediates in the Biosynthesis of the Phytochrome Chromophore. *Journal of Biological Chemistry, 270*(19), 11111-11118.

Terry, M. J., Wahleithner, J. A., & Lagarias, J. C. (1993). Biosynthesis of the plant photoreceptor phytochrome. *Archives of Biochemistry and Biophysics, 306*(1), 1-15.

Ting, C. S., Rocap, G., King, J., & Chisholm, S. W. (2001). Phycobiliprotein genes of the marine photosynthetic prokaryote Prochlorococcus: evidence for rapid evolution of genetic heterogeneity. *Microbiology, 147*(Pt 11), 3171-3182.

Towbin, H., Staehelin, T., & Gordon, J. (1979). Electrophoretic Transfer of Proteins from Polyacrylamide Gels to Nitrocellulose Sheets - Procedure and Some Applications. *Proceedings of the National Academy of Sciences of the United States of America, 76*(9), 4350-4354.

Tu, S. L., Gunn, A., Toney, M. D., Britt, R. D., & Lagarias, J. C. (2004). Biliverdin reduction by cyanobacterial phycocyanobilin:ferredoxin oxidoreductase (PcyA) proceeds via linear tetrapyrrole radical intermediates. *Journal of the American Chemical Society, 126*(28), 8682-8693.

Vermaas, W. (2001). Photosynthesis and Respiration in Cyanobacteria *eLS* (pp. 245 - 251). Encyclopedia of Life Sciences: Nature Publishing Group.

Vieira, J., & Messing, J. (1982). The pUC plasmids, an M13mp7-derived system for insertion mutagenesis and sequencing with synthetic universal primers. *Gene, 19*(3), 259-268.

Wiethaus, J., Busch, A. W., Dammeyer, T., & Frankenberg-Dinkel, N. (2010). Phycobiliproteins in Prochlorococcus marinus: biosynthesis of pigments and their assembly into proteins. *European Journal of Cell Biology, 89*(12), 1005-1010.

Wilbanks, S. M., & Glazer, A. N. (1993). Rod structure of a phycoerythrin II-containing phycobilisome. II. Complete sequence and bilin attachment site of a phycoerythrin gamma subunit. *Journal of Biological Chemistry, 268*(2), 1236-1241.

Wildman, R. B., & Bowen, C. C. (1974). Phycobilisomes in blue-green algae. *Journal of Bacteriology, 117*(2), 866-881.

Wilks, A. (2002). Heme oxygenase: evolution, structure, and mechanism. *Antioxidants & Redox Signaling, 4*(4), 603-614.

Wilks, A., & Schmitt, M. P. (1998). Expression and characterization of a heme oxygenase (Hmu O) from Corynebacterium diphtheriae. Iron acquisition requires oxidative cleavage of the heme macrocycle. *Journal of Biological Chemistry, 273*(2), 837-841.

Wood, A. M. (1985). Adaptation of photosynthetic apparatus of marine ultraphytoplankton to natural light fields. *Nature, 316*, 253.

Wruck, F., Katranidis, A., Nierhaus, K. H., Buldt, G., & Hegner, M. (2017). Translation and folding of single proteins in real time. *Proceedings of the National Academy of Sciences of the United States of America, 114*(22), E4399-E4407.

Yabuta, Y., Fujimura, H., Kwak, C. S., Enomoto, T., & Watanabe, F. (2010). Antioxidant Activity of the Phycoerythrobilin Compound Formed from a Dried Korean Purple Laver (Porphyra sp.) during in Vitro Digestion. *Food Science and Technology Research, 16*(4), 347-351.

Yanisch-Perron, C., Vieira, J., & Messing, J. (1985). Improved M13 phage cloning vectors and host strains: nucleotide sequences of the M13mp18 and pUC19 vectors. *Gene, 33*(1), 103-119.

Zhang, N., & Young, R. (1999). Complementation and characterization of the nested Rz and Rz1 reading frames in the genome of bacteriophage lambda. *Molecular & General Genetics, 262*(4-5), 659-667.

Zhao, K. H., Su, P., Tu, J. M., Wang, X., Liu, H., Ploscher, M., Eichacker, L., Yang, B., Zhou, M., & Scheer, H. (2007a). Phycobilin:cystein-84 biliprotein lyase, a near-universal lyase for cysteine-84-binding sites in cyanobacterial phycobiliproteins. *Proceedings of the National Academy of Sciences of the United States of America, 104*(36), 14300-14305.

Zhao, K. H., Zhang, J., Tu, J. M., Bohm, S., Ploscher, M., Eichacker, L., Bubenzer, C., Scheer, H., Wang, X., & Zhou, M. (2007b). Lyase activities of CpcS- and CpcT-like proteins from Nostoc PCC7120 and sequential reconstitution of binding sites of phycoerythrocyanin and phycocyanin beta-subunits. *Journal of Biological Chemistry, 282*(47), 34093-34103.

Zilinskas, B. A., & Greenwald, L. S. (1986). Phycobilisome structure and function. *Photosynthesis Research, 10*(1-2), 7-35.

Curriculum vitae

Persönliche Daten

Name	Marco Aras

Hochschulausbildung

Sep. 2014 Okt 2018	Doktorand in der Abteilung für Mikrobiologie von Prof. Dr. Nicole Frankenberg-Dinkel an der TU Kaiserslautern
Okt. 2010 – Jan. 2013	Studium der Biologie (Ruhr-Universität Bochum) Schwerpunkt: Molekulare Botanik und Mikrobiologie Abschluss: Master of Science, Note 1.5
Okt. 2007 – Sep. 2010	Studium der Biologie (Ruhr-Universität Bochum) Abschluss: Bachelor of Science, Note 2.0
Okt. 2004 – Sep. 2007	Studium der Wirtschaftswissenschaften (Ruhr-Universität Bochum)

Berufs- und schulische Ausbildung

Aug. 2002 – Jun. 2004	Ausbildung zum Bankkaufmann (Sparkasse Arnsberg-Sundern)
Sep. 2001 – Mai 2002	Grundwehrdienst Lipperlandkaserne Lippstadt
bis Juni 2001	Abitur St.-Ursula-Gymnasium Arnsberg

Berufserfahrung

Jun. 2014 – Aug. 2014	Praktikum als Junior Sales Contact bei Capsid GmbH/Jobvector
Apr. 2012 – Sep. 2012	Wissenschaftliche Hilfskraft (Lehrstuhl Biologie der Mikroorganismen, RUB)
Mar. 2010 – Jun. 2010	Wissenschaftliche Hilfskraft (Lehrstuhl Biologie der Mikroorganismen, RUB)
Sep. 2007 – Apr. 2011	Studentische Hilfskraft (Dr. Bergmann • Dr. Rhode & consulting group GmbH)

- Publikationen:

Ledermann, B., **Aras M.** and Frankenberg-Dinkel, N. (2017) *Biosynthesis of cyanobacterial light-harvesting pigments and their assembly into phycobiliproteins* Modern Topics in the Phototrophic Prokaryotes (Chapter 9, 305-341)

Overkamp, K. E., Langklotz, S., **Aras, M.**, Helling, S., Marcus, K., Bandow, J. E., Hoef-Emden, K. und Frankenberg-Dinkel, N. (2014) *Chromophore composition of the phycobiliprotein Cr-PC577 from the cryptophyte Hemiselmis pacifica* Photosynth Res. 122, 293-304

Gisk B, Wiethaus J, **Aras M**, Frankenberg-Dinkel N (2012) *Variable composition of heme oxygenases with different regiospecificities in Pseudomonas species.* Arch. Microbiol. 194(7):597–606

- Konferenzteilnahmen

Poster

Marco Aras, Marc Nowaczyk and Nicole Frankenberg-Dinkel (2017) *Metabolic channeling during phycoerythrobilin biosynthesis in cyanobacteria.* International Conference on Tetrapyrrole Photoreceptors of Photosynthetic Organisms (ICTTPO), Chicago, Illinois, USA

Marco Aras and Nicole Frankenberg-Dinkel (2015) *Metabolic channeling during phycoerythrobilin biosynthesis in cyanobacteria.* International Conference on Tetrapyrrole Photoreceptors of Photosynthetic Organisms (ICTTPO), Upper Galilee, Israel.

Vortrag

Marco Aras and Nicole Frankenberg-Dinkel (2017) *Metabolic channeling during phycoerythrobilin biosynthesis in cyanobacteria.* Tetrapyrrole Retreat, Fulda, Germany.

Eidesstattliche Erklärung

Ich erkläre hiermit an Eides statt, dass ich die vorliegende Dissertation selbstständig und ohne Benutzung anderer als der angegebenen Hilfsmittel angefertigt habe. Die aus fremden Quellen übernommenen Gedanken sind ausnahmslos als solche kenntlich gemacht. Die Promotionsordnung des Fachbereichs Biologie der TU Kaiserslautern ist mir in der derzeit gültigen Fassung bekannt. Die Ergebnisse anderer Mitarbeiter sowie anderer Autoren wurden klar gekennzeichnet. Die Dissertation oder Teile daraus wurden in keinem anderen Fachbereich oder keiner anderen Fakultät als Prüfungsarbeit eingereicht. Ich habe zu keinem früheren Zeitpunkt an einer anderen Universität ein Promotionsverfahren beantragt.

Kaiserslautern, den 16.10.2018
Marco Aras